A Study Of Seismic Design Spectra For Highway Bridges

by

Qin Liu

B.Eng. (Civil Engineering)

Dalian University of Technology, China, 1982

A thesis submitted to

The Faculty of Graduate Studies and Research

in partial fulfillment of the requirements

for the degree of

Master of Engineering

Department of Civil and Environmental Engineering

Carleton University, Ottawa

Aug. 1997

The master of Engineering Program in Civil and Environmental Engineering is a joint program with the University of Ottawa, administered by the Ottawa-Carleton Institute for Civil Engineering

Abstract

In light of the recent advances in earthquake engineering, this study reviews some important aspects of the earthquake resistant design for highway bridges, such as the design concept, philosophy and approaches. An overview and discussion of the seismic design code provisions for the earthquake resistant design of highway bridges are presented. The site amplification effects of different soil conditions to earthquake input ground motions with different a/v ratios are investigated. The calculated results are compared with the design spectra from codes and guidelines. The results indicate that current design codes underestimate seismic design loads in most of the considered soil cases, particularly for those of short-period bridges close to the source fields and for moderate to long-period bridges at some distance from source fields.

Acknowledgments

The author would like to take this opportunity to express her sincere gratitude to her supervisor Professor D.T. Lau for his great insights into this field and invaluable guidance through the course of this work.

The author wishes to thank Professor K.T. Law, Professor M.S. Cheung and Dr. J.H. Rainer for their helpful discussions and supports.

Special thank is due to the support of family members.

The financial support provided by the Department of Civil and Environmental Engineering of Carleton University is gratefully acknowledged.

TABLE OF CONTENTS

LIST OF FIGURES

CHAPTER 1 INTRODUCTION

1.1 Introduction

The dynamic behaviour and performance of highway bridges under seismic loads are subjects of major concern to bridge engineers in seismically active areas. As many highway bridges are an integral part of modern transportation networks, damages to these bridges during earthquakes may not only result in loss of life but can also cause severe economic losses. Severe damage or collapse of important highway bridges will also hamper immediate post-disaster rescue efforts and recovery.

During the 1971 San Fernando earthquake in California, more than 60 bridges on the Golden State Freeway collapsed or suffered severe damage to a total cost of $6.5 million. Although there have been many advances made in the area of earthquake resistant design of highway bridges since the 1971 San Fernando earthquake, the problem still exists today as evidenced by the large number of bridges damaged during the 1989 Loma Prieta earthquake, the 1994 Northridge earthquake in California (Moehle et al. 1995), and the 1995 Kobe earthquake in Japan (Bruneau et al. 1995, Anderson et al. 1995). During these recent events, structural failures were observed in bridge columns and piers, supporting joints, abutments and girders. The severity of the damage suffered by the highway bridges in recent earthquakes has clearly shown that many bridge structures, especially the older ones, are vulnerable to severe seismic damage and do not have the capacity to resist strong ground shakings.

In reviewing the damages to highway bridges in recent earthquakes, three typical types of failure can be identified as follows:

1. Loss of span due to underestimation in seismic displacements;

2. Failure of piers and columns due to the insufficient resistance of the substructure;

3. Failure of foundations and embankments due to the weakness of surrounding soils.

The observed earthquake performance and damage led to increased attention and concern on the level of safety provided by the current bridge design codes. Extensive research efforts have been carried out to examine the existing seismic design philosophy and procedures for highway bridges, as well as to improve the design methodology for this type of structure. The objective of many of these research activities, both experimental and theoretical, is to develop a unified design approach that will prevent collapse due to ground motions from the most severe earthquake, but accept the possibility of some damages that are reparable from a less severe earthquake event.

In the development of the earthquake resistant design concepts and codes for highway bridges, the 1971 San Fernando earthquake in southern California stands out as a major event. The 1971 San Fernando earthquake caused substantial damage to and collapse of numerous highway bridges designed in accordance to the provisions of the latest modern design code in effect at that time. Results of investigations after the earthquake revealed the inadequacy of the design and failure in the existing practice of structural detailing. This led to a major review of the adequacy of the design provisions in the seismic design codes for bridges in North America. Coordinated research efforts were made to better understand the dynamic response and behaviour of bridges subjected to earthquake

ground motions, and to develop new design procedures. Examples of these research efforts include research in New Zealand (Chapman 1979, Richards and Elms 1977), Japan (JSCE 1982) and the U.S. as well as other parts of the world (Gates 1976, 1979, Imbsen and Penzien 1986, Imbsen et al. 1979, Newmark 1979, Hall and Newmark 1979, Elms and Martin 1979, Sharpe and Carr 1976, Barenberg and Foutch 1987, Priestley 1996, Housner 1979, Seed et al. 1976, Basham et al. 1985, Mitchell et al. 1986 and 1991, Heideberecht and Lu 1987, Rainer and Pernica 1979).

As a result of the research, the importance of the role of structural ductility in seismic behaviour and earthquake resistant design of bridges is well recognized. In the inelastic ductile design concept, the design strength of the structure is reduced with the expectation that the structure will behave in a ductile manner and has sufficient redundancy for the redistribution of seismic loads after initial yielding failure of the structure. The current practice in earthquake resistant design of highway bridges relies on the capability of the ductile components in a bridge system, such as columns and piers, to absorb or dissipate the seismic energy imparted by the strong ground motions. To properly implement the ductile design concept, it is important to have a clear understanding and knowledge of the dynamic response and behaviour of the designed bridge system. A bridge structure should be designed and detailed in such a way that the ductile components, such as the plastic hinge regions of bridge piers and columns when seismic damages are expected to occur during a severe earthquake, will have sufficient reserved ductility capacity to accommodate the expected ductility demand of the system.

Design criteria have also been developed to take into consideration the effect of the characteristics of ground motions and the dynamic effect of the underlying soil deposit on the response of the bridge superstructure. Research results and findings have been incorporated in the recommendations of seismic design standards and guidelines (ATC 1981, ASSHTO 1983, CALTRANS 1976, Japan Road Association 1980, CHBDC 1996).

Among the design criteria considered, the effect of local soil conditions on the characteristics of input ground motions is a major concern in the earthquake resistant design of bridges, particularly for bridges located in or near areas of river sediment of soft soil. The failure of many highway bridges occurs because of the amplification effect of the underlying soil on the bedrock ground motions. Experience and observations from recent major earthquakes in California and other parts of the world have shown that bridges built on soft clay are particularly susceptible to failure during earthquakes. For example, significant ground motion amplifications were observed during the 1985 Mexico earthquake in areas of Mexico City of clay deposits, which caused extensive damage and collapse to high-rise buildings due to natural vibration periods of structures that resonate with the dominant vibration period of the amplified motions (Mitchell et al. 1986). In the 1989 Loma Prieta earthquake, the locations of damaged bridges are strongly correlated with the areas of soft soils where the level of ground shakings has been significantly amplified (Michell et al. 1991). Other bridge damages caused by the local soil amplification effect include the collapse of bridges during the 1994 Northridge earthquake. In this case, even though the bridges were built not on soft soil but on stiff or dense granular materials of 10 to 17 m deep, significant amplifications to the earthquake

ground motions still occurred and caused severe damage to highway bridges (Scott et al. 1994).

Analytical studies of the local soil effects have concluded that earthquake ground motions are strongly influenced by the type and depth of the soil deposit on top of the bedrock. In earthquake resistant design, the soil effect on ground motions is generally represented approximately by the concept of a soil factor. Except for the degree of details in different seismic design codes, this factor depends on the characteristics and depth of the soil deposit as well as the frequency characteristics of the bedrock motions. Significant contributions to the research on the soil effect on ground motions have been made by Seed et al. (1976), Heideberecht and Lu (1987), Dobry and Vucetic (1987), Naumoski et al. (1988), Elhmadi et al. (1990), Heideberecht et al. (1990), Krawinkler and Rahnama (1992) and Hosni and Heideberecht (1994) and others.

In the development of the earthquake resistant design concept and methodology, much of the development and research have focused on the behaviour and performance of buildings. Although there are many similarities on the seismic design philosophy of buildings and bridges, because of different lateral load resisting systems in the two types of structures, differences on design requirements and limitations can be significant. Firstly, bridges are relatively light structures and thus the dynamic behaviour of bridges is not significantly influenced by soil-structure interaction effects (Ciampoli and Pinto 1995) as compared to that of buildings (Fenves and Serino 1990, Wallace and Moehle 1990). Secondly, the consequence of structural failure in a bridge can be quite different from that in a building structure. Because of the lack of structural redundancy in a typical

highway bridge system, the failure of one structural member or connection between elements in a bridge usually has more serious consequences and may result in the collapse of the structure, which is unlikely to be the case in a building because a high degree of redundancy is generally found in building structural systems.

In view of the differences in seismic behaviour under different earthquake ground motions, it is important to note that the seismic design loads specified in current bridge design codes used in Canada (OHBDC 1991, CHBDC 1996) are derived based on earthquake records in western North America, particularly California, which may not be appropriate for the seismic design of highway bridges in other regions of Canada. In fact, there are many significant differences in the characteristics of the earthquake ground motions in eastern Canada from those on the west coast in terms of the frequency content.

1.2 Objectives and Outline of the Thesis

In light of the recent advances and new research findings in earthquake engineering, the intent of this thesis is to determine the level of protection and the adequacy provided by the seismic design provisions in current bridge design codes and standards. More specifically, the objectives of this thesis are as follows:

(1) to review and compare different approaches in the earthquake resistant design of highway bridges in current bridge design codes;

(2) to investigate the level of protection provided by the seismic design code provisions in commonly used U.S. and Canadian bridge design codes and standards;

(3) to estimate the degree of adequacy of the representation of soil amplification effects in current bridge design codes due to different types and depths of local soil deposits.

The thesis is divided into five chapters. Chapter 1 gives a brief introduction on the motivation, objectives and scope of the present study.

The seismic resistant design concept for highway bridges is discussed in Chapter 2. The design philosophy, approach, methods of analysis and design criteria are discussed. The different requirements in the ductile design of bridges from that of buildings are also discussed.

Following the discussion of the design concept of highway bridges, a conceptual comparison of the design objectives and design approaches of commonly used codes and standards for the earthquake resistant design of bridges is presented in Chapter 3.

Chapter 4 presents the results obtained from a study on the soil amplification effects due to different types of soil and seismic ground motions. The results are compared with those specified in the existing design codes. Finally, a summary and conclusions are presented in Chapter 5.

CHAPTER 2 EARTHQUAKE RESISTANT DESIGN CONCEPT FOR HIGHWAY BRIDGES

2.1 Introduction

The overall objective of earthquake resistant design of highway bridges is to design the bridge structure with sufficient strength and overall stiffness as well as reserved ductility capacity, so as to prevent failure or excessive damage that leads to the collapse of the bridge, in the event of an earthquake. This is rather a complex problem. In earthquake resistant design of bridges, there are many uncertainties in defining the severity of the potential earthquake hazards. The one area that needs more detailed investigation is the influence of the local underlying soil condition on the response of the bridge structure.

The seismic design provisions in modern bridge design codes are based on the concept of ductile design. In ductile design of highway bridges, bridge structures are expected to behave inelastically during moderate to strong earthquakes, and the damage is controlled through hysteretic energy dissipation. In recent years, extensive research has been carried out on the seismic design of bridges and buildings (Hall and Newmark 1979, Housner 1979, Newmark 1979 and Housner and Jennings 1982). Conceptually, earthquake resistant designs for bridges and buildings are quite similar. However, because of the differences in responses and failure modes of bridges and buildings during

earthquakes, the design requirements of these two types of structures can be quite different. Buildings are typically designed to have strong columns and weak beams. For such a structural system with multiple redundancy, redistribution of seismic loads after yielding failure of structural members can be easily accommodated to achieve a ductile design. On the other hand, typical highway bridges inherently have less structural redundancy than buildings with a relatively small number of supporting columns and longer spanned superstructures. For such a bridge structural system, the failure of a single structural element or connection may lead to a catastrophic collapse of the superstructure. This is generally not the case for a building. Typical weak links in a bridge system are the connections between the bridge deck and the supporting piers or columns and abutments. As columns and piers are the main lateral load-resisting elements in a bridge structure, plastic hinges are expected to develop in columns and piers during earthquakes. Consequently in earthquake resistant design of bridges, particular emphasis is required on the inelastic ductile design of bridge columns and piers together with the need to ensure that adequate displacements or seat widths are provided at supporting joints to accommodate the large plastic displacement of columns and piers. The strength and ductility of columns and piers require special attention in the earthquake resistant design of bridges (Hall and Newmark 1979).

This chapter discusses the basis of the design code provisions for the earthquake resistant design of bridges. The design philosophy, principle of capacity design, design criteria, seismic design approaches and methods of analysis are discussed.

2.2 Design Philosophy

The objective of earthquake resistant design of highway bridges is to control damage in critical structural components to prevent the total collapse of the structure in case of a severe earthquakes, while allowing the possibility of some damage during moderate ground shakings. With regard to earthquake response, the seismic design objectives for highway bridges can be summarized as follows:

1) The designed bridge structural systems should be able to resist small to moderate earthquakes within the elastic range of behaviour.

2) The seismic loads from large earthquakes should not lead to collapse of all or part of the bridge systems.

The first design objective considers the case of earthquakes with high probability of occurrence, which may occur several times during the lifetime of the bridge with a relatively small-to-moderate intensity. The resistance to small-to-moderate earthquakes within the elastic range implies that the structural responses do not exceed the response level that corresponds to the yielding level of the system. In the design process, the strength-control aspect is contained in the specification of the minimum equivalent static lateral seismic force as determined from an elastic analysis.

The second design objective considers the case of severe earthquakes with a low probability of occurrence but with strong intensity. The resistance to large earthquakes without collapse implies that the bridge structure must have sufficient ductility to allow extensive energy absorption without reaching a collapse state. By considering the post-yielding behaviour in the bridge structure, the ductility-control aspect is contained in the

specification of a force reduction factor in conjunction with the specification of a minimum support length to accommodate the large displacement expected in such a ductile system.

2.3 Principle of Capacity Design

One form of implementation of ductile design of highway bridges is the concept of capacity design, which was first developed in New Zealand (Gates 1979). The basic concept of capacity design is that the structural members and components, including girders and columns, are designed such that inelastic hinges are permitted to form only in columns and piers. Satisfactory performance of the bridge is ensured by detailing the columns or piers so that they can sustain the large plastic deformations imposed on them without significant degrading of the strength and stiffness.

In capacity design, the response of a bridge depends on the capacity of the support columns to displace inelastically under the design earthquake motions. The columns should be designed to withstand multiple cycles of excursion into the inelastic range of behaviour without excessive strength and stiffness degradation beyond those corresponding to the elastic response level. In order to ensure this level of performance, the relationship between the flexural strength and the plastic hinge rotation in the column is required. By using this relationship and having an estimation of the expected level of ductility demand of the bridge structure, the flexural strength of the bridge column plastic hinge, which is compatible with the expected ductility level, can be obtained. Then in the design of a column member, a force reduction factor can be used to obtain the design strength of the member from the elastic strength.

2.4 Design Criteria

Earthquake resistant design criteria are, in general, means of specifying the desired earthquake resistant capability of the structures. The purpose of the design criteria is to provide a level of earthquake resistance that is appropriate to the desired performance of the bridge. Earthquake resistant design criteria for highway bridges are developed based on considerations of the potential earthquake hazards, the effects of the underlying soil at a site, the dynamic response of the bridge including the vibrational characteristics of the bridge structure and the ductility capacity of the bridge structural system.

Seismic hazards are usually represented in design codes by means of a seismic zoning map. The seismic hazard at a site is determined with considerations of the seismological conditions of the site, which include the locations of nearby active faults, the local geological conditions and data or historical records of past earthquakes that occurred in nearby regions. The seismic zoning map is usually developed with a risk level considered acceptable in engineering design practices, typically 10% of excedence in 50 years for buildings and bridges (Basham et al. 1985), and lower for more important structures. Parameters of horizontal acceleration or velocity are often used to characterize the intensity of the ground motions. Recent research on seismic hazard in Canada has shown that the ratio of the horizontal acceleration to velocity is a useful parameter to characterize the frequency contents of earthquake ground motions (Heidebereeht and Lu 1987, Naumoski et al. 1988). Therefore, the a/v ratio is considered an important parameter in the seismic design of structures.

From observations in many earthquakes, it has been found that the site response can be greatly influenced by local geology and soil conditions. In seismic design provisions, the intensity of the surface ground motion is modified by the use of a soil coefficient to take into account the effect of underlying soil deposits over the bedrock motion. Surface motions may be estimated from bedrock motions by using the time history or response spectrum analysis for the site. The soil effects can then be determined by comparing the intensity of surface ground shakings to that of the bedrock motions. Wide variations in the properties and characteristics of soil conditions are often classified into 3 or 4 categories. The amplification effect of the soil deposit is usually represented by means of the ratio of the pseudo-acceleration response of the soil medium at the ground surface level to that at the bedrock. A site coefficient can be determined based on the statistical study of site responses to selected appropriate design earthquakes with suitable variations in the overall intensity, frequency content and duration of strong ground motions. These should be compatible with the seismic hazard of the site and reflect the level of uncertainties in typical earthquake ground motions.

The structural properties of a bridge, which have significant influences on the dynamic response of the system, are the structural mass and its distribution in the system, the natural vibration period, the damping ratio, as well as the ductility capacity of the structural system and its components. In bridge design codes, bridges are commonly categorized into a few types according to the number of spans and the complexity of the configuration of the superstructure. For design, bridges are divided into single span bridges or multi-span bridges. Multi-span bridges are further categorized into regular

bridges or irregular bridges. Regular bridges are those with no abrupt or unusual changes in the mass distribution, stiffness or geometry along its span and no large differences in these parameters from span-to-span or support-to-support. Any bridge that does not meet the definition of a regular bridge is considered an irregular bridge. For different types of bridges, different methods of analysis are often specified in the codes to be utilized to determine the seismic response of the bridge structural components. A force reduction factor is used to reduce the linear elastic response spectra for the design of inelastic ductile elements and components. The reduction in the design force level is applied due to considerations of the structural redundancy and ductility capacity of designed members or components.

2.5 Seismic Design Approaches

Two alternative design approaches are commonly adopted in the earthquake resistant design of highway bridges: the strength design approach and displacement design approach. The strength design approach is the traditional approach adopted in many existing codes. In this approach, the seismic design forces are determined in relation to acceleration response spectra, and then the adequacy of the displacement capacity of the structural system is checked. On the other hand, the displacement design approach is a relatively new approach, which recognizes that seismic damage in a structural system is a direct result of the large displacement experienced by the structure during an earthquake. Thus in this approach, the expected displacement of the system is used as the starting point for the design.

2.5.1 Strength Design Approach

In the strength design approach, two major steps are involved to predict the stresses and displacements of the components of a bridge structure. The first step is to determine the seismic load, and the second is to determine the effect of this load on the structure.

In seismic strength design, the seismic design load is determined from a design spectrum. The design spectrum specifies the level of the seismic design force as a function of the natural vibration period and damping of a bridge structure.

The effect of the seismic design load is evaluated from an elastic response analysis of the structure by using an appropriate analysis method, such as, the equivalent lateral static force method, the response spectrum analysis method or the time-history analysis method. Structural member forces can be determined by using the elastic response analysis, in which equivalent static lateral forces are obtained from the maximum credible earthquake of a site. However, it is uneconomical for a bridge structure to resist the effect of seismic load from a severe earthquake entirely in the elastic range because of the low probability of occurrence of such an event. A reduction in the design member forces is thus applied to account for the post yielding behaviour of the structure. The reduction factor varies with different structural components, such as piers, column bents and abutment walls, based on the expected ductility capacity of the components and on the experience and the performance of different types of structural components in severe earthquakes. It is assumed that plastic hinges will develop in piers when the seismic forces exceed the seismic design forces.

The "force design" approach is adopted in a number of current bridge design codes, including the bridge design recommendations and guidelines published by the California Department of Transportation (CALTRANS 1977), ATC (1981) and AASHTO (1982), which are the most commonly used bridge seismic design codes in the U.S.

In typical seismic code provisions, a force modification factor is employed to ensure that energy dissipation occurs with the formation of plastic hinges in ductile columns. The relationship between the force reduction factor R and the displacement ductility factor μ in the strength approach of the seismic design can be illustrated by a simple elasto-plastic system as shown in Figure 2.1. The force reduction factor, $R = F_{max} / F_y$, depends on the properties and characteristics of the structural system. It can be expressed in terms of the displacement ductility factor, $\mu = \Delta_{max} / \Delta_y$. Assuming the inelastic system attains equal maximum displacement as the elastic system, as shown in Figure 2.1 (a), the factor R can be expressed as follows:

$$R = \mu = F_{max} / F_y \tag{2.1}$$

For another case in which the potential energy of the inelastic system at maximum displacement is equal to that of the elastic system, as shown in Figure 2.1 (b), the factor R can be determined as follows:

$$R = \sqrt{2\mu - 1} \tag{2.2}$$

Recent research results by Penzien (1995) have shown that the relationship between the force reduction factor and the global ductility demand depends on the vibration period T of the single-degree-of-freedom system. For T greater than 0.5 s, it is found that the global ductility demand μ is equal to the force reduction factor R.

2.5.2 Displacement Design Approach

The displacement design approach is based on considerations of displacement ductility demand rather than force requirements. In this approach, the design procedure attempts to provide the appropriate member detailing, such as member size and reinforcement content, to achieve a specified displacement at an assumed location (normally at the center of the seismic force). The difference between the displacement design approach and the strength design approach is that, in the displacement design approach, the equivalent displacement cannot be converted backward to establish a relationship between the design force level and displacement ductility factor.

Three steps are involved in the displacement design procedure. The first step involves an estimate of the initial structural yield displacement and determination of the limit of acceptable inelastic displacement. Care should be given to ensure that the inelastic displacement due to plastic hinge rotation is not overestimated because the plastic hinge rotation is limited by its member strength. The second step involves an estimate of the structural damping property at the level of the expected ductility and the location of the plastic hinge by using an appropriate relationship between ductility and damping. With an estimated design displacement, the third step consists of establishing a relationship between the design displacement and the maximum curvature or compression strain imposed on the member cross-section. And then, the member dimensions and reinforcement content can be determined according to the calculated required member strength. Details of the displacement-based design approach can be found in publications by Qi and Moehle (1991), Moehle (1992) and Wallace (1996).

2.6 Methods of Analysis

Depending on the type of bridge structure and the complexity of the structural configuration, different methods and levels of approximation and accuracy can be employed to determine seismic forces in bridge structures. In current design practice of bridges, acceptable methods of analysis are:

1. Equivalent static force analysis;
2. Response spectrum analysis;
3. Time-history analysis.

The method of analysis for determining earthquake load effects is based on the desired level of accuracy in the calculation of the expected bridge performance. Minimum requirements may be specified in the design codes according to the complexity of the bridge structures to achieve a pre-defined acceptable level of accuracy in the estimation of seismic forces.

2.6.1 Equivalent Static Force Analysis

The equivalent lateral static force method is a simplified method of analysis for determining the seismic behaviour of bridges with satisfactory accuracy for the design of relatively simple bridges. In this approach, the seismic load effect is approximately represented by equivalent lateral static forces distributed over the structural system.

Specifically, in the uniform load method, the seismic load effect is approximately represented by an equivalent uniform load applied on the bridge superstructure. This method is commonly used in the codes to obtain the effect of seismic design loads for regular bridges. The accuracy of the uniform method has been examined by Imbsen et al.

(1979) with the conclusion that this method can yield accurate results for structures of straight, non-skewed alignment with balanced span and equal column stiffness. It is found that the relative contribution of the columns to the transverse stiffness of the entire structure has an influence on the accuracy of the results.

Another form of equivalent static force analysis method is called the pushover analysis. This method is actually an event scaling analysis that can determine the sequence of inelastic actions. In pushover analysis, an event is defined as a change in the member stiffness of the structure due to cracking, development of a plastic hinge, yielding of a soil spring in the analysis model of the soil foundation, or other occurrence that leads to significant changes in the stiffness property of the structure. The failure mode of the bridge is determined by a step-by-step force-deformation analysis procedure. At each event, the properties of the structural system is modified to reflect the occurrence of the event in the form of an updated member stiffness or the introduction of a hinge mechanism. By using a stepwise linear elastic analysis procedure, the pushover analysis can determine the ultimate deformation capacities of the bent or the frame of a bridge system. The inelastic deformation demands at assumed plastic hinge locations can be determined. Details of the analytical procedure can be found in Priestley (1996).

2.6.2 Response Spectrum Analysis

The response spectrum analysis procedure generally provides reliable results for seismic design of highway bridges. Two analysis methods are used in current design practices depending on the structural type of the bridges and the level of requirement to resist earthquake load. These are:

1. Single mode spectral analysis;
2. Multi-mode spectral analysis.

The single mode spectral analysis method is used to calculate the seismic design forces for bridges whose responses are dominated by the fundamental mode of vibrations. The deformation mode shape is determined by applying a uniform horizontal load to the structure in the direction of the ground motion component being considered. The horizontal seismic design forces are determined according to the fundamental vibration mode of the bridge, which is affected by the distribution of mass and stiffness over the length of the bridge. The method can be applied to many types of bridges with both continuous and non-continuous superstructures.

The multi-mode spectral analysis method can be considered as a simplified special case of modal analysis, in which the period and mode shape of each mode and the corresponding maximum response are determined in reference to a response spectrum. In this method, the bridge structural system is modelled by an appropriate mathematical model. The maximum response of each vibration mode is then obtained in a linear dynamic analysis of the bridge model. Since the maximum response of the individual modes do not necessarily occur at the same time, the maximum value of a force or displacement can be estimated by an appropriate combination rule, such as the Square Root of the Sum of Squares (SRSS) or Complete Quadratic Combinations (CQC) methods (Wilson et al. 1981).

2.6.3 Time History Analysis

In time history response analysis, the equations of motion of a bridge system are solved by direct integration in a step-by-step procedure. This analysis method can be applied to both linear and nonlinear analysis of bridge structural systems. In this direct time step integration method, the time history of seismic input is divided into short intervals that may be taken as equal. The response of the nonlinear system is calculated for each time step increment by assuming that the system behaves as a linear system having the properties at the beginning of the time step interval. At the end of each time step, the properties of the system are modified or updated to conform to the current deformation and stress states of the system at that time.

For nonlinear time-history analysis of a bridge system, reliable results can be obtained only if the bridge model used in the analysis can accurately represent the bridge's vibration behaviour at large amplitudes of motion. And the statistical results are examined when the model responds to several ground motions. For a complex bridge, the nonlinear time-history analysis procedure can produce realistic predictions of the behaviour of the bridge structural system during severe earthquakes. But full nonlinear modelling of a large complex bridge system is costly and may lead to enormous results if incorrect parameters are used in the analysis. It is therefore recommended that nonlinear inelastic model should be introduced slowly, starting with a full linear elastic model to maintain confidence in the validity of the results obtained.

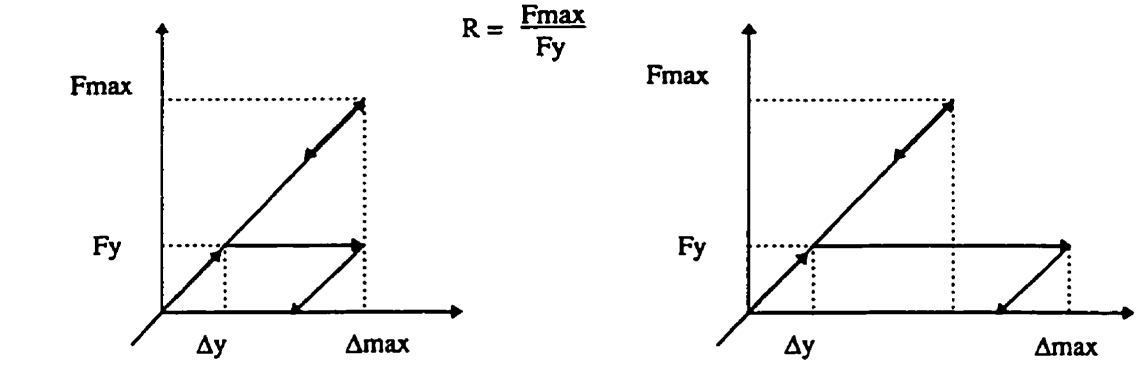

(a) Equal Maximum Displacement (b) Equal Maximum Potential Energy

Figure 2.1 Force Reduction Factor for Seismic Loading Equating Elastic and Inelastic Response

CHAPTER 3 CURRENT BRIDGE SEISMIC DESIGN CODES

3.1 Introduction

There are a number of highway bridge seismic design codes and guidelines commonly used in North America, such as the AASHTO (1993), ATC (1981), OHBDC (1991), CSA (1988) and CHBDC (1996). Bridge seismic design codes undergo continual revisions in an attempt to reflect the latest advances and new technologies in bridge and earthquake engineering. Some part of the code development is also based on observations and lessons learned from the performance of highway bridges during past strong earthquakes.

The development of seismic bridge design codes in North America can be divided into two periods, prior to the 1971 San Fernando earthquake and after. The seismic design code published by the American Association of State Highway Officials (AASHO 1965) was a typical bridge design code used prior to the 1971 San Fernando earthquake. In that design code, the seismic design load was defined as an equivalent lateral static force applied at the center of gravity of the structure. The equivalent lateral static load is taken as 2% to 6% of the dead weight of the structure depending upon the allowable foundation loads and the foundation type. The 1965 AASHO code did not address any influences from the geological conditions of the site, dynamic response characteristics and the expected ductile behaviour of bridges. Immediately following the San Fernando earthquake, the California Department of Transportation (CALTRANS 1977) initiated investigations and research efforts to improve the seismic design methodology

for highway bridges (Gate 1976, CALTRANS 1977). As a results of the concerted studies and research, significant improvements to the earthquake resistant design of highway bridges were achieved. Many of the research findings were incorporated into the seismic design codes and standards by the Applied Technology Council (ATC 1981) and the American Association of State Highway and Transportation Officials (AASHTO 1983).

The development of seismic bridge design codes in Canada began in 1979, with the first edition of the Ontario Highway Bridge Design Code published by the Ontario Ministry of Transportation and Communications (OHBDC 1979). An overview of the development of seismic design provisions in OHBDC is presented in the next section of this chapter. Another highway bridge design standard is issued by the Canadian Standards Association (CSA 1988), in which seismic design procedures were adopted from the 1985 National Building Code of Canada (NBCC 1985). Many of the seismic design provisions in the 1985 NBCC were specifically developed for buildings and may not be appropriate to apply to the design of bridges. Presently, a new design standard for highway bridges is proposed as the Canadian Highway Bridge Design Code (CHBDC 1996). In general, many aspects of the CHBDC (1996) are similar to the recommendations in AASHTO (1993) and ATC (1981).

In earthquake resistant design, the response spectrum method is often selected as the method of analysis to determine the seismic design load for the structure and the components. This is because design spectra can be easily constructed to quantify the earthquake hazard as opposed to other methods of analysis. Design spectra provide a quantitative description for both the intensity and the frequency content of the design

earthquakes. The design spectra are obtained from the ground motion parameters multiplies by suitable spectral amplification factors that contain the soil amplification effects. The seismic design load is generally determined from the design spectrum as a product of a response coefficient and the bridge's structural weight. The response coefficient is commonly obtained from the design spectra depending on the fundamental period of the bridge structure.

In the following sections, a brief overview of current seismic bridge design provisions, including the CALTRANS (1990) which plays an important role in the development of seismic bridge design codes, is presented. The approaches adopted in different codes to determine the seismic design load for highway bridges are summarized. The conceptual comparison and discussions of current seismic design codes are also presented.

3.2 Current Seismic Bridge Design Provisions

3.2.1 CALTRANS

After the 1971 San Fernando earthquake, CALTRANS initiated extensive studies to examine the inadequacy of seismic design provisions for bridges at the time. As a result of those research efforts, the seismic design specifications for highway bridges by the California Department of Transportation (CALTRANS) were revised with major improvement on the seismic design methodology for bridges. The earthquake design criteria in CALTRANS include the following considerations:

1. The location of the bridge relative to active faults;

2. The effect of a maximum credible earthquake from an active fault;

3. The effect of overlying soils at a site;

4. The dynamic responses of the bridge to the ground motion;

5. The reduction in force level for ductility and risk consideration.

In the latest CALTRANS recommendations (CALTRANS 1990), the elastic earthquake design load, Q, is determined as follows:

$$Q = ARSW \tag{3.1}$$

where A is the maximum expected acceleration at bedrock or "rock-like" material for the site, R is the normalized 5% damped elastic acceleration response spectrum on "rock" like material for the site, S is the soil amplification spectral ratio, and W is the dead load of the bridge or bridge component. For individual structural components, the design member force is obtained by dividing the elastic earthquake force Q by a reduction factor Z. The factor Z varies depending on the type of structural components. For ductile components, such as bridge columns and piers, the reduction factor varies from 2 to 8 and for non-ductile components, such as connections, it varies from 0.8 to 1.0. This design procedure is a "force design" approach.

ARS curves are given by a combined 5% damped elastic response spectra as function of the ground acceleration, soil depth and natural period of a bridge structure, as shown in

Figures 3.1 to 3.2. For a specific bridge at a site, the response coefficient C can be obtained directly from the design spectra.

3.2.2 ATC (1981) and AASHTO (1993)

In 1981, the development of "Seismic Design Guidelines for Highway Bridges" by ATC represented a major improvement for the earthquake resistance design practice of highway bridges. The improvements were mainly the results of analytical and experimental research on the seismic response and behaviour of bridges following the 1971 San Fernando earthquake (Imbsen and Penzien 1986). Later the recommendations on the earthquake resistant design of highway bridges by ATC (1981) were adopted by AASHTO to became the AASHTO's standard specifications for seismic design. Consequently, the AASHTO and ATC guidelines are identical in their seismic design provisions, which were based on modifications to the CALTRANS approach.

The design seismic load in ATC and AASHTO is obtained as the product of the elastic seismic response coefficient C_{sn} and the equivalent weight of the superstructure. The value of C_{sn}, for the n^{th} vibration mode is given as follows:

$$C_{sn} = \frac{1.2AS}{T_n^{\frac{2}{3}}} < 2.5A \qquad (3.2)$$

where A is the acceleration ratio, S is the site coefficient, and T_n is the vibration period of the n^{th} mode. The site coefficient was derived based on a statistical response spectra analysis of 104 earthquake records in the western United States by Seed et al. (1976). Several factors were taken into account in determining the design loads. These are briefly discussed next.

Importance Category: The importance categories defined in the AASHTO (1993) and ATC (1981) are *essential* and *other* bridges, which takes into consideration the impact of the potential loss of the bridge. Bridges classified as *essential* bridges should maintain their function after a design earthquake.

Seismic Performance Category: Four seismic performance categories are specified in AASHTO and ATC, based on the acceleration coefficient and the bridge importance classification. The purpose of classifying seismic performance categories is to specify the minimum analysis and design requirements for the determination of design forces.

Site Coefficient : The site coefficient S is used to account for the effects of site conditions on the bridge response. Generally the wide range of possible vibration in local soil deposits is difficult to quantify. In the AASHTO and ATC guidelines, the soil conditions are classified into three categories, with a site coefficient assigned to each category. The value of the site coefficient depends on the soil profile. It ranges from 1.0 to 1.5 for rocklike materials to soft and medium-stiff clays.

On the seismic performance category, two different minimum analysis procedures are specified for the types of bridges classified as "regular" and "irregular" bridges. The minimum analysis procedure required is based on the following two elastic response analysis methods:

1. Single-mode spectral method;

2. Multimode spectral method.

3.3.3 OHBDC

The first edition of OHBDC was published in 1979, and followed the 1965 AASHO approach with a modification on the response coefficient *C*, as shown in Figure 3.3, in order to permit the use of the regional seismicity data of Ontario with comparable level of safety in areas of Canada and the U.S. with similar seismic risks.

The equivalent static lateral load is calculated by the following equation:

$$Q = CIFW \tag{3.3}$$

where C is the response coefficient which depends on the seismicity of the site as represented by a number of parameters including normalized elastic response spectrum, the maximum expected zonal acceleration ratio A, and the soil amplification effects; I is the importance coefficient which is equal to 1.3 for all bridges designed for post disaster service and 1.0 for all other bridges; F is the framing coefficient which is equal to 1.0 for structures where single column or pier resists the horizontal loads, and equal to 0.8 for continuous frames; W is the weight of the bridge structure.

In OHBDC, the design spectra are developed for four categories of alluvium soil depths (0 - 3 m, 3 - 25 m, 25 - 45 m, and greater than 45 m). The maximum expected zonal acceleration ratio varies from 0.02 to 0.12g. As mentioned above, the effect of structural ductility and structural damping are considered in the response coefficient curves of C.

In the second edition of OHBDC (1983), the same seismic design provisions remain essentially unchanged.

The current edition of OHBDC (1991) makes reference to the new Canadian seismic zoning maps developed by Basham et al. (1985). The new seismic zoning maps are developed on the basis of two ground motion parameters that characterize the intensity of ground motion, peak horizontal acceleration a and peak horizontal velocity v. The acceleration and velocity maps provide independent ground motion reference levels to better reflect the seismic risk with a probability of excedence of 10% in 50 years. Compared to the 1970 zoning map in NBCC, the new maps have seven seismic zones instead of four zones. The major changes of the seismic load provisions in the 1991 OHBDC are:

1. The response coefficient C is calculated by using the velocity-related zonal ratio v instead of the maximum expected zonal acceleration a. The shapes of design spectra remain the same as in the previous edition but are normalized to the velocity ratio v. The zonal velocity ratio varies from 0.1 to 0.3 m/s in the 1991 OHBDC.

2. The minimum support length N was equal to six times the computed elastic displacement in the previous edition, and currently is determined by the following equation:

$$N = 0.2 + 0.0017L + 0.0067H \tag{3.4}$$

where L is the length of the bridge deck to the adjacent expansion joint, and H is the average height of columns or piers.

3.2.4 CSA (1988)

The provisions in the 1988 CSA standard for the seismic design of bridges are basically adopted from the seismic design provisions of the 1985 NBCC. The equivalent static load Q is determined by Equation 3.5, which is based on the 1985 NBCC static base shear formula that assumes that the vibration period of the design bridge structure is less than 0.25 seconds.

$$Q = v_0 K I F W, \quad I F \leq 1.6 \tag{3.5}$$

where v_0 is the velocity-related coefficient calculated as the product of c_v multiplied by v; c_v is the velocity response coefficient equal to 0.62 for Za greater than Zv, and 0.44 for Za equal to Zv, and 0.31 for Za less than Zv; v is the zonal velocity ratio; and Za and Zv are the acceleration-related and velocity-related seismic zones; K is the framing coefficient which equals 1.0 for structures with single column bents, piers or abutments to resist the horizontal loads, and 0.8 for continuous frames; I is the importance coefficient which equals 1.3 for all bridges representing an important element in the highway network and 1.0 for all other bridges; F is the foundation factor, which equals 1.0 for rocklike material of soil type I, 1.3 for firm and stiff soil of type II, and 1.5 for soft soil of type III; finally, W is the weight of the bridge structure.

For important bridges or bridges with complex structural configurations and for bridges located in seismic zone Zv = 4 (v = 0.2 m/s) or higher, dynamic analysis is required as specified in AASHTO (1983) and ATC (1981). Other detailed requirements on restraint of the horizontal and vertical response motions are also specified.

3.2.5 CHBDC

On the earthquake resistant design part, the proposed new 1996 CHBDC (1996) is nearly identical to AASHTO (1993) and ATC (1981). The seismic design loads in CHBDC (1996) are given as the product of the elastic seismic response coefficient C_{sn} and the equivalent weight of the superstructure. The value of C_{sn} for the n^{th} vibration mode is the same as that in the AASHTO (1993) and ATC (1981), as given in Eq. 3.2.

The factors considered in determining the design loads in CHBDC are very similar to those in AASHTO (1993) and ATC (1981). However, there are some differences, as follows:

Importance Categories: The importance categories are classified as "critical", "essential" and "other bridges". In CHBDC (1996), the additional classification of "critical" bridges is defined as bridges that must satisfy the performance requirement of emergency purposes immediately after a large earthquake. For critical bridges, a 1000-year return period event is considered for the design earthquake in CHBDC.

Seismic Performance Zones: Four seismic performance zones are specified, based on the zonal acceleration ratio. The seismic performance zones use acceleration-related seismic zones of the NBCC unlike other existing seismic bridge design codes (OHBDC 1991, CSA 1988) which primarily use velocity-related seismic zones in their requirements. The reason for this change is that the seismic performance parameters must be compatible with the requirements in the AASHTO code so that the different requirements on method of analysis and minimum support length in AASHTO can be adopted.

Site Coefficient: The site coefficient S is assigned according to four different types of soil conditions. In the first three cases of S equal to 1.0 to 1.5 for soil type I to III, the provisions in CHBDC are similar to those in AASHTO and ATC, which are based primarily on statistical analysis on site effects by Seed et al. (1976). The CHBDC additionally adds a soil coefficient category equal to 2.0 for soil type IV of very soft clay or silt with depths great than 12 m. This is the result of the experience from the 1985 Mexico earthquake during which large amplifications to the earthquake motion were observed in clay deposits.

Based on the importance category and seismic performance zone of a bridge, the minimum analysis requirement is specified with five different types of analysis procedures in CHBDC. These are listed as follows:

1. Uniform load method;
2. Single mode spectral method;
3. Multi-mode spectral method;
4. Time-history method;
5. Static push-over method (Inelastic static method).

The different seismic design approaches of various design codes and guidelines are summarized in Table 3.1.

3.2.6 Combination of Factored Loads

The factored load combinations are required by codes to determine seismic design forces for structural members and connections. The purpose of using load factors is to take into account the uncertainty in determining the magnitude of the loads and their

variability, the uncertainty in the calculation of the load effects and the consequences of failure. In common analysis procedures, seismic forces are modified by the force reduction factor and then combined independently with forces from other loads. The load factors can be applied to the load effects for each member.

The load factors and load combination factors in different codes can be different depending on the calibration procedures adopted in the codes. For ultimate limit state design, the load combination involving earthquake load and the load factors of different codes are briefly described in this section.

In AASHTO and ATC, the factored load combination including earthquake is given as follows

$$\text{Group Load} = 1.0\,(D + B + SF + E + EQ) \tag{3.6}$$

where D is the dead load; B is the load effect due to buoyancy, SF is stream flow pressure, E is the load due to earth pressure and EQ is the earthquake load.

In CALTRANS, the group load combination involving earthquake is similar to Equation 3.6 with the additional load effect of prestressing as follows

$$\text{Group Load} = 1.0\,(D + B + SF + \alpha_E E + PS + EQ) \tag{3.7}$$

where α_E is the load factor for loads due to earth pressure, which may vary from 0.5 to 1.5. PS is the load due to the prestressing effect.

In OHBDC, the group load combination is given in the form

$$\text{Group Load} = \alpha_D D + \alpha_E E + \alpha_P PS + 0.7W + 1.3EQ \tag{3.8}$$

where α_D and α_P are load factors for dead loads and prestressing effects. The variation of the load factor α_D can range from 0.65 to 1.5 depending on different dead load types, and

0.5 to 1.25 for α_E depending on the characteristics of the earth pressure load, and 0.95 to 1.05 for α_P. W is the wind load.

In CSA, the load factors and load combination including earthquake are given as follows

$$\text{Group Load} = \alpha_D D + \alpha_{Ds} Ds + \alpha_E E + \alpha_B B + \alpha_S S + 1.3F + 1.3C + 1.3EQ + 1.3A \quad (3.9)$$

where α_{Ds}, α_B and α_S are load factors respectively for dead loads due to wearing surface (Ds), hydrostatic pressure including buoyancy (B), and effects of shrinkage, creep, differential settlement, and bearing friction (S). The variation ranges of the α factors are, 0.9 to 1.2 for α_D, 0 to 1.6 for α_{Ds}, 0.8 to 1.3 for α_E, 0 to 1.2 for α_B, and 0.8 to 1.2 for α_S. F is the load due to stream flow and ice pressure. C is the collision load and A is the snow load.

In CHBDC, the load factors and load combination are given as

$$\text{Group Load} = 1.0D + 1.0EQ \quad (3.10)$$

As it can be observed in Equations 3.6 to 3.10, the load factor for earthquake load is 1.0 in the design specifications of AASHTO, ATC, CALTRANS and CHBDC, and 1.3 in OHBDC and CSA. These load factors for the earthquake effect are used in the response spectra study of the different codes presented in the next chapter.

3.3 Discussions

This section presents a general discussion of some important aspects of the various seismic design codes for highway bridges. A comparison of the concept of the design approach and methodology used in these different codes are also presented.

3.3.1 Ductility Capacity

The ductile design concept is the most significant design aspect that affects the ability of bridge structures to withstand strong earthquakes. The ductile design concept permits the reduction of the structural design strength in accordance to the expected ductility capacity and redundancy of the bridge structure. The seismic response and performance of a bridge structure is greatly controlled by its ductile behaviour and hysteretic energy dissipation through plastic deformations. The concept of ductile design is adopted by most of the current seismic design codes and guidelines in different forms.

Using a response reduction factor R in the AASHTO, ATC and CALTRANS design guidelines, structural components that permit inelastic hinges to form without significant degradation in their stiffness and load carrying capacity are designed with the reduced design strength modified by the reduction factor R. The members and connections must be detailed to ensure that the ductile capacity of the bridge structural system can be achieved. On the other hand, in the OHBDC and CSA standards, the effect of ductility is assumed to be implicitly included in the design spectra.

For structures with limited redundancy for redistribution of loads after initial yielding, such as bridges, the concept of capacity design forms the particular important basis for the earthquake resistant design of this type of structures. In capacity design, bridge structures are detailed to ensure that inelastic deformations occur only in properly designed and detailed ductile components, such as columns and piers, and nonductile components, such as joints and connections, are designed with sufficient strength to remain elastic during the dynamic response to avoid any damage or failure. In the design

codes of AASHTO, ATC and CALTRANS, columns and piers are designed with strengths lower than the expected forces obtained from an elastic analysis, so that plastic hinges will develop in these members when seismic forces exceed the design forces. Other structural members and components, such as connections, are designed for expected or greater than expected elastic forces resulting from a maximum credible earthquake. The design codes OHBDC and CSA do not contain any specifications concerning capacity design that would specify the plastic hinge locations which require particular attention to structural detailing in order to accommodate the expected large inelastic deformation at these locations.

3.3.2 Methods of Analysis for Design

The uniform load method is an equivalent static load method that is a simplified procedure to determine the effects of the seismic load on the structure. In the uniform load method, the bridge response is assumed to be dominated by the fundamental mode of vibration. Studies have shown that the uniform load method yields results with good accuracy for regular bridges. As it is easy to apply, the uniform load method is adopted in many design codes, such as the CALTRANS and the OHBDC codes.

Another similar method of analysis is the single mode spectrum method. The main difference between the uniform load method and the single mode spectrum method is in the distribution of the lateral seismic force. In the single mode spectrum method, the seismic force is applied at the center of the bridge structure. The next level of sophistication is the multi-mode spectral analysis method, which requires more effort to compute multiple vibration periods and mode shapes for more complex bridge structural

systems in their linear range of responses excited by the design earthquakes. The CHBDC (1996) permits using inelastic analysis for critical bridges, such as time-history or static push-over analysis, which gives more realistic results and economical bridge designs.

The CHBDC (1996) adopts similar design approaches as AASHTO (1993). In the 1996 CHBDC, the significant adverse influence of very soft soil on the amplification of earthquake ground motions is included. On seismic performance requirements, important bridges classified as *critical* are required under all circumstances to remain functional following a maximum credible earthquake to provide emergency services. This greatly limits the damage level to such important bridges. In terms of analysis requirements for critical bridges, the analysis procedure must be able to produce realistic predictions on the behaviour of the bridge during maximum credible events.

Recent research on seismic ground motions in Canada has found that the earthquakes in eastern and western Canada have different characteristics on the frequency content, which can significantly affect structural response (Heideberecht and Lu 1987, Naumoski et al. 1988 and Hosni and Heideberecht 1990). Although some of these research findings have been incorporated in the seismic design provisions of the National Building Code of Canada since the 1985 edition, it is unclear how the frequency content and other seismic design parameters affect the design of highway bridges. Particularly in the 1991 OHBDC, response coefficient curves are used to represent the reduction of the design force due to ductility in an implicit way.

Table 3.1 Summary of Load Determination Approaches

Step	Factor	CALTRANS 1990	AASHTO 1992 ATC 1981	OHBDC 1991	CSA - S6 1988	CHBDC 1996
1	Design input motion	Acceleration ratio (A)	Acceleration ratio (A)	Zonal velocity ratio (v)	Zonal velocity Ratio (v)	Zonal Acceleration Ratio A
2	Importance classification	Essential IC= I Other IC= II	Essential IC= I Other IC= II	Importance factor 1.0 or 1.3	Importance factor 1.0 or 1.3	Essential I Other II Critical III
3	Seismic performance categories or zones	Four categories: Category A, B, C and D	Four seismic categories: Category A, B, C and D	No	No	Four Seismic zones: Zone 1, 2, 3 and 4
4	Soil effects (S) or foundation factor (F)	Included in the design response spectra	S = 1.0 Soil profile I S = 1.3 Soil profile II S = 1.5 Soil profile III	Included in the design response spectra	F = 1.0 Soil profile I F = 1.3 Soil profile II F = 1.5 Soil profile III	S = 1.0 Soil profile I S = 1.3 Soil profile II S = 1.5 Soil profile III S = 2.0 Soil profile IV
5	Method of min. analysis requirements	Equivalent static analysis $T = 3.2\sqrt{W/P}$	Single-mode & multi-mode spectral methods	Equivalent static analysis $T = 3.2\sqrt{W/P}$		Uniform load Single-mode, Multi-mode Time-history Static push-over
6	Response coefficient	Provided by the design response spectra curves	$C_{sm} = \frac{1.2AS}{T_m^{2/3}}$	Provided by the design response spectra curves	C = 0.62 vF, (a > v) C = 0.42 vF, (a = v) C = 0.31 vF, (a < v)	$C_{sm} = \frac{1.2AS}{T_m^{2/3}}$
7	Force reduction factor (R)	Piers or Columns: 2 - 8 Connections: 0.8 - 1	Piers or Columns: 2 - 5 Connections: 0.8 - 1	Included in the design response spectra	Included in the design response spectra	Piers or Columns: 1.5 - 5 Connections: 0.8 - 1
8	Combination of direction of the action	100% (in one dir.) + 30% (in perp. dir.)	100% (in one dir.) + 30% (in perp. dir.)	No	No	100% (in one dir.) + 30% (in perp. dir.)

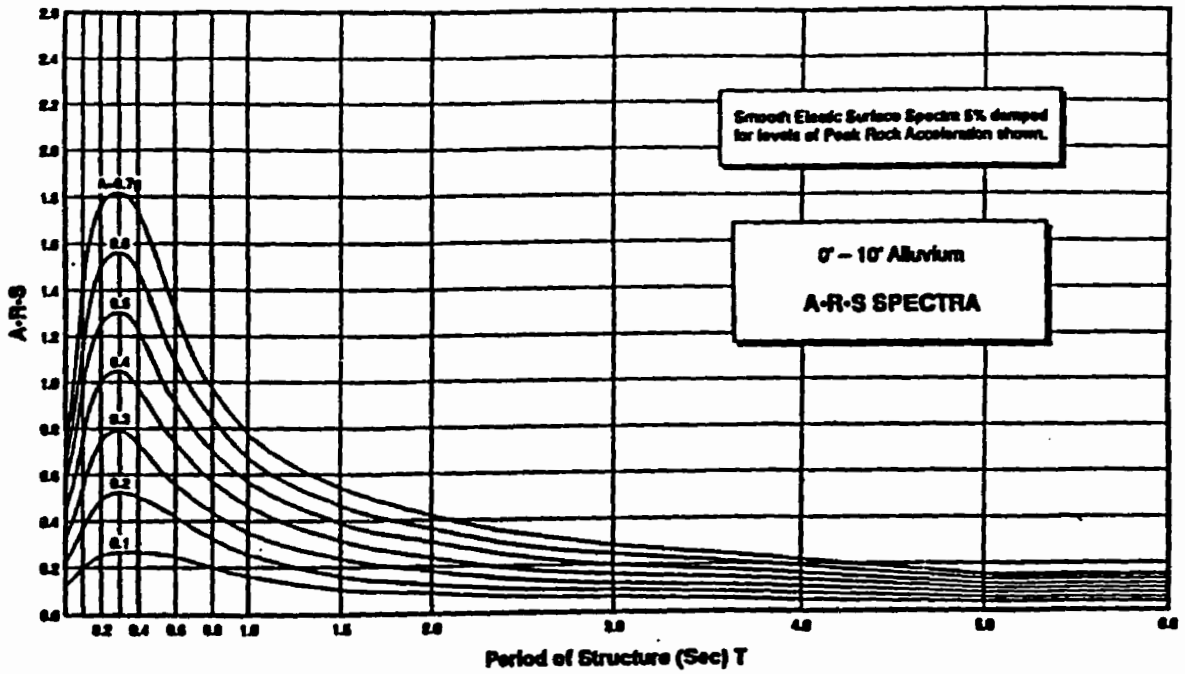

(a)

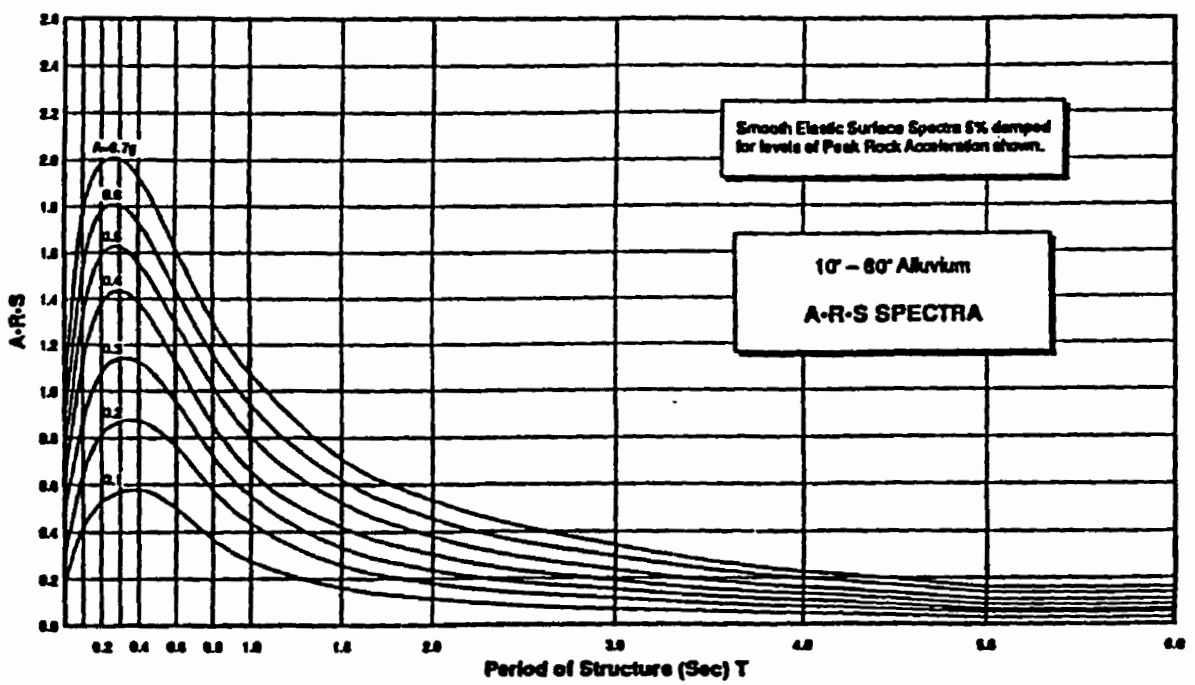

(b)

Figure 3.1 CALTRANS 1992 Design Spectra (c), (d)

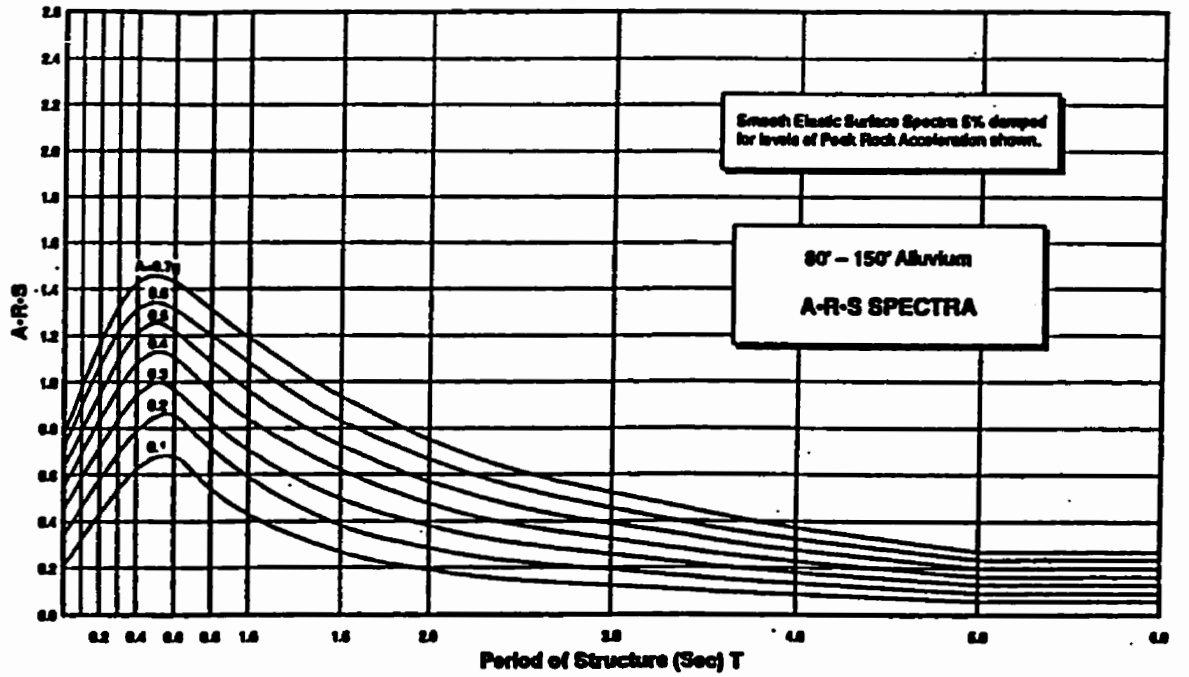

(c)

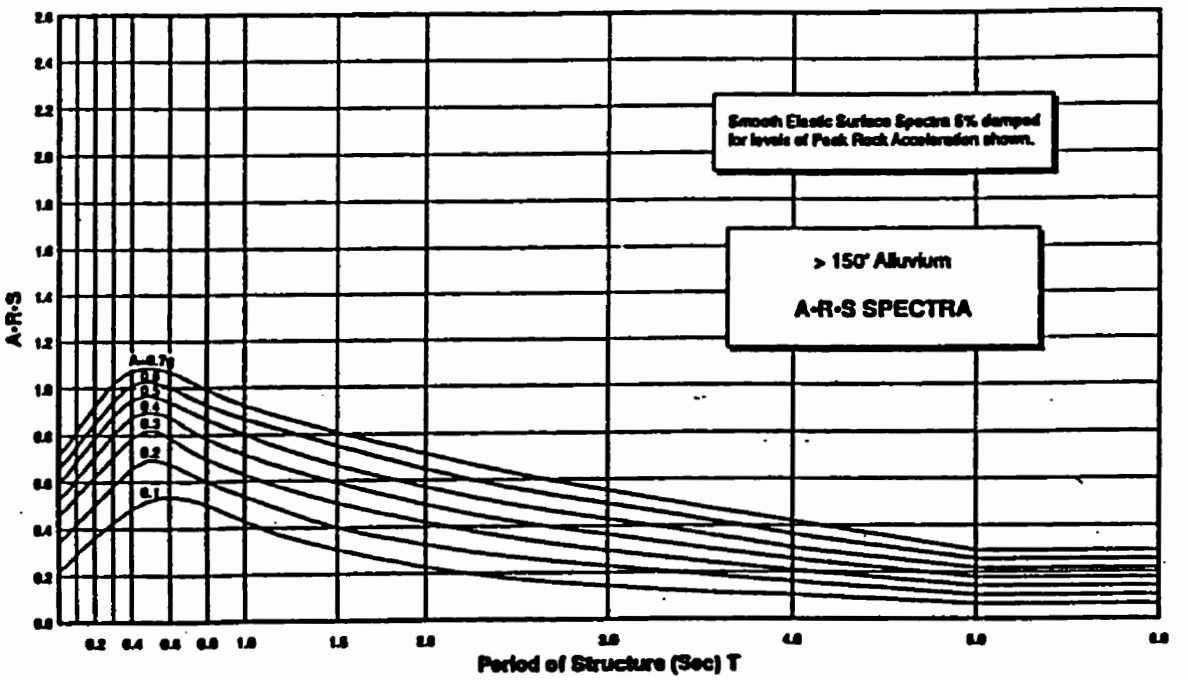

(d)

Figure 3.2 CALTRANS 1992 Design Spectra (a), (b)

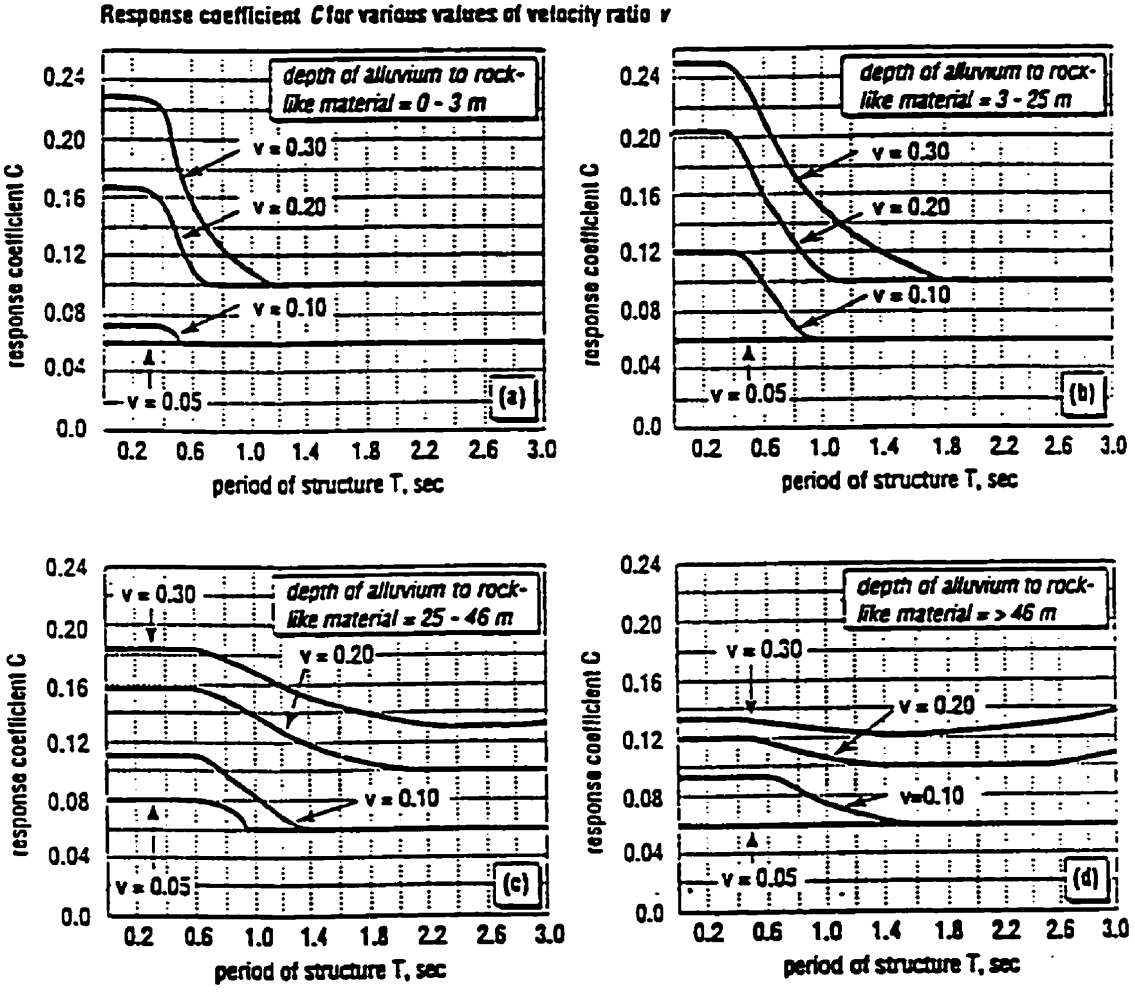

Figure 3.3 OHBDC 1991 Design Spectra

CHAPTER 4 COMPARATIVE STUDY OF DESIGN CODE PROVISIONS

4.1 Introduction

This chapter presents a comparative study of the adequacy of the design spectra adopted in typical bridge design codes and standards with the requirements from selected ground motion records. In particular, the effects of the ground motion characteristics as represented by the a/v ratios and underlying soil deposits are studied. In the present study, the effect of soil-structure interaction is not considered because bridge structures are usually not heavy in weight so that the soil-structure interaction effect can be ignored. Although the influence of the ductile response of the bridge structure is important in seismic performance, it is not covered here in this study as the focus is placed on the significance and influence of the soil amplification effects of different soil deposits. The linear elastic design spectra from AASHTO, ATC, CHBDC and CALTRANS are compared to the calculated ground surface response spectra. Since the design spectra in OHBDC and CSA already include the effect of structural ductility, it is noted here that the comparison may not be entirely consistent. However, since no clear engineering justification has been provided in OHBDC and CSA to support the above observation, a comparative study will be valuable to provide useful information.

The soil effects are evaluated for three different types of soil at three different depths. To compare the sensitivity of the structural response to different soil properties, one

linear soil model and two nonlinear soil models are considered. Three sets of ground motion records with high, intermediate and low a/v ratios are selected. The response spectra of bedrock ground motions are also studied, which are compared to the corresponding code design spectra for rock-like material.

The computer program FLUSH (Lysmer et al. 1975) is used to generate the response spectra for different soil models subjected to different earthquake motions.

4.2 Seismic Ground Motions

Information of seismicity in Canada is presented in the seismic zoning maps of the NBCC (1995), as shown in Figure 4.1. In the NBCC, two seismic zoning maps are given, one based on the peak horizontal acceleration parameter Z_a and the other based on the peak horizontal velocity parameter Z_v. The two seismic maps provide two independent ground motion reference levels with a probability of excedence of 10% in 50 years. The two seismic parameters Z_a and Z_v are used to better characterize the seismic hazard at a site due to the differences in the ground motion characteristics from nearby and distant earthquakes. Furthermore, it has been recognized that the ratio of the peak ground horizontal acceleration to peak ground horizontal velocity (*a/v*) is an important parameter to represent the characteristics of the ground motion expected at a particular site. Research has shown that the *a/v* ratio is a suitable parameter for quantifying the frequency content of the ground motions. A motion with significant high frequency content and a high *a/v* ratio is typically associated with a near source earthquake, whereas a motion more dominated by low frequency content and thus a low *a/v* ratio is often more associated with a distant source earthquake.

As examples of seismicity in major cities in Canada, locations with expected in the high, intermediate and low a/v ratio categories are, respectively, Ottawa, Vancouver and Prince Rupert. Table 4.1 shows the seismic parameters for the three cities. It is shown in Table 4.1 that Ottawa has a high a/v ratio (a/v = 2), which is representative of the seismicity in eastern Canada, whereas Vancouver has an intermediate a/v ratio (a/v =1) and Prince Rupert has a low a/v ratio (a/v =0.48), which are typical of the seismicity in western Canada.

For each a/v ratio, a set of 4 ground motion records are selected, as shown in Table 4.2. The acceleration time history of the ground motion records with high, intermediate and low a/v ratios are shown in Figures 4.2 to 4.4.

All the selected input ground motions are scaled to an intensity level of a peak ground horizontal acceleration (PHA) of 0.2 *g*. All the response spectrum analyses are based on the parameter of PHA.

4.3 Soil Models

In the study, three different depths of the soil profile are considered: 15 m, 25 m and 45 m. The ranges considered are related in reference to those used in OHBDC 1991, CHBDC 1995 and NBCC 1995. In OHBDC, the soil depths are categorized by the ranges of 0 to 3 m, 3 to 25 m, 25 to 45 m, and greater than 45 m. In CHBDC and NBCC, the depth of 15 m is the common dividing value used for all different soil types. Uniform soil deposit is assumed for each soil case. Soil stiffness is an important parameter that can significantly affect the level of shaking at the ground surface as the bedrock motions propagate upwards through the soil depth. The shear modulus value under low strain of

58 MPa, 120 MPa, and 168 MPa are chosen respectively as representative of soft, firm and stiff soils.

Since soils behave nonlinearly under large strain during strong shaking, soil properties vary during the vibration of strong shakings. The changes in the soil properties are related to the shear strain in different types of soils considered in the study. To compare the different nonlinearity behaviour of soils to ground motions, three different soil models are used in this analysis, which consists of one linear soil model and two nonlinear soil models. A damping ratio of 5% is assumed in the linear soil model. For the two nonlinear soil modes, the shear modulus and damping properties of the soil mass vary with the effective shear strain under the dynamic conditions. The relationship of the hysteretic damping ratio with the effective shear strain is plotted in Figure 4.5. The corresponding relationship for a shear modulus reduction factor with the effective shear strain is plotted in Figure 4.6. The nonlinear soil model 1 is determined based on data from Seed and Idriss (1977), and the nonlinear soil model 2 is the soil model used by Hosni and Heidebrecht (1994). It is observed from Figures 4.5 and 4.6, that the nonlinear soil model 1 has a softer behaviour than that of the nonlinear soil model 2 throughout the range of effective shear strain of interest in the present study. Since the dynamic properties of soils vary in a wide range, the two sets of data used in this study are representative of the behaviour limits for clay soils.

4.4 Site Dynamic Response

The site response to the input ground motions is computed using the computer program FLUSH developed by Lysmer et al. (1975). The program can perform dynamic

analysis in the frequency domain to obtain the response of the soil deposit to an input acceleration time history. The program solves the dynamic equations of motion by linear interpolation. It is applicable to analyze linear visco-elastic systems. To account for the non-linear behaviour of the soil layer, an equivalent linear analysis model and procedure have been adopted by continually updating the soil dynamic properties in the analysis process. The shear modulus and damping ratio of the soil deposit are updated to values compatible with the effective strain and vibration amplitude of the soil layer as the shaking progresses. Although the program is capable of taking into account the soil-structure interaction effect in two-dimensions, only free field ground motions on the ground surface are considered.

4.5 Comparison of Design Code Response Spectra

A dynamic response analysis is carried out for each specified soil deposit subjected to the selected ground motions. The parameters of variations considered are the soil type, soil depth and nonlinear soil behaviour. The results of the free field motions on the ground surface due to input motions at the bedrock are compared to the corresponding response spectra for the design earthquakes having 0.2 g peak horizontal acceleration. The results are also compared with linear elastic design spectra from AASHTO, ATC, CHBDC and CALTRANS. The load factors for the earthquake load effect as specified in the codes and discussed in Section 3.2.6 are considered. Since the earthquake load factor is equal 1.0 in all of the selected code specifications for comparison here, the comparison of the code design spectra and the response spectra of the selected ground motions is

consistent on the same basis. The analysis results indicate that the soil deposit can greatly modify the ground motions on the surface felt by the bridge superstructure.

4.5.1 Comparison of Response Spectra for Bedrock Ground Motions

Figures 4.7 to 4.9 show the results of the elastic response spectra of the three sets of input ground motions at base rock, which are compared to the code design spectra for a rock site. For ground motions with a high a/v ratio, as shown in Figure 4.7, the results show that the code design spectra are conservative for bridge structures having natural periods greater than 0.5 s. The CALTRANS design spectrum is unconservative for bridge structures with short periods (less than 0.5 s), which implies that for stiff bridge structures, such as wall type piers, the CALTRANS design code may underestimate the actual force from near field earthquakes. The design loads specified by AASHTO, ATC and CHBDC are generally considered to be adequate or conservative for bridge structures in a short period range less than 0.5 s.

For the set of input ground motions with an intermediate a/v ratio, as shown in Figure 4.8, the results show that the code design spectra are comparable with those of the selected ground motions, except in the period range of 0.2 to 1.0 s. A large structural response is observed near the resonant period of 0.25 s, which implies that bridge structures having fundamental periods in this range can be vulnerable to earthquakes of intermediate distance from the source field.

For the set of input ground motions with a low a/v ratio, as shown in Figure 4.9, it has been observed that the response to the Long Beach ground motion record is significantly different from that of the other three records. It appears that the bridge response is

sensitive to some detailed characteristics of the input ground motions and the effect can sometimes be very significant. In general, the results in Figure 4.9 show that the code design spectra are comparable with those of the selected ground motions, except in the short period range between 0.25 to 0.5 s, periods greater than 2.5 s, and all of the Long Beach ground motion record. A large structural response is observed near the resonant period of 0.3 s.

The results clearly show that the response of the bridge structure is very sensitive to the frequency content of the input ground motions.

4.5.2 Comparison of Response Spectra for Soil Depth of 15 M

Figures 4.10 to 4.36 show the comparison of the elastic response spectra for the soil depth of 15 m. Three different soil types of soft, firm, and stiff soils are considered. Each is subjected to the selected three input ground motions. For each specified soil deposit and input ground motion, the nonlinear soil behaviour is investigated by comparing the response of the two different soil models to that of the linear soil model.

4.5.2.1 Comparison of Soft Soils

The comparison of the elastic response spectra for soft soils with a depth of 15 m are shown in Figures 4.10 to 4.18.

For the linear soil model, as shown in Figures 4.10, 4.13 and 4.16, to input motions of different a/v ratios, similar trends are observed in their response spectra. Very significant responses are observed at periods near 0.3 s in all the cases.

Figures 4.10 to 4.12 show the response spectra of soft soils with a 15 m depth to a set of high a/v input ground motions. The nonlinear soil behaviour is investigated. For the linear soil model, as shown in Figure 4.10, the results show that the responses of bridge structures are amplified significantly within the short period range between 0.1 to 0.5 s. The peak response at the resonant period is about 5 times higher than that specified in the codes. In Figure 4.11, it can be observed that the nonlinear soil model 1 damps out the high frequency structural response and the peak response value is reduced by approximately 70%. The CALTRANS design spectrum is conservative and it represents the envelope of the dynamic response for the selected high a/v input ground motions. The design loads specified by AASHTO, ATC and CHBDC are generally conservative for bridge structures having periods greater than 0.75 s, but it may be unconservative for the period range from 0.1 to 0.6 s. For the nonlinear soil model 2, as shown in Figure 4.12, the results show that design loads specified by the codes are unconservative at the period range less than 0.7 s.

Very high structural response is closely observed near the resonant period of 0.5 s because the natural frequency of the structure matches with the predominant frequency of the site. The structural response is highly amplified near that resonant period, so that bridge structures with vibration periods in this range are particularly vulnerable. Such type of behaviour was experienced during the 1985 Mexico earthquake where severe structural damages were observed due to soil-structure resonance.

By comparing the results obtained from the two nonlinear soil models, it can be found that the code design spectra are closer to what have been observed in the nonlinear soil

model 1 than in the nonlinear soil model 2. The results also show that the responses of soil are very sensitive to the soil dynamic properties. The amplification potential of nonlinear soil model 2 is more severe than that of nonlinear soil model 1 when subjected to high a/v ratio earthquakes.

Figures 4.13 to 4.15 show the response spectra of soft soils of 15 m depth to intermediate a/v input ground motions. The influence of the soil dynamic property is investigated. Similar trends of behaviour in Figure 4.10 are observed for the linear soil model, as shown in Figure 4.13. Very high responses are observed near the resonant period of 0.3 s. The linear soil model is used for the purpose of comparing the two nonlinear soil models. In Figure 4.14, it can be observed again that the nonlinear soil model 1 damps out the high frequency structural response so that the peak response value is reduced by approximately 70%. It is observed that there are more than one period ranges between 0.2 to 1.5 s for which the spectra are significantly higher than other periods. The CALTRANS design spectrum is conservative at periods less than 0.8 s but unconservative for periods greater than 0.8 s. The design standards AASHTO, ATC and CHBDC are unconservative for period ranges near 0.3 s and between 1.0 to 1.5 s where maximum responses occur. They are conservative for long periods greater than 2 s. For the nonlinear soil model 2, as shown in Figure 4.15, soil-structure resonance is observed near the period of 0.5 s.

Figures 4.16 to 4.18 show the comparison of the response spectra of soft soil with 15 m depth to a set of low a/v input ground motions. The influence of the soil dynamic property is similar to that observed for intermediate a/v input ground motions, with the

exception of the behaviour of the nonlinear soil model 2. As shown in Figure 4.18, there are more than one period ranges between 0.2 to 1.5 s for which the spectra are significantly greater than that of other period ranges. It should be mentioned that the spectrum of the Long Beach ground motion record at long periods behaves differently compared to the other three records. The results show that the code design spectra are unconservative especially at the middle period range where maximum responses are observed.

The effect of input ground motions having different a/v ratios can be observed by comparing the results shown in Figures 4.10 to 4.18 for high a/v ground motions. The maximum spectral response is significantly reduced in the short period range, whereas for intermediate and low a/v ratios the responses may be significantly amplified at the period range of 1.0 to 1.5 s. This implies that long span bridges having long fundamental periods are particularly vulnerable to earthquakes with intermediate and low a/v ratios.

4.5.2.2 Comparison of Firm Soils

Similar comparison of the behaviour of firm soils of 15 m depth to different ground motions are shown in Figures 4.19 to 4.27.

For the linear soil model, as shown in Figures 4.19, 4.22 and 4.25, to input motions of different a/v ratios, similar trends are observed in the response spectra as in the case of soft soil.

The response spectra of the two nonlinear soil models subjected to high a/v ratio ground motions, as shown in Figures 4.20 and 4.21, are similar. Soil-structure resonance is observed at periods near 0.5 s, but the peak value is about 50 - 60% less than that of the

linear model. In Figure 4.20, the CALTRANS design spectrum is comparable with the obtained spectra except at the resonant periods between 0.4 to 0.6 s. The design spectra of AASHTO, ATC and CHBDC are unconservative for periods less than 0.7 s. In Figure 4.21, it is observed that the code design spectra are unconservative for the period range between 0.1 to 0.6 s.

However, there is a significant difference in the response spectra obtained from the two nonlinear soil models subjected to intermediate to low a/v ratio ground motions, as shown in Figures 4.23, 4.24, 4.26, and 4.27. Soil-structure resonance is observed at periods near 0.3 s in the nonlinear soil model 2, as shown in Figures 4.22 and 4.25, but it is not the case for the nonlinear soil model 1. For the nonlinear soil model 1, significant high spectral responses occur in the middle range of periods between 0.5 to 1.3 s. The CALTRANS design spectrum is unconservative at periods greater than 0.5 s, whereas AASHTO, ATC and CHBDC are unconservative at periods between 0.2 - 1.5 s but comparable for long periods greater than 1.5 s.

4.5.2.3 Comparison of Stiff Soils

The comparison of stiff soils with a depth of 15 m are shown in Figures 4.28 to 4.36. In the linear soil model, similar results are observed to those of firm soils, as shown in Figures 4.28, 4.31 and 4.34.

The nature of spectra of two nonlinear soil models to high a/v ratio ground motions, as shown in Figures 4.29 and 4.30, is similar. A soil-structure resonance is observed at periods near 0.4 s for the nonlinear soil model 1, and 0.25 s for the nonlinear soil model 2. The peak values are reduced by 50 - 60% as compared to that of the linear model. In

Figure 4.29, the CALTRANS design spectrum is generally comparable except at near the resonant periods between 0.25 to 0.5 s. AASHTO, ATC and CHBDC are unconservative at periods less than 0.7 s where the maximum response occurred. In Figure 4.30, it is observed that the code design spectra are unconservative at the period range less than 0.6 s.

There are some similarities in the response spectra of the two nonlinear soil models subjected to intermediate to low a/v ratio ground motions, as shown in Figures 4.32, 4.33, 4.35, and 4.36. Resonant behaviour is observed in all cases. The resonant period is shifted to a longer period at 0.6 s for the nonlinear soil model 1 as compared to that for the nonlinear soil model 2 which is in the range of 0.15 to 2.5 s. The behaviour of lower spectral values over a wider period range is observed for the nonlinear soil model 1 as compared to that observed for the nonlinear soil model 2. This is because soils in model 1 are softer than those of model 2. The CALTRANS design spectrum is unconservative for the specified soil condition, as can be observed in Figure 4.32 in the period range between 0.4 to 1.2 s, whereas AASHTO, ATC-6 and CHBDC are unconservative at periods between 0.2 - 1.5 s but comparable for long period ranges greater than 1.5 s. Similarly, code design spectra are found to be unconservative within certain period ranges for other cases, as it can be observed in Figures 4.33, 4.35, and 4.36.

4.5.2.4 Discussions

The response of different soil types having a depth of 15 m to different sets of ground motions is found to be sensitive to their dynamic properties and input motions. The observations can be summarized as follows:

1. For the linear soil model, there is no significant difference found in calculated response spectra for all cases.

2. Nonlinear soil models reduce the peak response significantly as compared to that of the linear model.

3. Design loads specified by the codes are found to be unconservative in some period ranges, with the exception of the one shown in Figure 4.11 in a short period range of less than 0.7 s for high a/v ratio earthquakes, and in short to moderate period ranges between 0.2-2.0 s for intermediate to low a/v ratio earthquakes.

4. A lower peak spectral value and wider period range that has high spectral response are found in the cases of softer soils and lower a/v ratio earthquakes. A higher peak spectral value and narrower period range that has high response are found in the cases of stiffer soils and higher a/v ratio earthquakes.

5. Surface motions are amplified more in the short period range in the cases of high a/v ratio input motions, and in short to moderate period ranges for intermediate and low a/v ratio earthquakes. The low a/v ratio earthquakes also cause higher response at long periods than that of high a/v ratio.

6. Nonlinear soil model 1 usually leads to lower responses in short to moderate period ranges less than 1.5 s than those of nonlinear soil model 2.

4.5.3 Comparison of Response Spectra for Soil Depth of 25 m

Figures 4.37 to 4.63 show the comparison of the elastic response spectra for the soil depth of 25 m. For each specified soil deposit and input ground motion, the nonlinear soil

behaviour is investigated by comparing the response of the two different soil models to that of the linear soil model.

4.5.3.1 Comparison of Soft Soils

Similar comparison of soft soils with a depth of 25 m are shown in Figures 4.37 to 4.45. Less significant spectral response is observed in the soil depth of 25 m than the previous case of the 15 m soil depth.

For the linear soil model, as shown in Figures 4.37, 4.40 and 4.43, to different sets of a/v ratio input motions, the results show that resonant behaviour is shifted to a longer period near 0.5 s as compared to the case with the depth of 15 m. The results also show that for the specified soil type, the influence of input ground motions is significant as it can be observed from the shape of the response spectra.

For the nonlinear soil model 1, as shown in Figure 4.38, it can be observed that the code design spectra are conservative. Especially, the design load specified by CALTRANS is conservative for bridge structures having periods less than 1.0 s. For the nonlinear soil model 2, as shown in Figure 4.39, the CALTRANS design spectrum is comparable to the observed behaviour of the specified soil. The design loads specified by AASHTO, ATC-6 and CHBDC are generally over conservative for bridge structures having periods greater than 0.75 s, but unconservative for shorter periods. By comparing the results from the two nonlinear soil models, it can be found that the CALTRANS design spectra satisfy the design load requirements for bridge structures constructed on soil described by the two soil models and subjected to high a/v ratio earthquakes.

For the nonlinear soil models subjected to intermediate to low a/v ratio ground motions, as shown in Figure 4.41, 4.42, 4.44 and 4.45, it can be observed that the significant high spectral response occurs in short to long period ranges. The CALTRANS design spectrum is conservative for bridge structures having periods less than 1.0 s and unconservative at periods greater than 1.0 s. The design loads specified by AASHTO, ATC-6 and CHBDC are conservative (nonlinear soil model 1 and intermediate a/v ratio earthquakes) at the period range less than 0.6 s, but unconservative for greater than that period. In the case of low a/v ratio earthquakes, however, it is over conservative at periods less than 1.5 s, and unconservative for the periods of greater than 1.5 s. The results imply that the design loads specified in the codes are unconservative for structures having a long fundamental period. Especially for low a/v ratio earthquakes, the specified soil deposit can amplify ground motions significantly in the long period ranges.

4.5.3.2 Comparison of Firm Soils

Figures 4.46 to 4.54 show results of firm soils with a depth of 25 m to different sets of ground motions. Similar observations can be made in the nature of the shapes of response spectra as those of the 15 m depth with the same soil type. Generally, less significant structural response is found in this soil depth.

For the linear soil model, as shown in Figures 4.46, 4.49 and 4.52, it is found that the expected resonance period is shifted from ranges near 0.25 s to 0.4 s.

For the high a/v input ground motion case, the period range where high spectra occurred is generally found to be lower than 1.0 s. As can be observed in Figure 4.47, for the nonlinear soil model 1, the CALTRANS design spectrum is conservative. For the

nonlinear soil model 2, as shown in Figure 4.48, the period range when the design load is unconservative is between 0.1 to 0.7 s. The design loads specified by AASHTO, ATC-6 and CHBDC are conservative for bridge structures having periods greater than 0.8 s, but unconservative for the period range between 0.15 to 0.8 s. By comparing the results from the two nonlinear soil models, it is be found that the CALTRANS design spectrum is safe for the soil type of nonlinear model 1 when subjected to high a/v ratio earthquakes.

There is a significant difference in the spectral response of the two nonlinear soil models when subjected to intermediate to low a/v ratio ground motions, as shown in Figures 4.50, 4.51, 4.53, and 4.54. Soil-structure resonance is observed at periods near 0.6 s of the nonlinear soil model 2, as shown in Figures 4.51 and 4.54, but not in the case of the nonlinear soil model 1. For the nonlinear soil model 1, significant high spectral response occurs in the middle period range between 0.2 to 2.0 s, with the expectation of the case of the Long Beach record at periods greater than 1.5 s. The CALTRANS design spectrum is unconservative for periods greater than 0.9 s for the nonlinear soil model 1, and greater than 0.4 s for the nonlinear soil model 2. AASHTO, ATC-6 and CHBDC are unconservative at the middle period range between 0.3 to 1.5 s, and comparable to the results for long periods greater than 1.5 s.

4.5.3.3 Comparison of Stiff Soils

For the stiff soil type with a depth of 25 m, the results are shown in Figures 4.55 to 4.63.

General similar observations in the shapes of calculated spectra are found in stiff soils with a depth of 15 m. Slight differences in the peak values of responses are found. The

period ranges, where the high spectral response occurs, fall in short periods (0.7 s) for soils subjected the high a/v ratio earthquakes and the nonlinear soil model 1 subjected to other sets of earthquakes. And these periods fall in the short to middle period ranges for the nonlinear soil model 2 to sets of earthquakes with intermediate to low a/v ratios. Design loads specified by the codes are found to be unconservative within these period ranges.

4.5.3.4 Discussion

The responses of the studied soil types of depth 25 m are observed to be sensitive to their dynamic properties and input motions, which are similar to the behaviour observed in previous cases of shallower soil depth. The differences in the response of the two soil depths are summarized as follows:

1. There are differences observed in calculated response spectra. Resonance behaviour occurs at more than one period range of softer soils.

2. Code design spectra are found to be conservative for a few types of soils subjected to high a/v ratio earthquakes, but they are unconservative for most types of soils at certain period ranges.

4.5.4 Comparison of Response Spectra for Soil Depth of 45 m

Results form the soil depth of 45 m are shown in Figures 4.64 to 4.90. The same study case as the previous analysis is applied to this soil depth. Generally lower spectral responses are observed compared to the other two soil depths.

4.5.4.1 Comparison of Soft Soils

The comparison of soft soils with a depth of 45 m to different sets of ground motions are shown in Figures 4.64 to 4.72. Less significant spectral response is observed in the soil depth of 45 m than that of 25 m.

To compare the linear soil model to different sets of input motions, as shown in Figures 4.64, 4.67 and 4.70, the results show a lower response at short periods less than 0.5 s and a higher response at moderate periods near 1.5 s compared to that of the same soil with less depth.

For the nonlinear soil model 1, as shown in Figures 4.65, 4.68 and 4.70, it can be observed that the code design spectra are over conservative, except the one in Figure 4.70 (low a/v), which is unconservative at a period range greater than 3.0 s. For the nonlinear soil model 2, as shown in Figures 4.66, 4.69 and 4.71, the CALTRANS design spectrum is comparable to this specified soil, except at middle periods between 1.0 to 2.0 s for intermediate to low a/v ratio earthquakes. The design loads specified by AASHTO, ATC-6 and CHBDC are unconservative for bridge structures having periods less than 2.5 s, as shown in Figure 4.69. But it is comparable except at middle periods between 1.0 to 2.0 s, as shown in Figure 4.71.

The results imply that the design loads specified in the codes are conservative or comparable with few exceptions for soft soils at the depth of 45m.

4.5.4.2 Comparison of Firm Soils

The response spectra of the firm soil with a depth of 45 m to different sets of ground motions are shown in Figures 4.73 to 4.81. Less significant spectral responses are observed in the soil depth of 45 m than both in 15 and 25 m.

Figures 4.73, 4.76 and 4.79 show calculated spectrum curves for the linear soil model to different sets of a/v ratio input motions. Similar shapes of response spectra are found in this type of soil, where the peak spectral response occurs at the period near 0.7 s. A lower peak response is observed in Figure 4.73 than in Figures 4.76 and 4.79, which is not the case for firm soils with shallower soil depths. The results imply that for this specified soil type, the variations of soil deposit depths and input ground motions are significant when the linear soil model is assumed.

The significant difference in spectra of the two nonlinear soil models subjected to different sets of ground motions is shown in Figures 4.74, 4.75, 4.77, 4.78, 4.80 and 4.81. A soil-structure resonance is observed at short to moderate period ranges, as shown in Figures 4.75, 4.78 and 4.81, but it is not the case for the nonlinear soil model 1. For the nonlinear soil model 1, the period ranges, where significant high spectra occur, are shifted from short periods to short and moderate periods, and from moderate to long periods corresponding to the input ground motions of high, intermediate and low a/v ratios, as shown in Figures 4.74, 4.77 and 4.80. For the nonlinear soil model 1, the CALTRANS design spectrum is fairly conservative with the exception of the Long Beach record. And AASHTO, ATC-6 and CHBDC are comparable at the period range near 0.3 s, as shown in Figure 4.74, and between 1.5 to 3.0 s, as shown in Figure 4.77.

4.5.4.3 Comparison of Stiff Soils

The stiff soils with a depth of 45 m to different sets of ground motions are shown in Figures 4.82 to 4.90. Similarly, less significant spectral responses are observed in the soil depth of 45 m.

For nonlinear soil models, the shape of the response spectrum is quite different. In Figure 4.83, moderate spectral responses are observed within periods 1.5 s. The CALTRANS design spectrum is over conservative and AASHTO, ATC-6 and CHBDC are comparable.

In Figure 4.84, high spectral responses are observed within periods 1.0 s. The CALTRANS design spectrum is comparable at periods within 0.9 s, except at periods near 0.25 s, and over conservative at periods of greater than 0.9 s. AASHTO, ATC-6 and CHBDC are unconservative for structures having natural periods less than 0.9 s and conservative for that period and greater.

In Figure 4.86, high spectral responses are observed in the period range between 0.2 to 2.2 s. The CALTRANS design spectrum is conservative except at periods between 1.5 to 2.5 s and AASHTO, ATC-6 and CHBDC are unconservative except at periods less than 0.3 s and greater than 3.0 s.

In Figure 4.87, peak spectral responses are observed at periods near 0.3 and 1.0 s. The code design spectra are unconservative for structures having natural periods less than 1.5 s and conservative for the range greater than that period.

In Figure 4.89, moderate spectral responses are observed over all the periods. The shape of the response spectrum of the Long Beach record is different from the other

records, since it has a much high response at periods greater than 2.0 s. The CALTRANS design spectrum is over conservative within the period of 1.3 s and comparable at periods of greater than that period, except the Long Beach record. AASHTO, ATC-6 and CHBDC are unconservative except for structures having natural periods less than 0.5 s.

In Figure 4.90, high spectral responses are observed within periods 1.5 s. The code design spectra seem to be unconservative.

The results imply that lower spectral responses generally occur in the case of a deeper soil depth subjected to the high a/v ratio earthquakes compared to those of shallower soil depths. For soils subjected to intermediate to low a/v ratio earthquakes, the higher response can be found in wider period ranges.

4.5.4.4 Discussions

The responses of soil types with a depth of 45 m appear to behave softer compared to the other two shallower soil depths. This may be reasonable because a deeper soil deposit dissipates more seismic energy.

1. Design loads specified by the codes are found to be conservative or comparable for the nonlinear soil model 1 with a depth of 45 m as compared to the other two soil depths.

2. The spectra with lower peak spectral values are observed in the cases of softer soils to lower a/v ratio earthquakes.

4.5.5 Conclusions

The dynamic response analyses for different soil deposits and input ground motions were performed. The parameters considered are the soil type, soil depth and nonlinearity

of soil behaviour and input ground motion characteristics. The general conclusions are summarized as follows:

1. The responses of soil deposits are very sensitive to the properties of the soil and characteristics of the input ground motions, especially for softer soils. The shapes of the spectral response can vary significantly.

2. Nonlinear soil models generally reduce the peak response significantly as compared to the linear model. The peak responses calculated using nonlinear soil model 1 are found to be lower than those from the nonlinear soil model 2.

3. For high a/v ratio earthquakes, high spectral response generally occurs within short periods. For the cases of intermediate a/v ratios, similar behaviour occurs in short to moderate period ranges and moderate to long period ranges for low a/v ratio earthquakes.

4. For the same soil type, the case of a shallower soil depth causes a higher response and a deeper soil depth leads to a lower response.

5. Design loads specified in the codes are found to be unconservative for some period ranges. The CALTRANS design load is more comparable to the calculated spectra using nonlinear soil model 1 than the other codes.

Table 4.1 Seismic Parameters for the Three Cities

City	Z_a	Z_v	a	v
Ottawa	4	2	0.20	0.10
Vancouver	4	4	0.21	0.21
Prince Rupert	3	5	0.13	0.27

Table 4.2 Selected Ground Motion Records

a/v	Event Name	Year	a_{max} (m/s^2)	v_{max} (m/s)	a/v	Soil condition
High	Parkfield	1966	0.434	0.255	1.7	Rock
	Montana	1935	0.146	0.072	2.03	Rock
	Nahanni	1985	1.101	0.462	2.38	Rock
	Seguenay	1988	0.107	0.016	7.09	Rock
Intermediate	El Centro	1940	0.345	0.334	1.04	Stiff soil
	San Fernando 1	1971	0.15	0.19	1.01	Rock
	San Fernando 2	1971	0.18	0.205	0.88	Rock
	Kern County	1952	0.179	0.177	1.1	Rock
Low	Long Beach	1933	0.097	0.236	0.41	Rock
	El Centro	1934	0.16	0.209	0.77	Rock
	San Fernando 3	1971	0.129	0.186	0.69	Stiff soil
	San Fernando 4	1971	0.106	0.17	0.62	Stiff soil

(a) Contours of peak horizontal ground velocities, in unit of m/s, having a probability of exceedance of 10% in 50 years

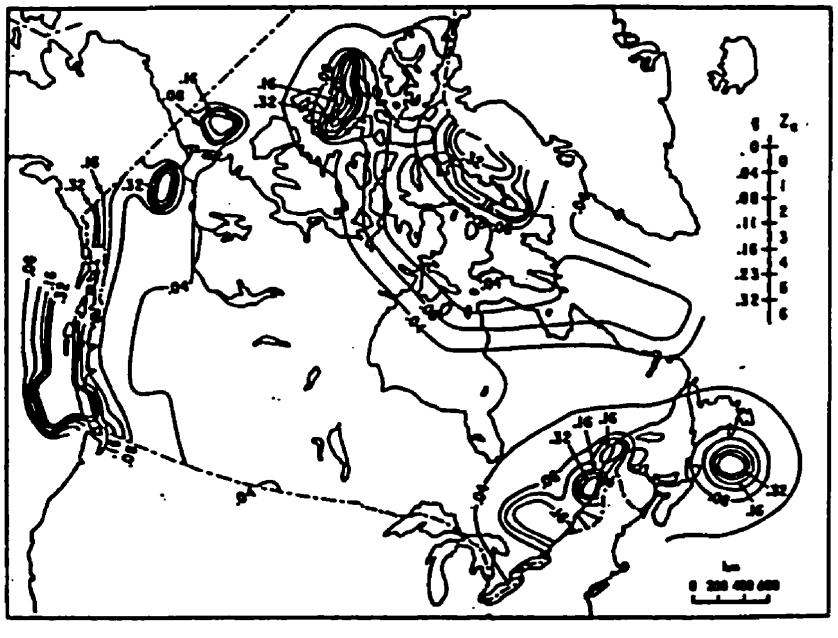

(b) Contours of peak horizontal ground accelerations, in unit of g, having a probability of exceedance of 10% in 50 years

Figure 4.1 Seismic Zoning Maps in NBCC (1995)

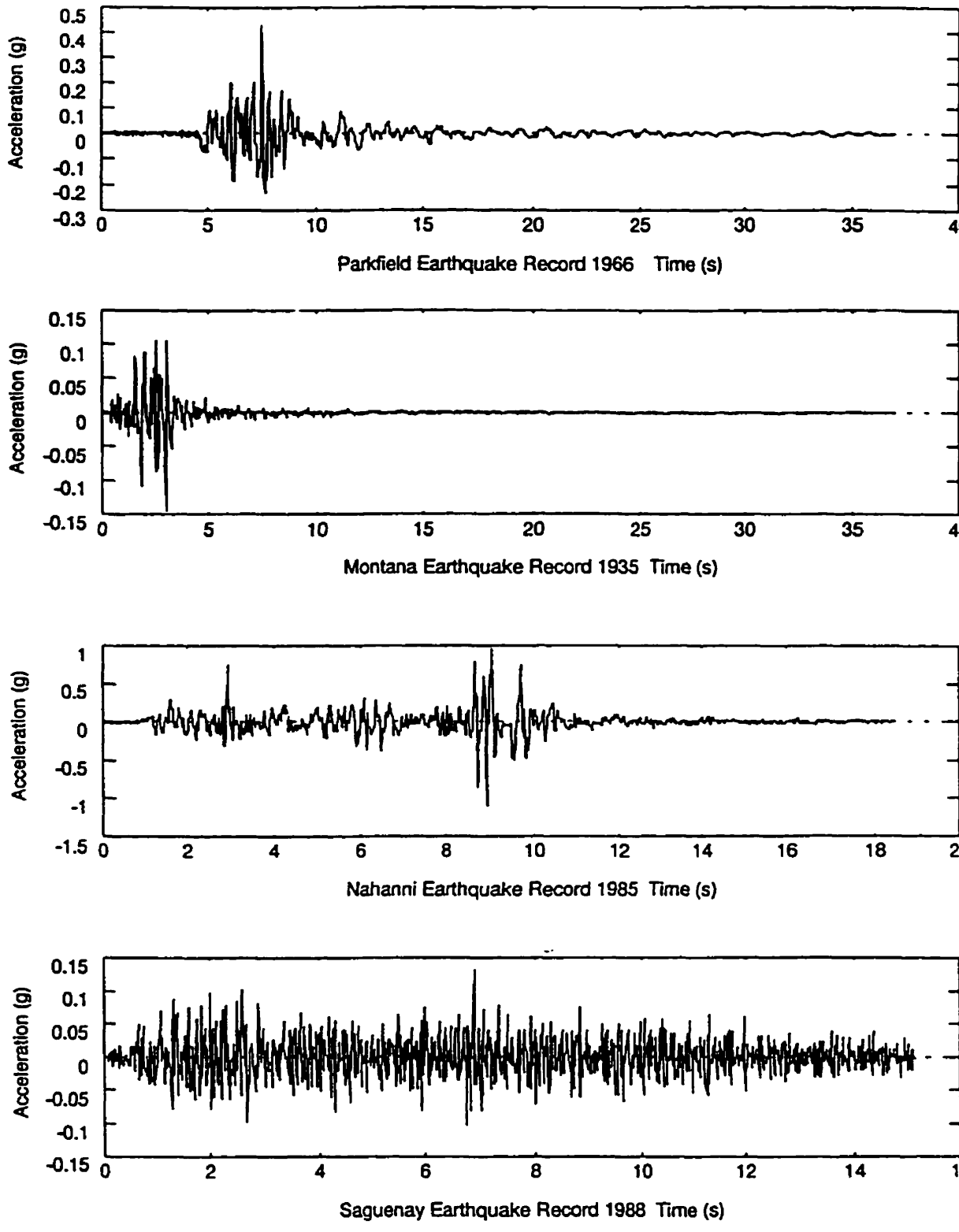

Figure 4.2 Time History of Selected Ground Motion Records with High a/v Ratios

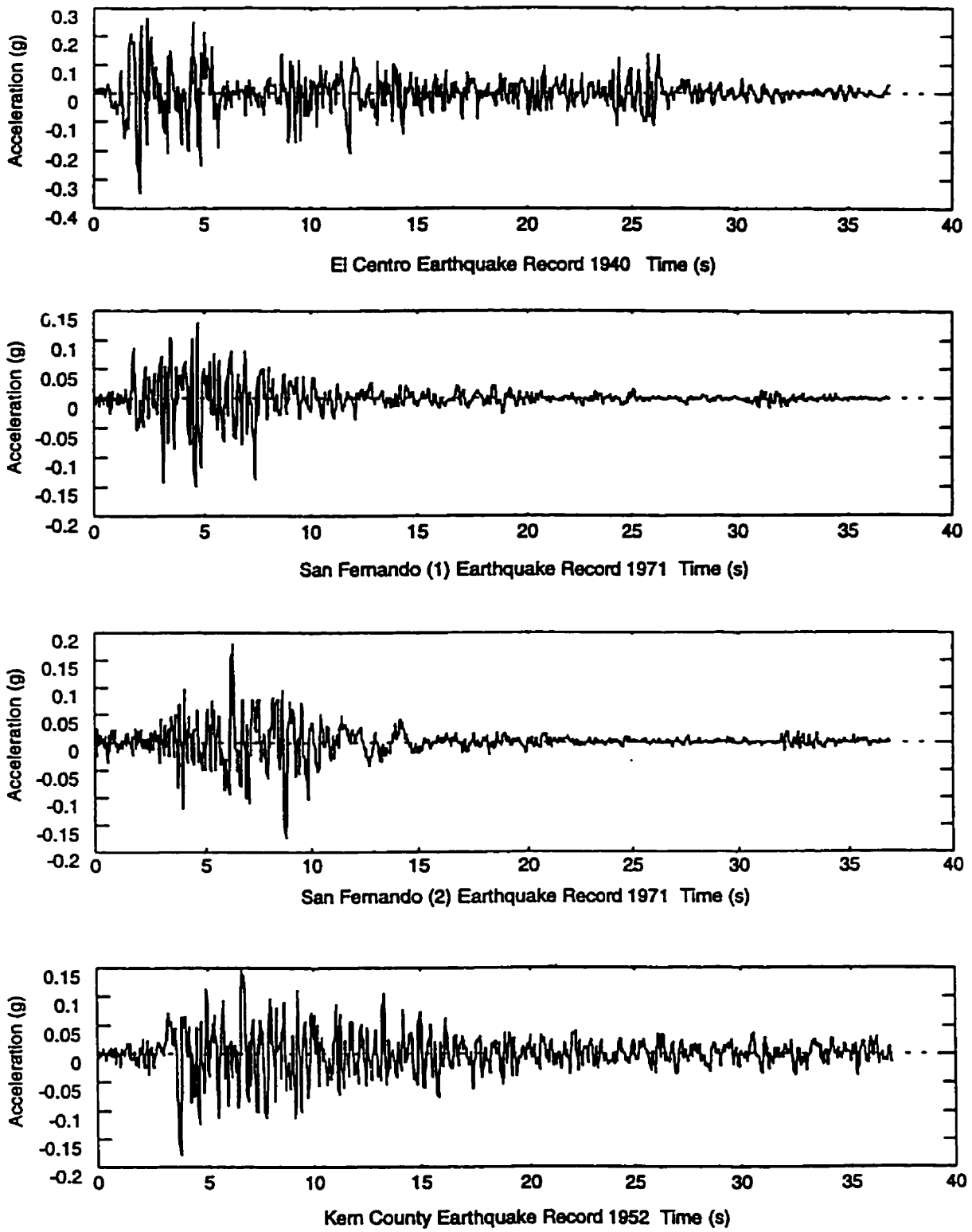

Figure 4.3 Time History of Selected Ground Motion Records with Intermediate a/v Ratios

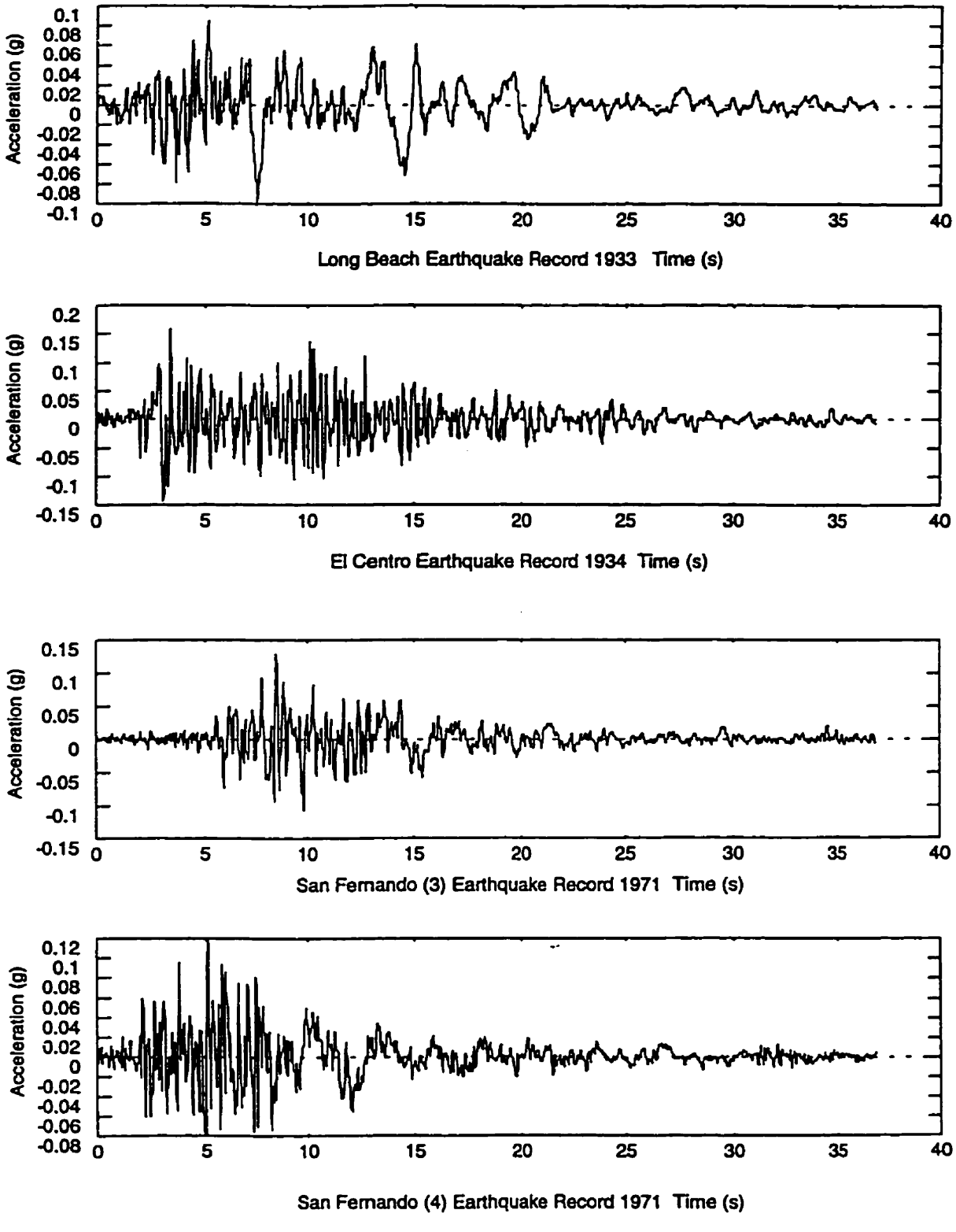

Figure 4.4 Time History of Selected Ground Motion Records with Low a/v Ratios

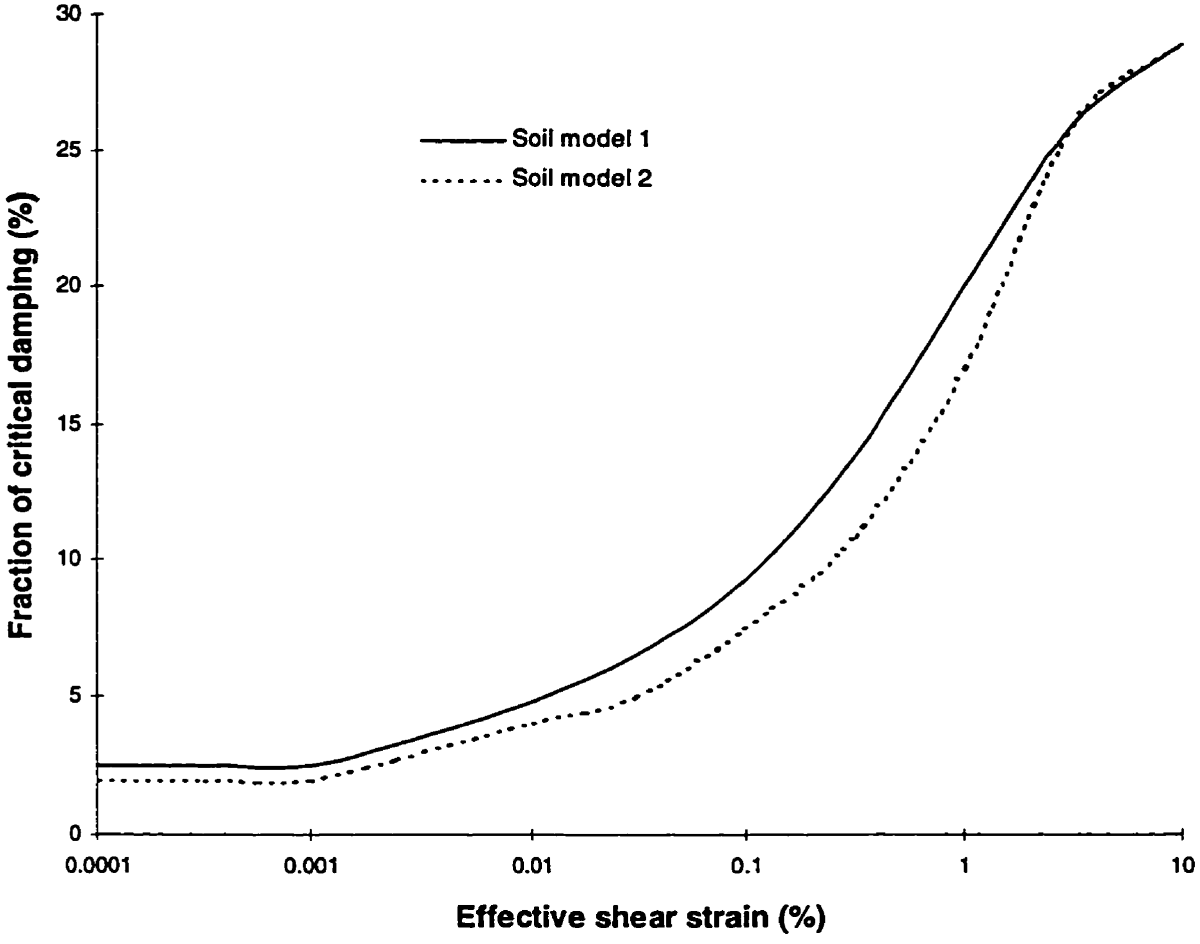

Figure 4.5 Hysteretic Damping Ratio Versus the Effective Shear Strain

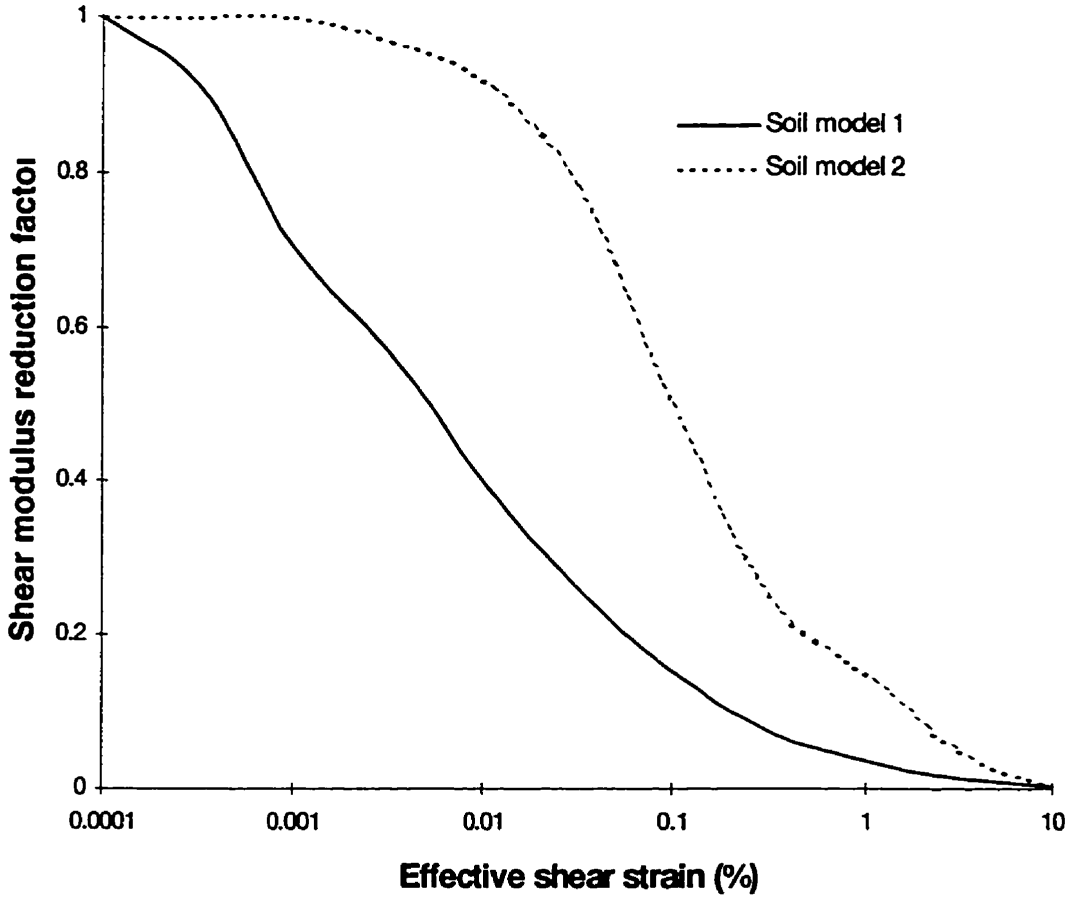

Figure 4.6 Shear modulus Reduction Factor Versus the Effective Shear Strain

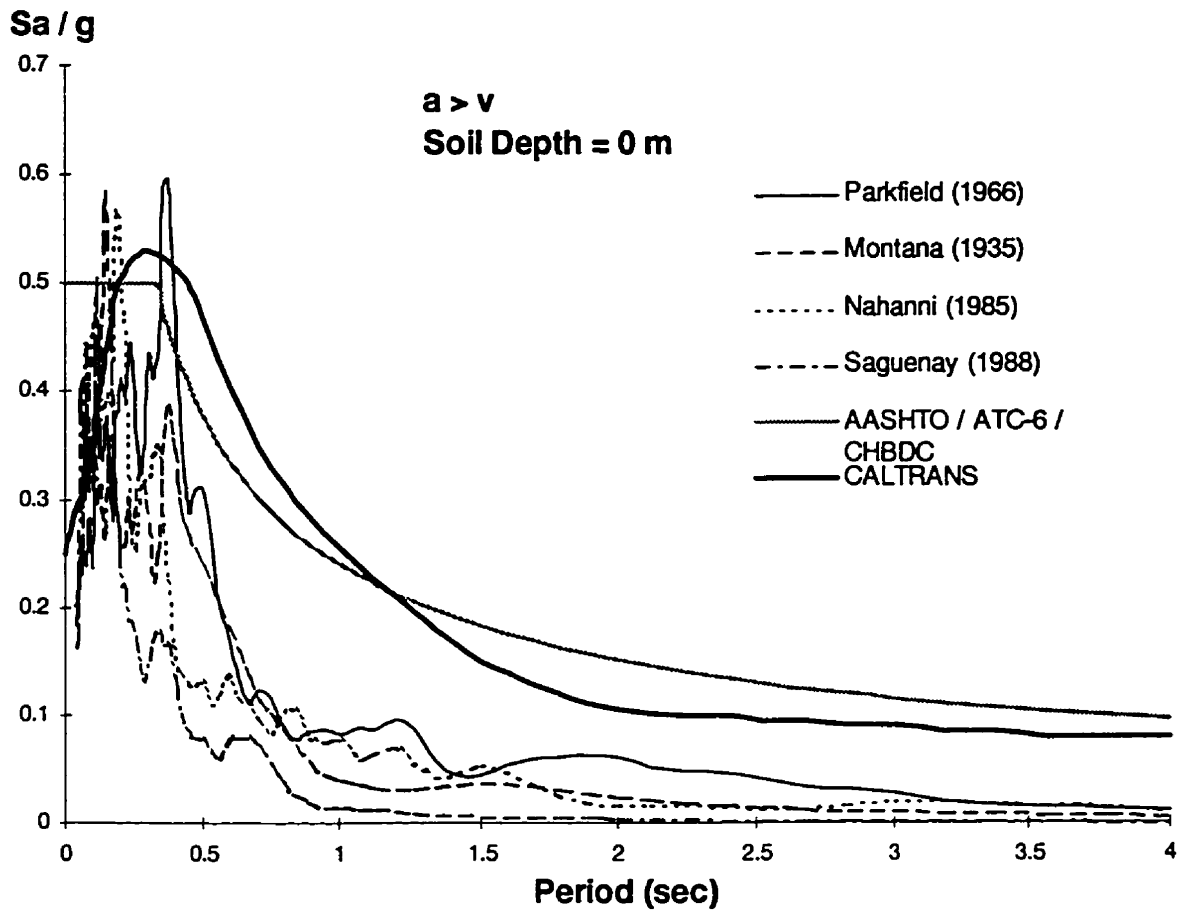

Figure 4.7 Comparison Of Response Spectra For High a/v Earthquakes At The Bedrock To Code Design Response Spectra With 0m Soil Depth

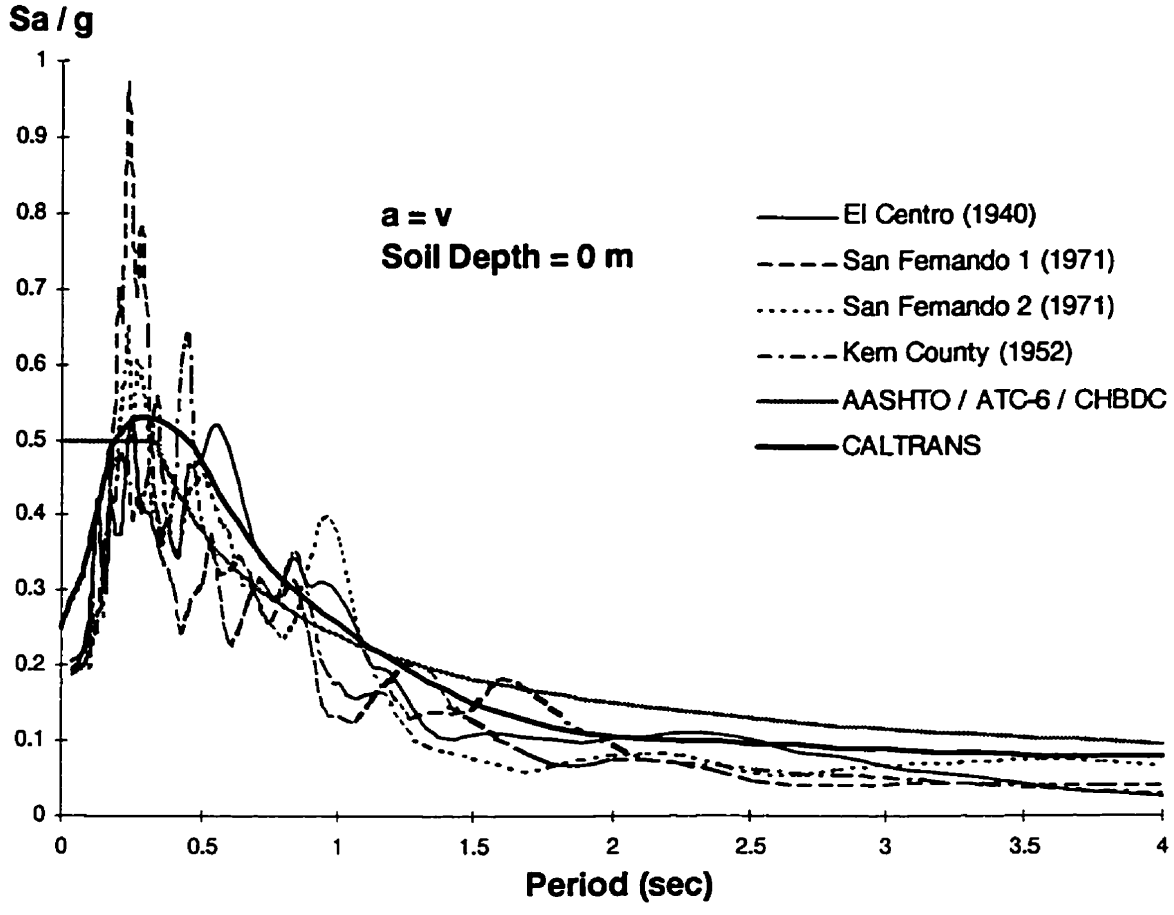

Figure 4.8 Comparison Of Response Spectra For Intermediate a/v Earthquakes At The Bedrock To Code Design Response Spectra With 0m Soil Depth

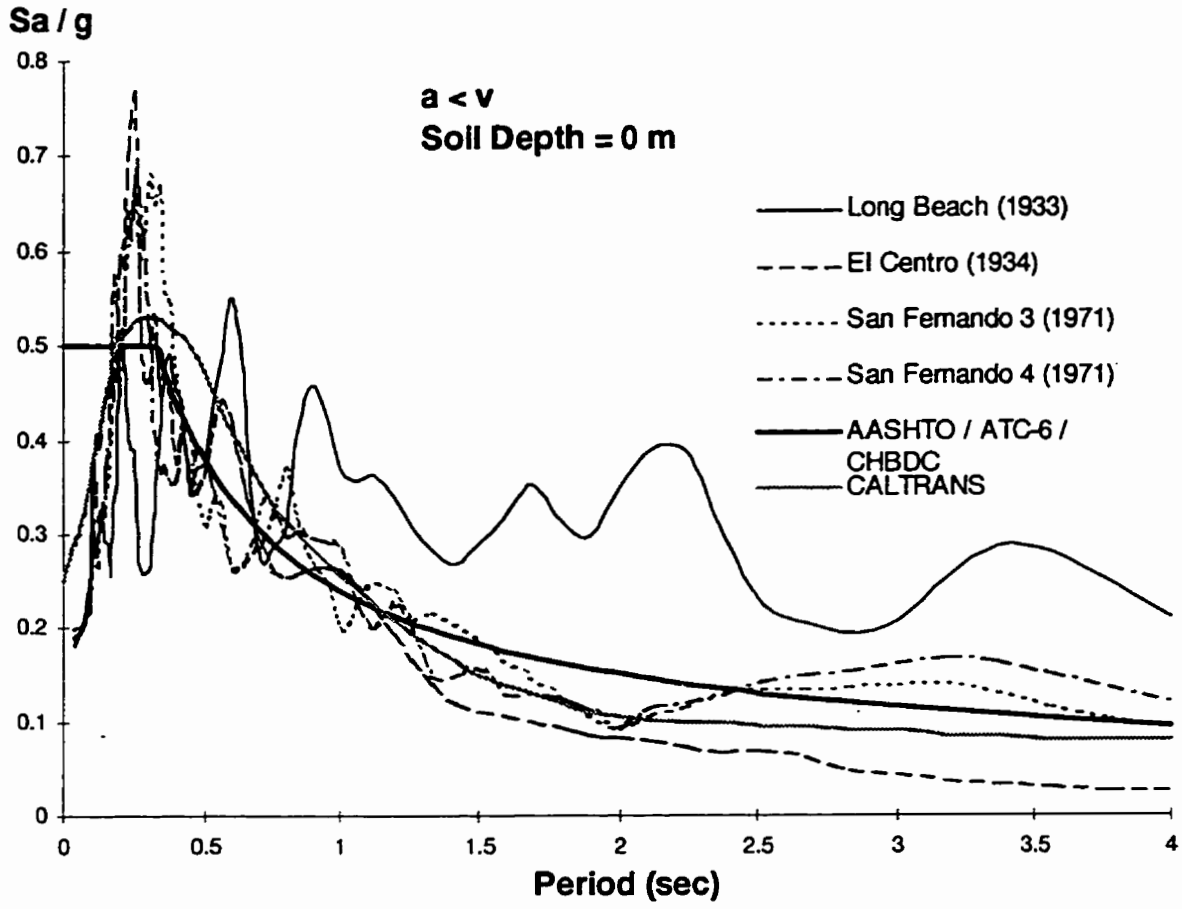

Figure 4.9 Comparison Of Response Spectra For Low a/v Earthquakes At The Bedrock To Code Design Response Spectra With 0m Soil Depth

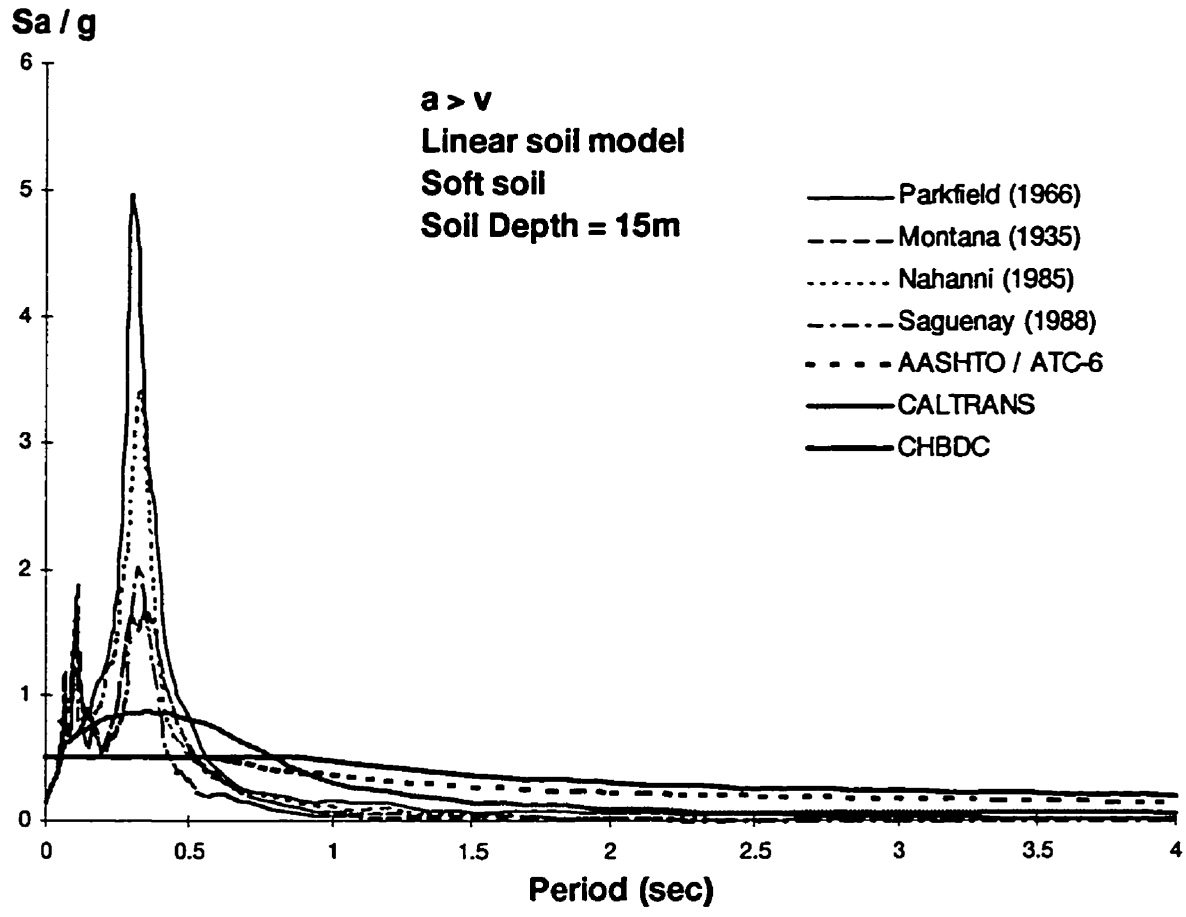

Figure 4.10 Comparison Of Response Spectra For Linear Model of Soft Soil with 15m Depths Subjected High a/v Earthquakes To Code Design Response Spectra

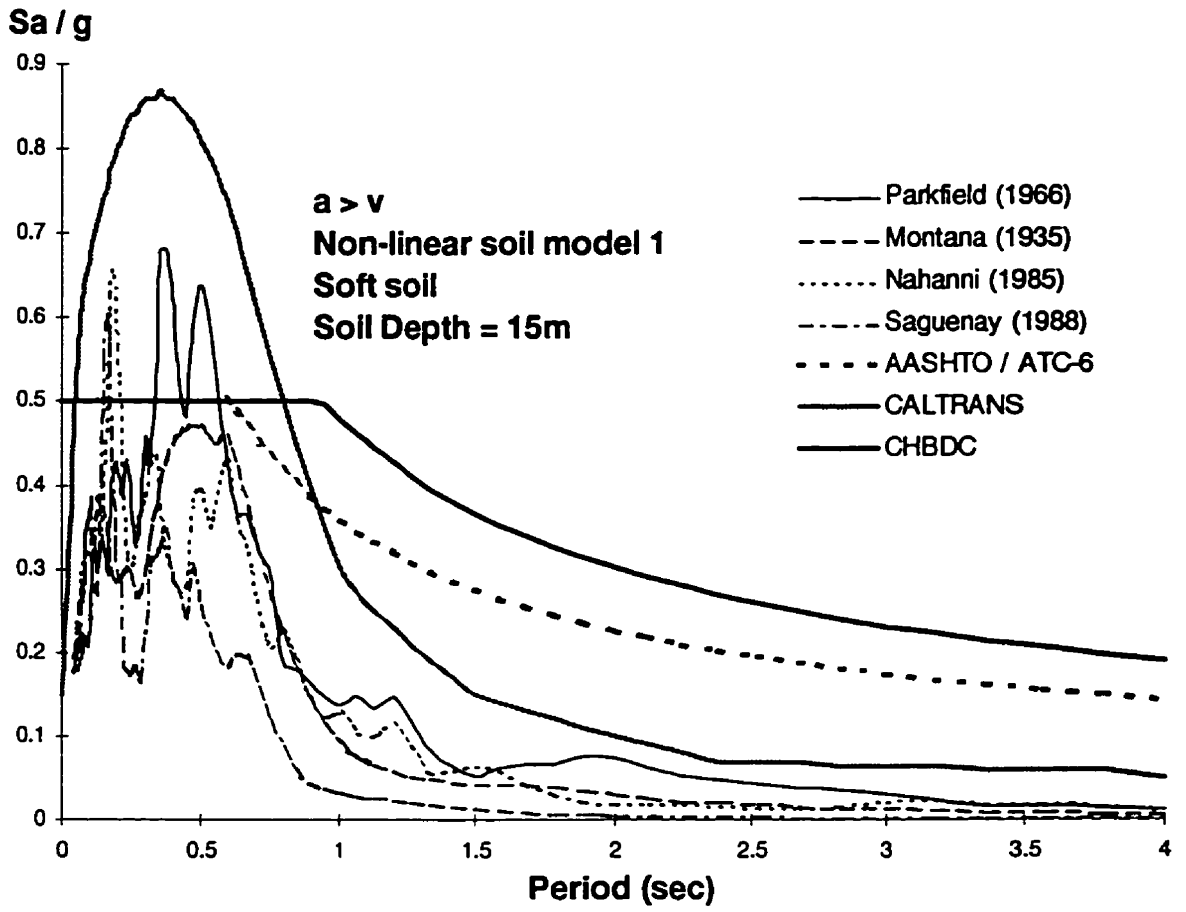

Figure 4.11 Comparison Of Response Spectra For Nonlinear Model 1 of Soft Soil with 15m Depths Subjected High a/v Earthquakes To Code Design Response Spectra

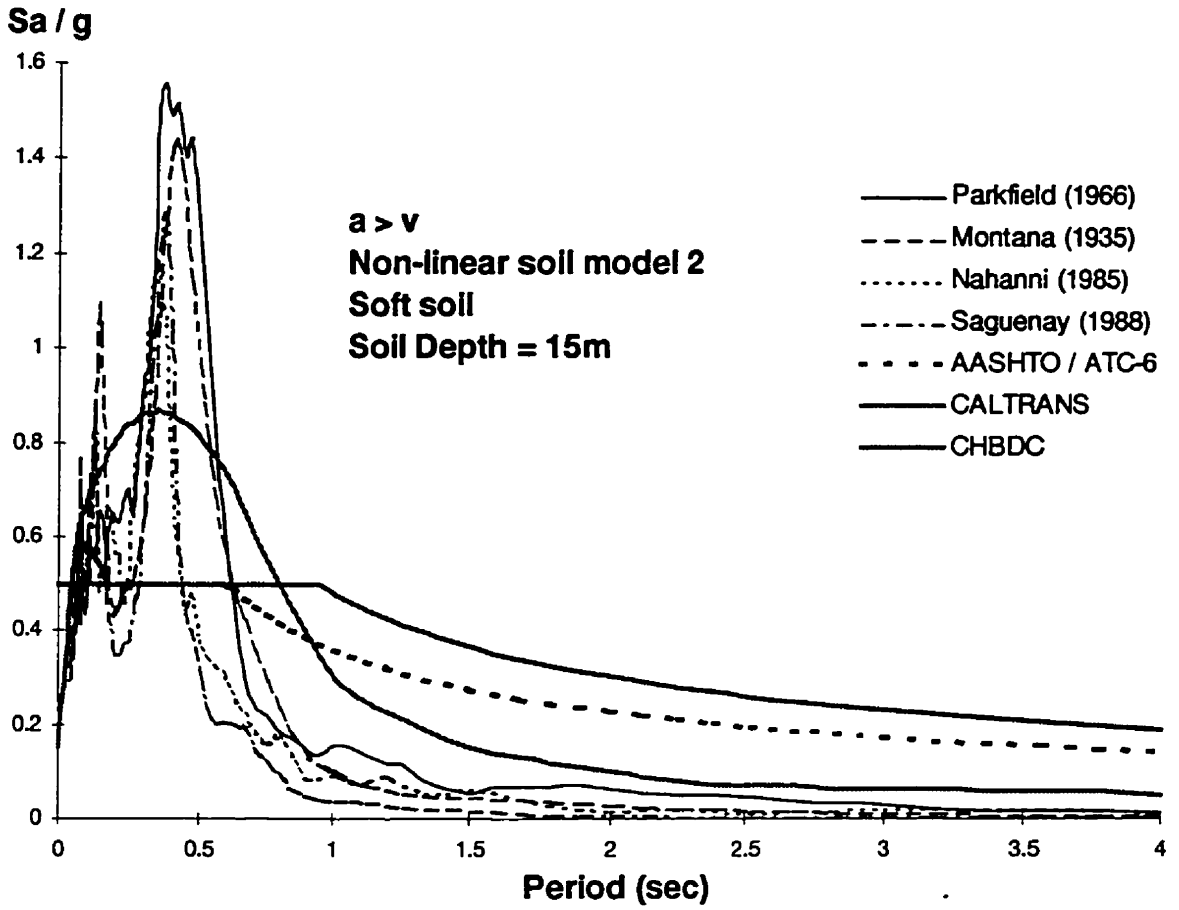

Figure 4.12 Comparison Of Response Spectra For Nonlinear Model 2 of Soft Soil with 15m Depths Subjected High a/v Earthquakes To Code Design Response Spectra

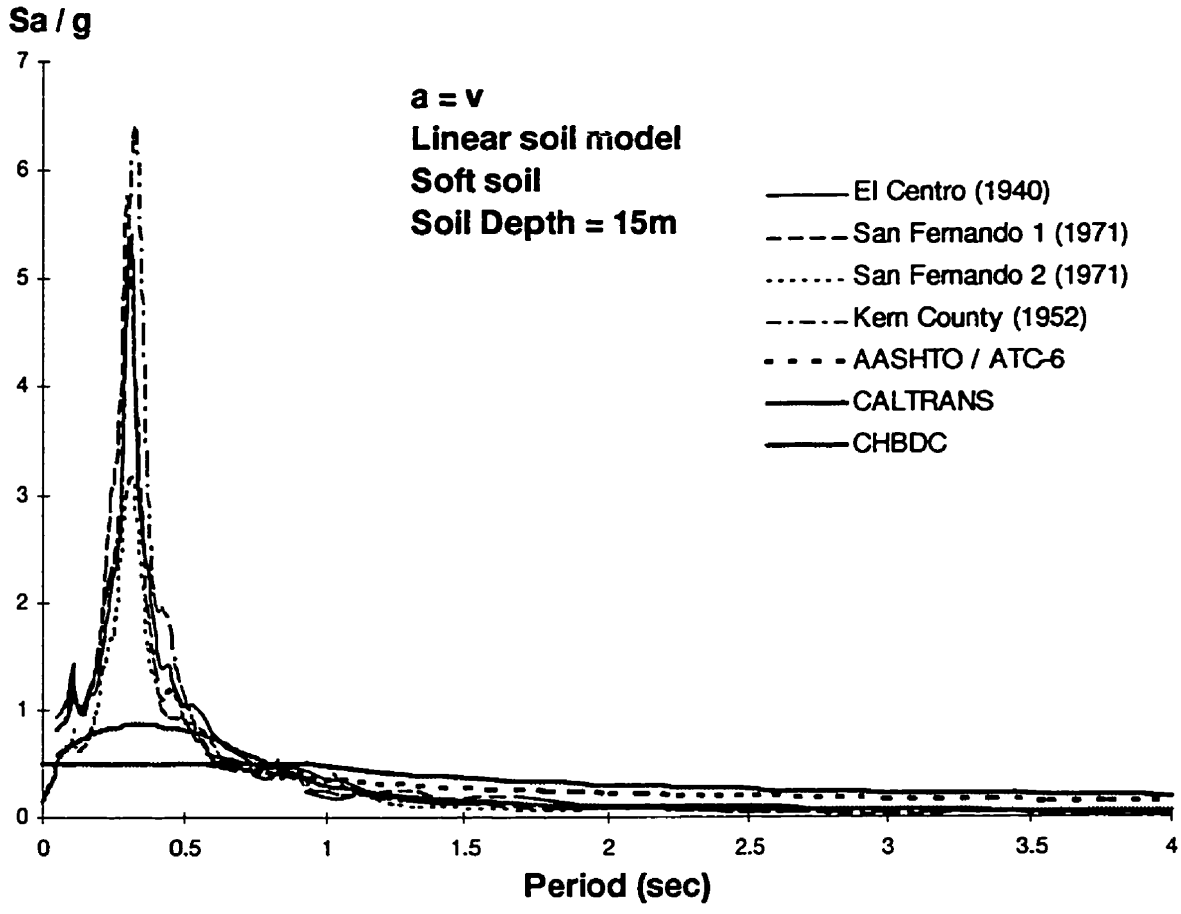

Figure 4.13 Comparison Of Response Spectra For Linear Model of Soft Soil with 15m Depths Subjected Intermediate a/v Earthquakes To Code Design Response Spectra

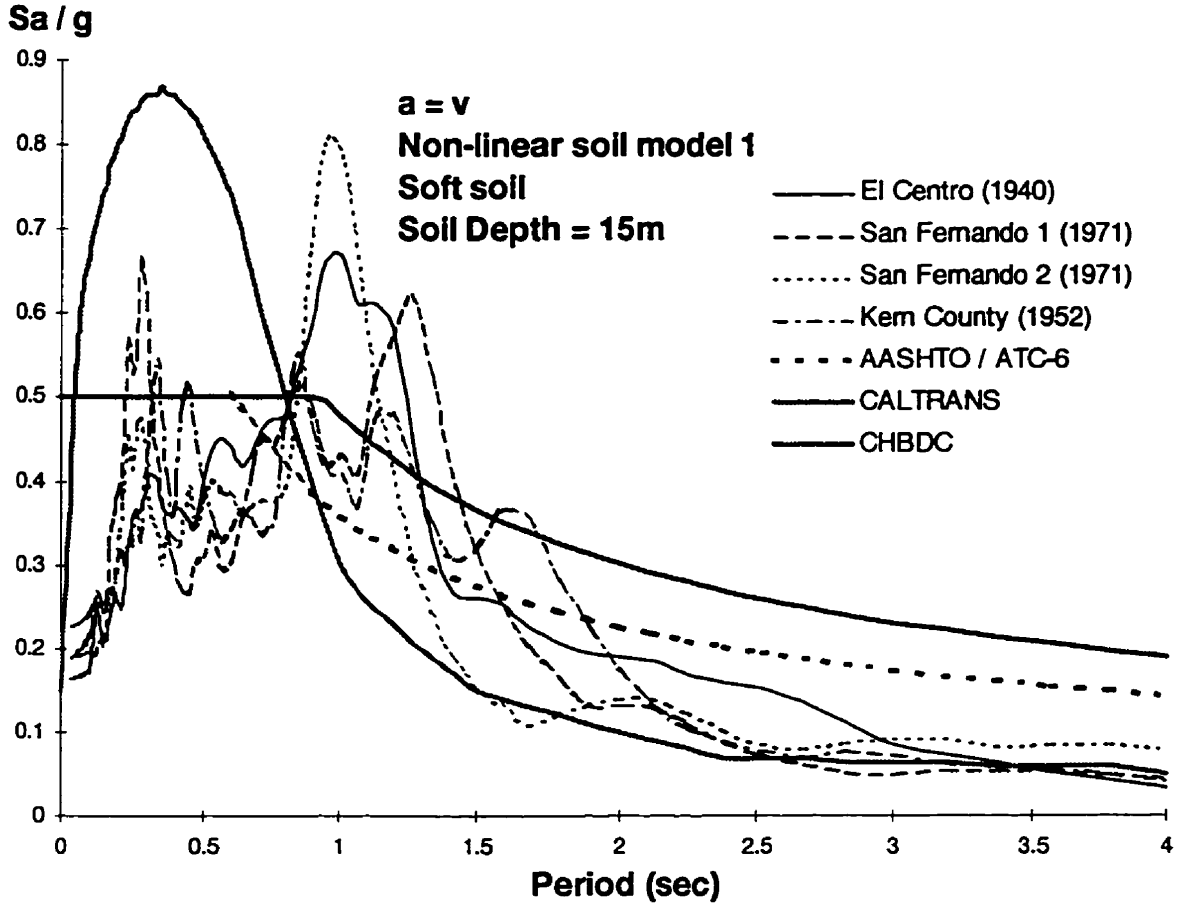

Figure 4.14 Comparison Of Response Spectra For Nonlinear Model 1 of Soft Soil with 15m Depths Subjected Intermediate a/v Earthquakes To Code Design Response Spectra

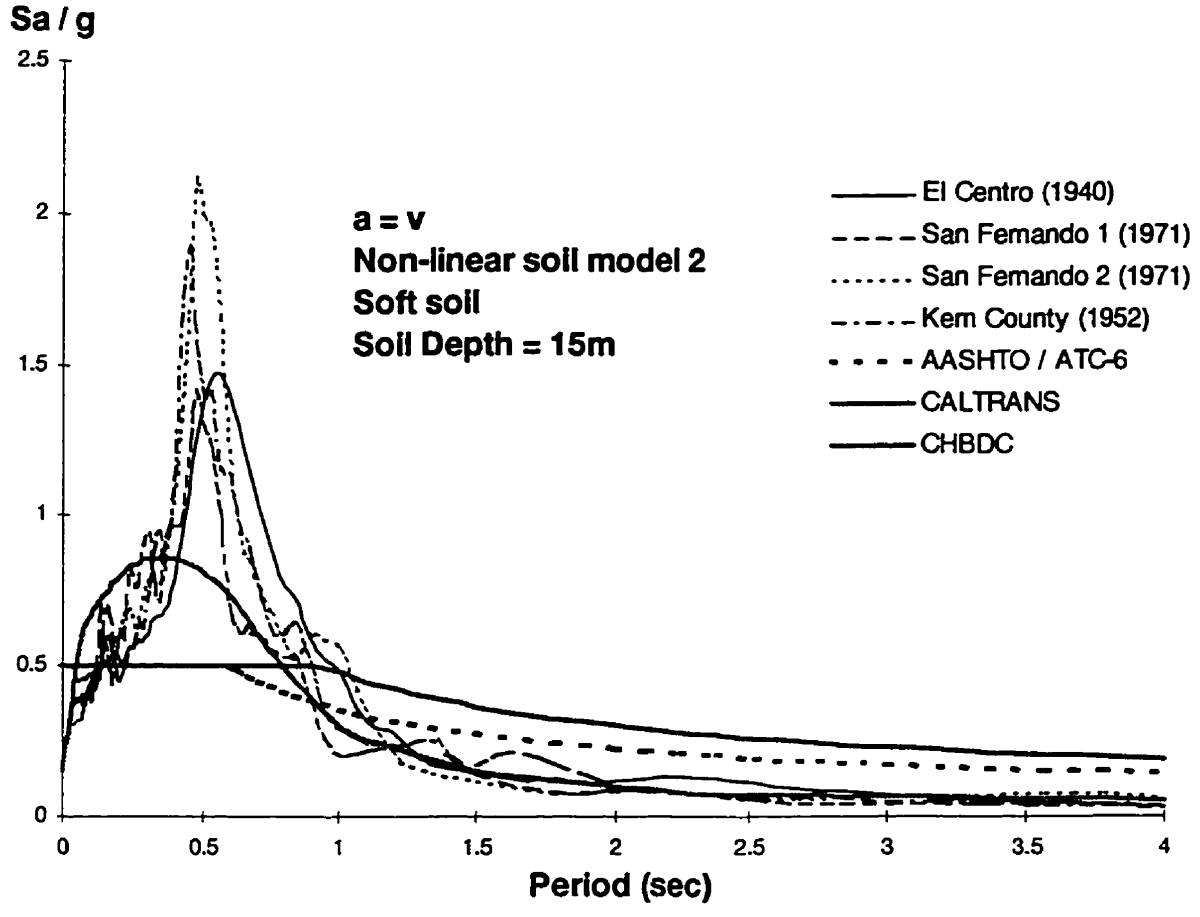

Figure 4.15 Comparison Of Response Spectra For Nonlinear Model 2 of Soft Soil with 15m Depths Subjected Intermediate a/v Earthquakes To Code Design Response Spectra

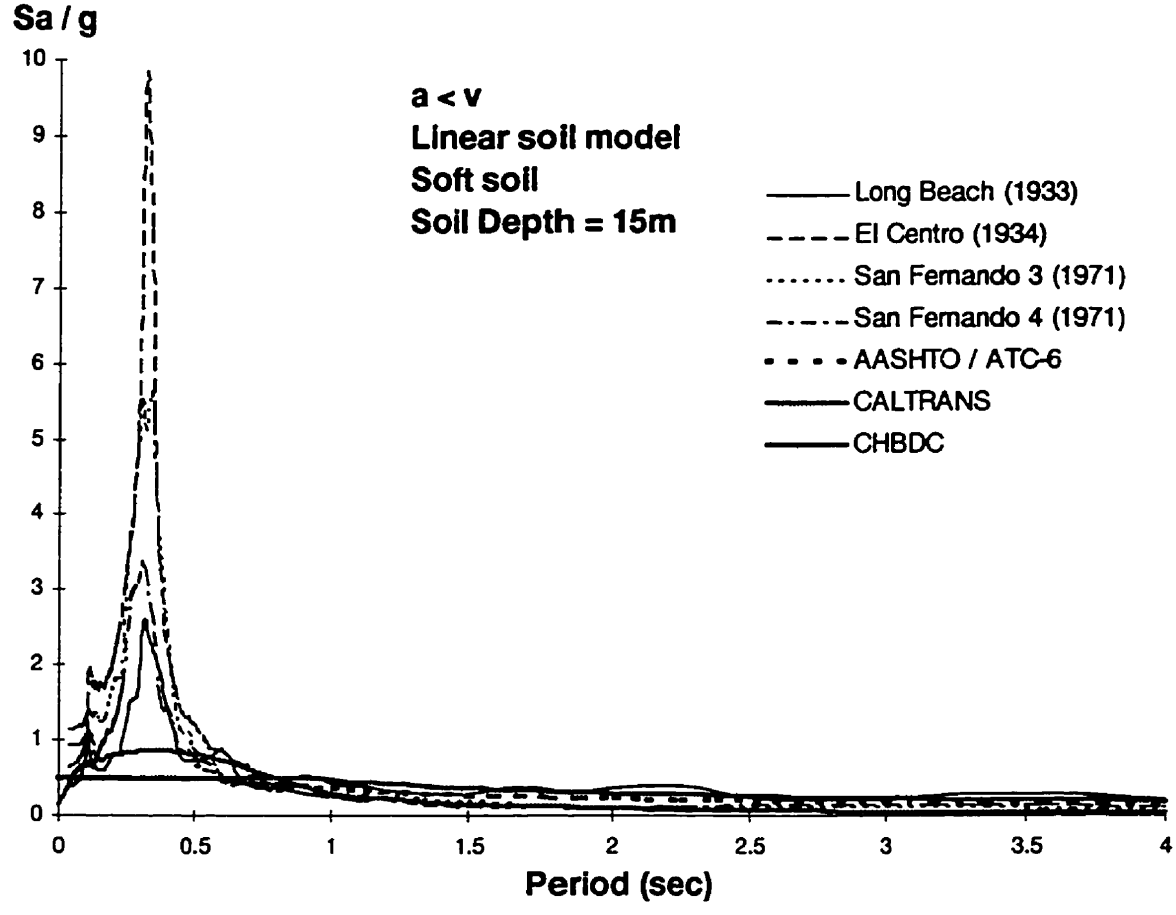

Figure 4.16 Comparison Of Response Spectra For Linear Model of Soft Soil with 15m Depths Subjected Low a/v Earthquakes To Code Design Response Spectra

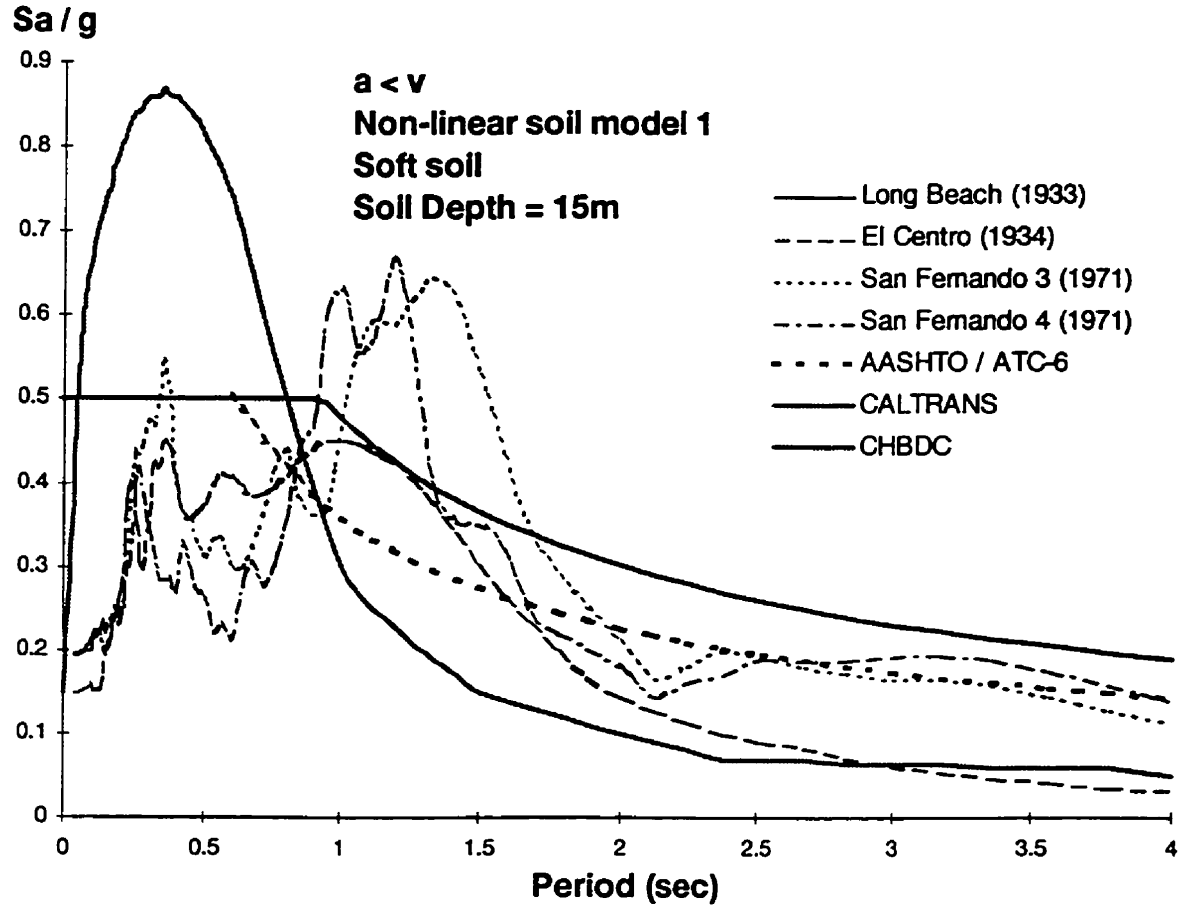

Figure 4.17 Comparison Of Response Spectra For Nonlinear Model 1 of Soft Soil with 15m Depths Subjected Low a/v Earthquakes To Code Design Response Spectra

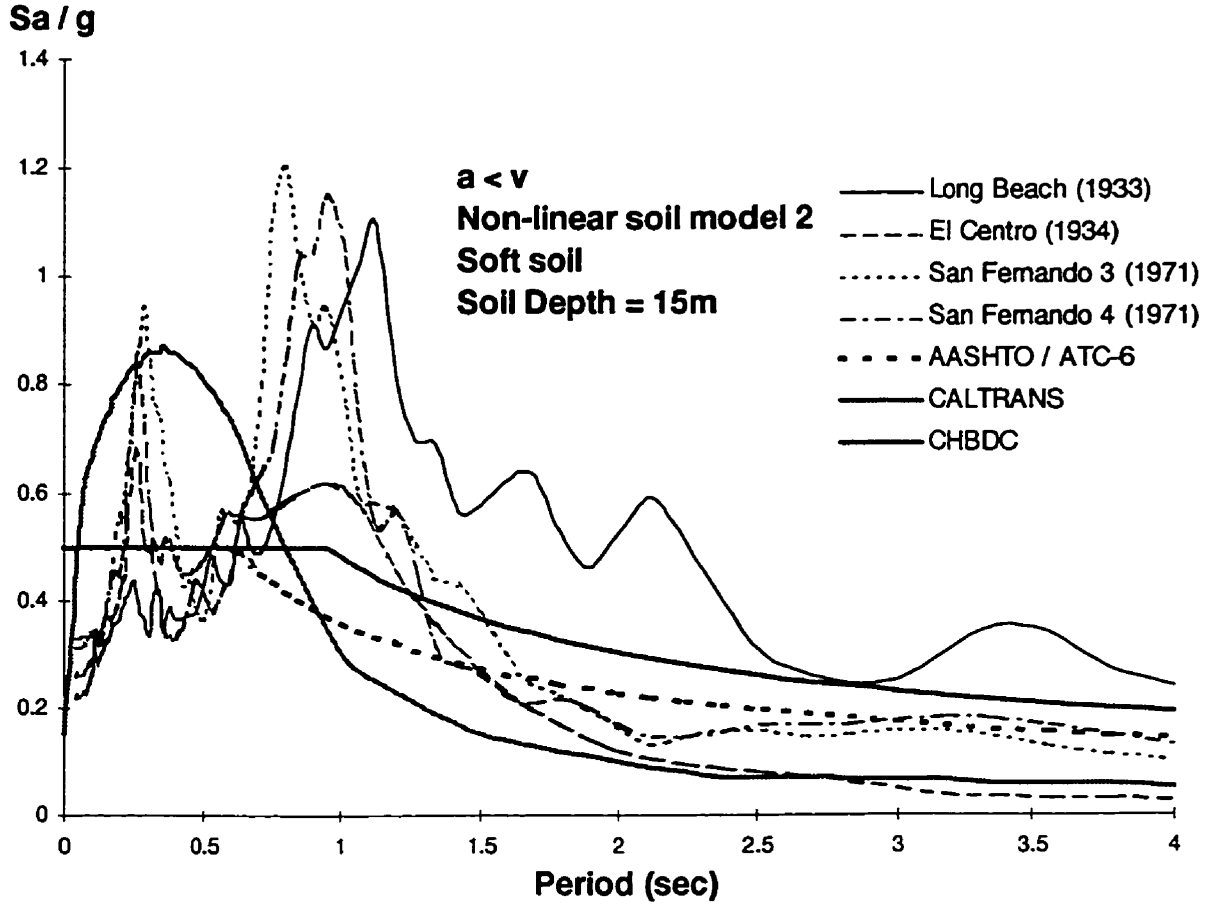

Figure 4.18 Comparison Of Response Spectra For Nonlinear Model 2 of Soft Soil with 15m Depths Subjected Low a/v Earthquakes To Code Design Response Spectra

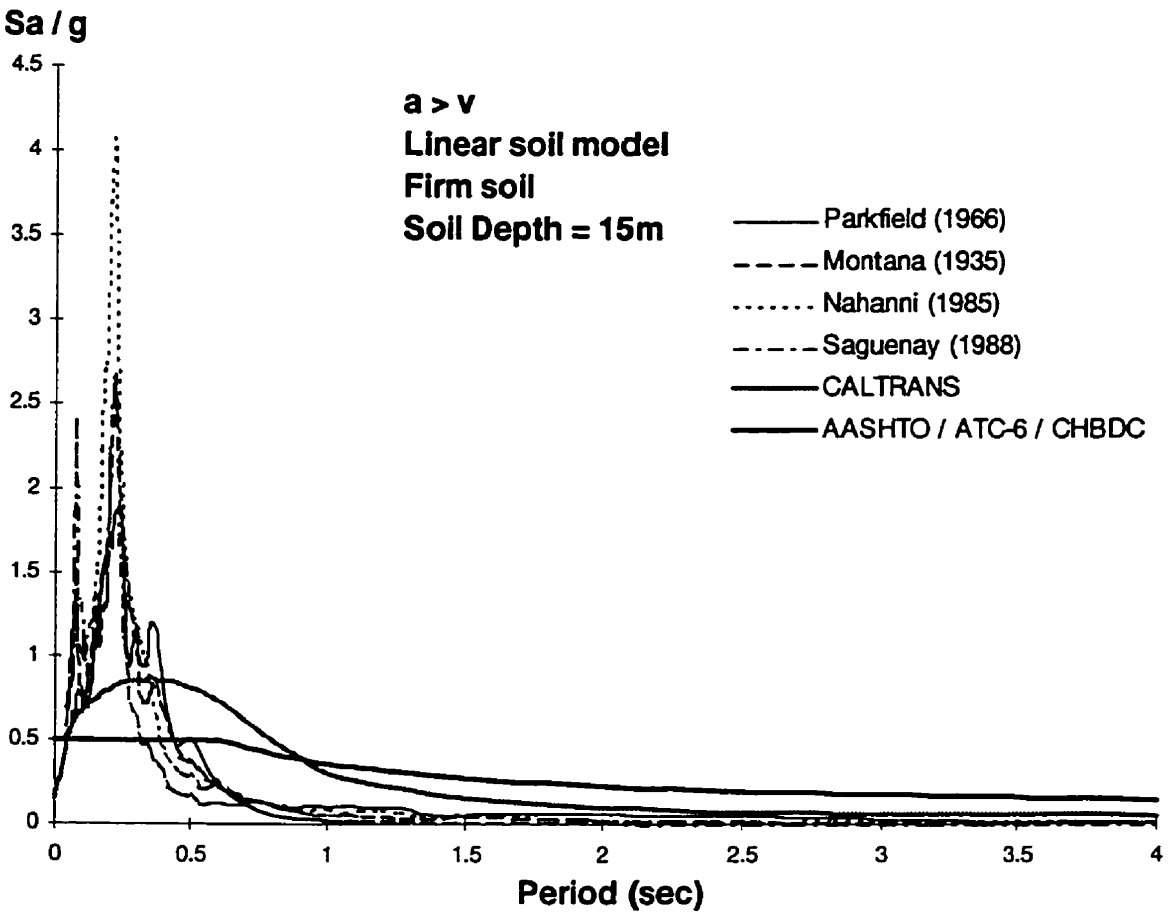

Figure 4.19 Comparison Of Response Spectra For Linear Model of Firm Soil with 15m Depths Subjected High a/v Earthquakes To Code Design Response Spectra

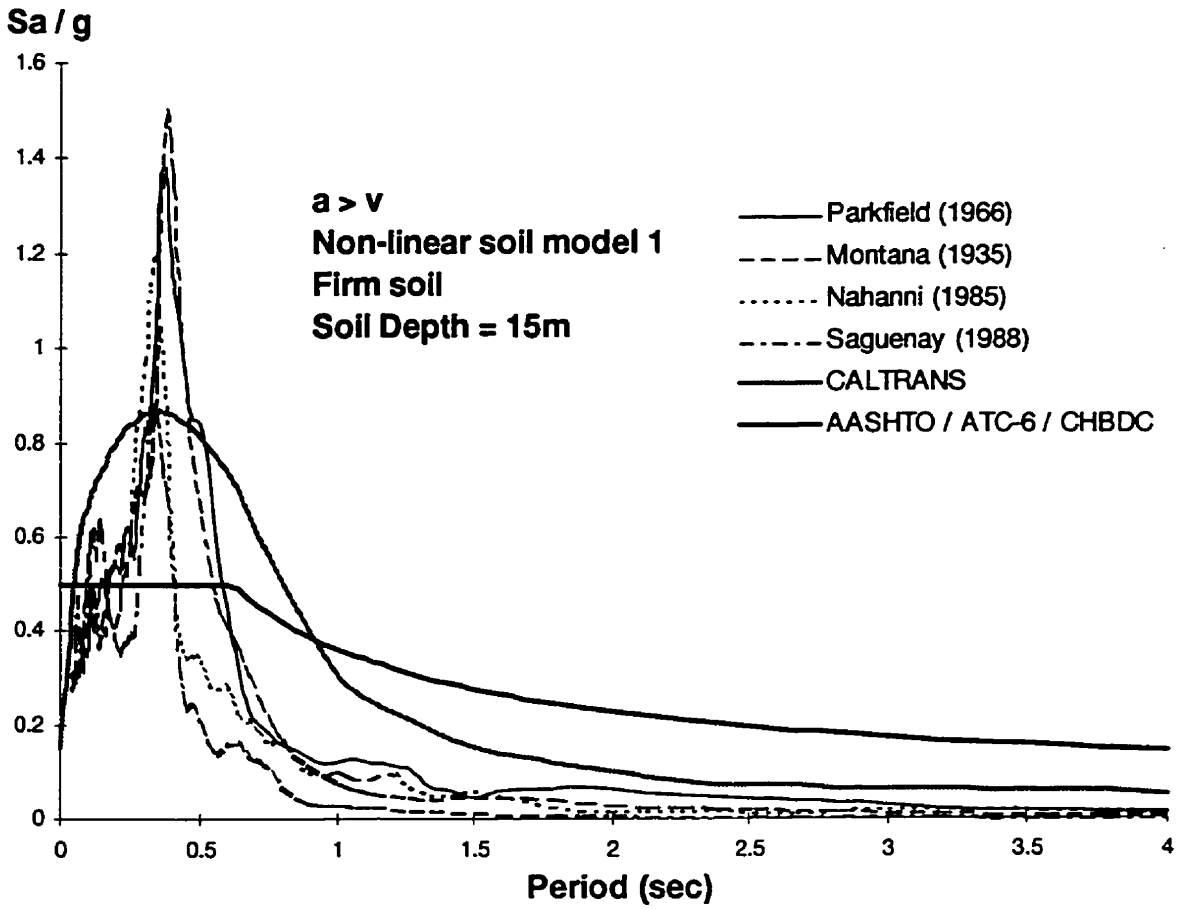

Figure 4.20 Comparison Of Response Spectra For Nonlinear Model 1 of Firm Soil with 15m Depths Subjected High a/v Earthquakes To Code Design Response Spectra

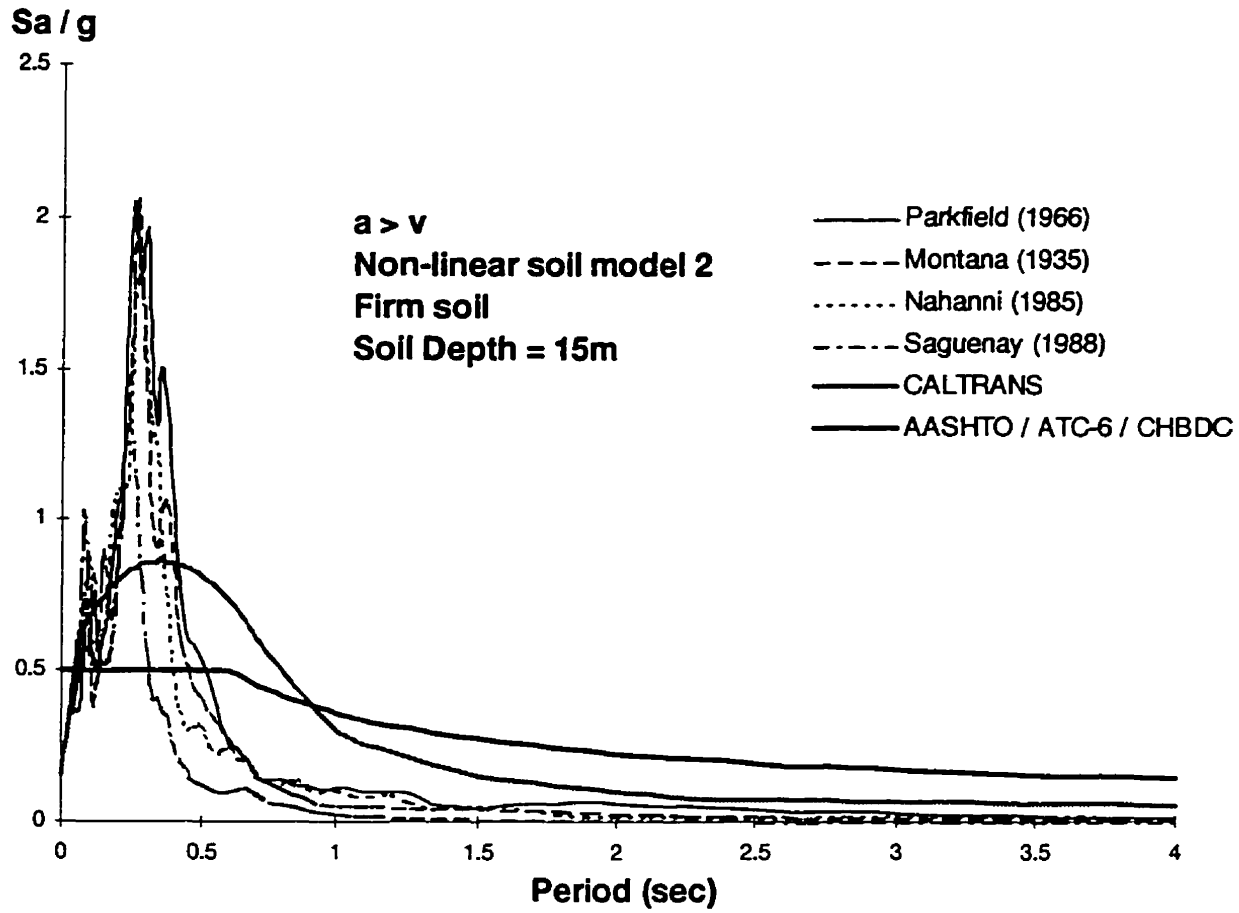

Figure 4.21 Comparison Of Response Spectra For Nonlinear Model 2 of Firm Soil with 15m Depths Subjected High a/v Earthquakes To Code Design Response Spectra

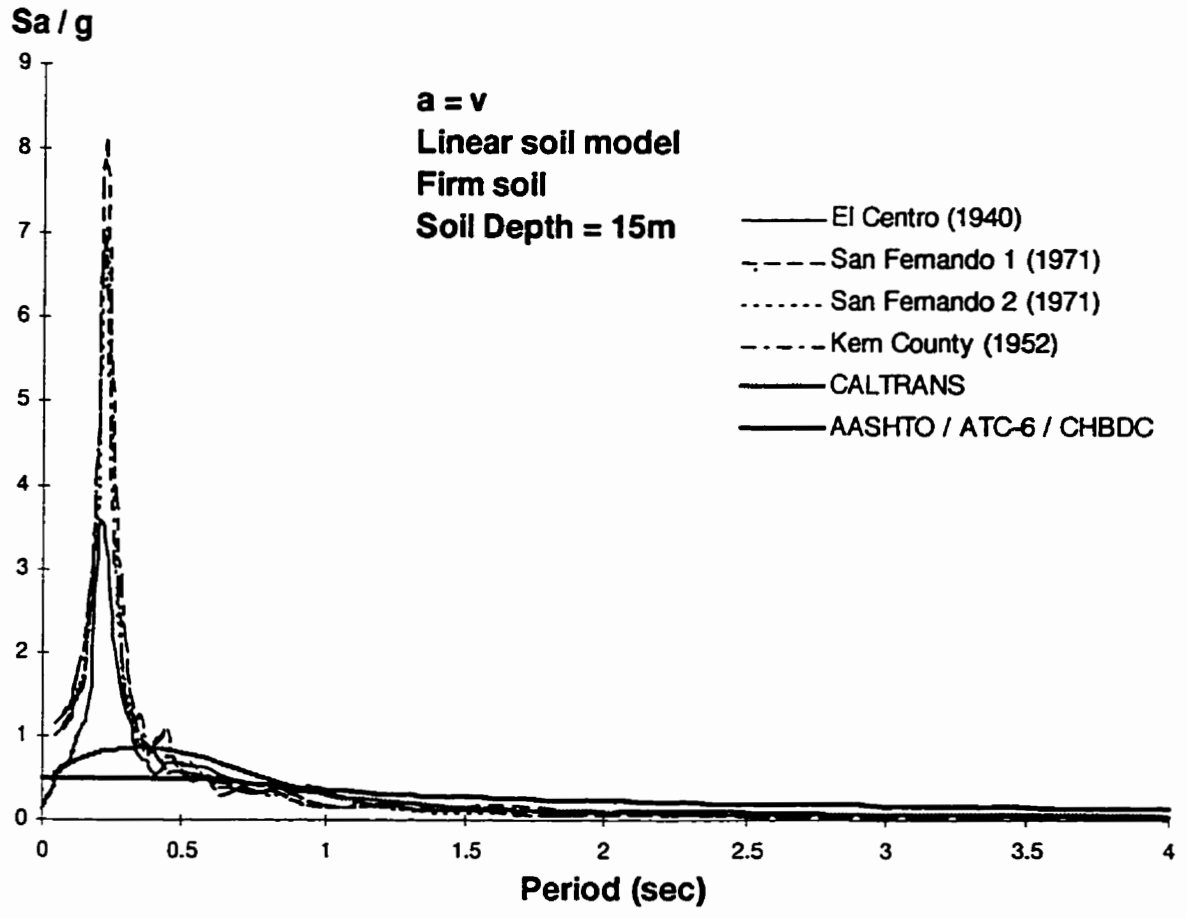

Figure 4.22 Comparison Of Response Spectra For Linear Model of Firm Soil with 15m Depths Subjected Intermediate a/v Earthquakes To Code Design Response Spectra

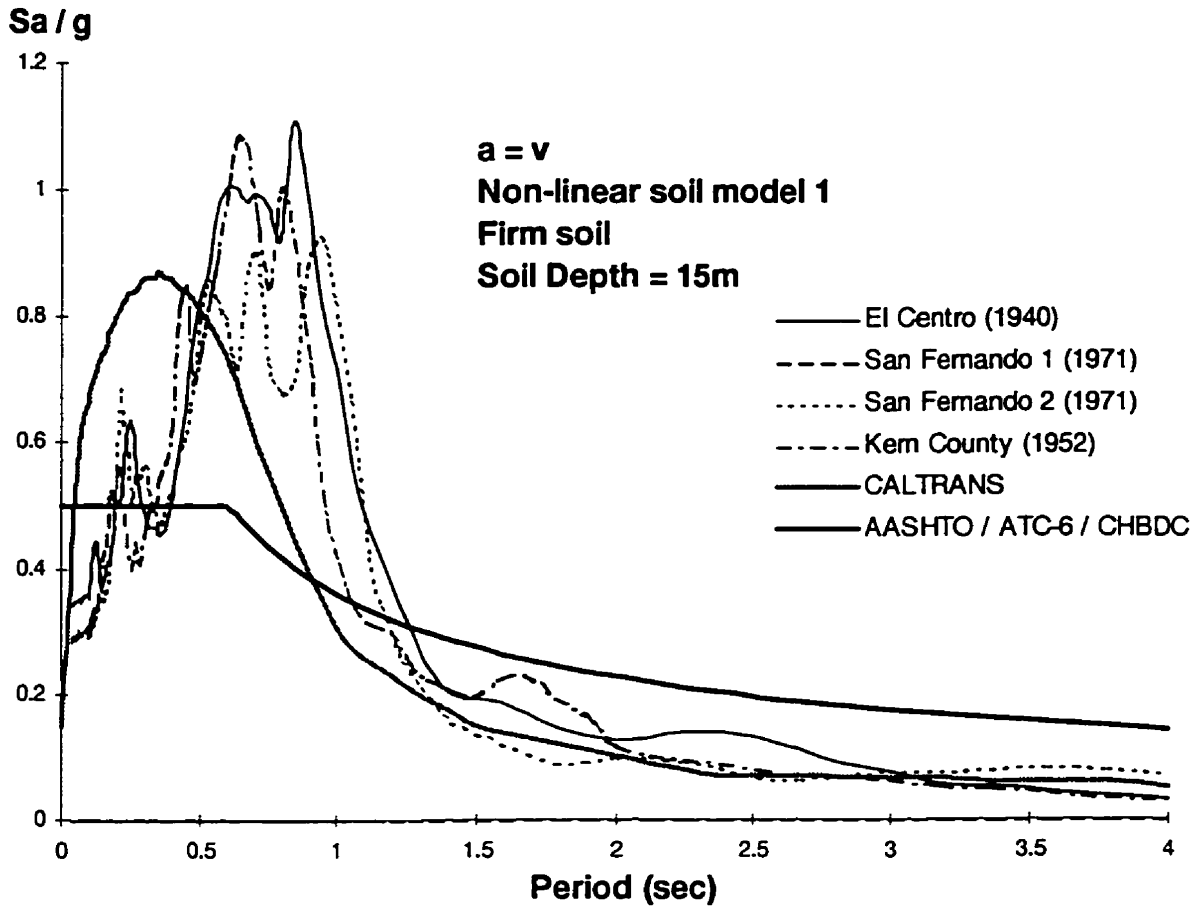

Figure 4.23 Comparison Of Response Spectra For Nonlinear Model 1 of Firm Soil with 15m Depths Subjected Intermediate a/v Earthquakes To Code Design Response Spectra

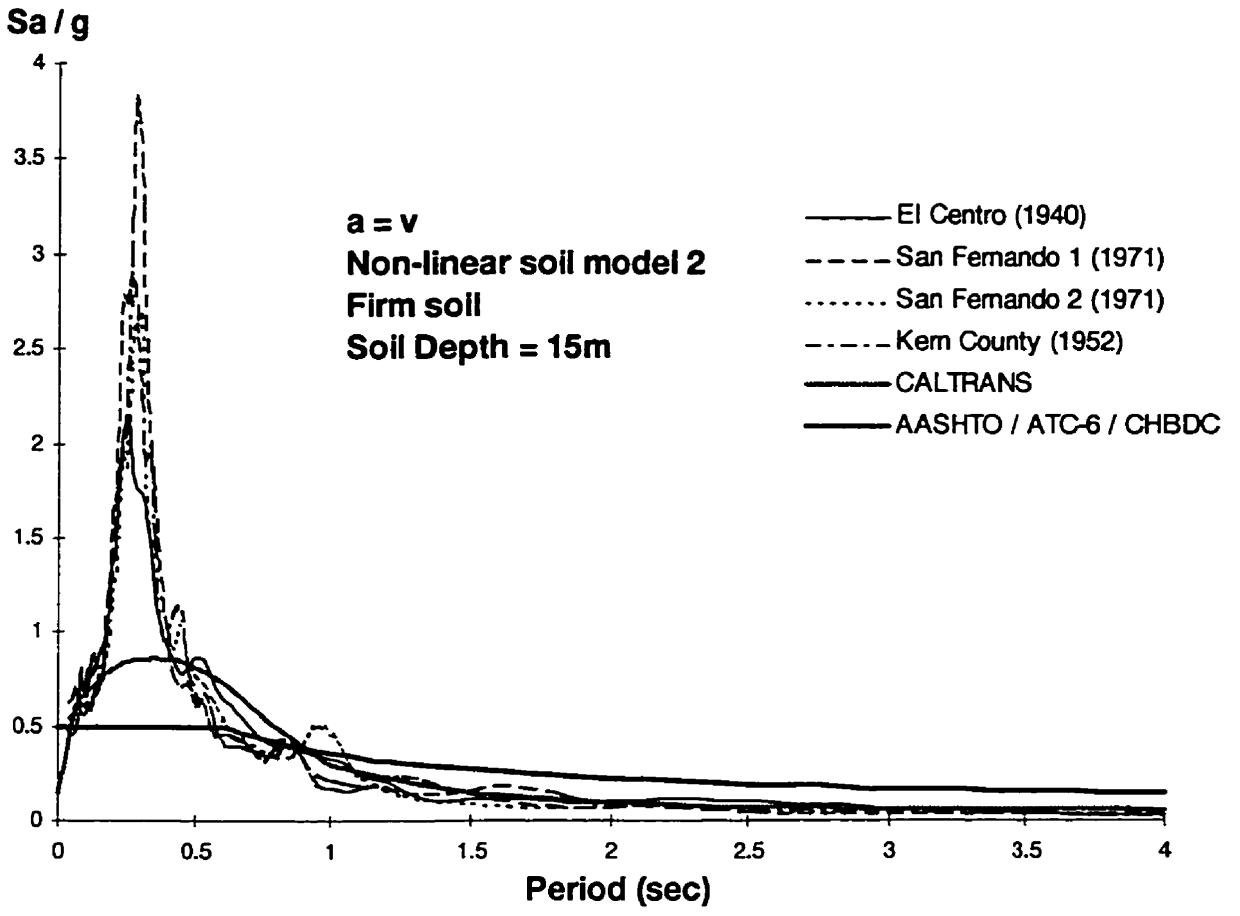

Figure 4.24 Comparison Of Response Spectra For Nonlinear Model 2 of Firm Soil with 15m Depths Subjected Intermediate a/v Earthquakes To Code Design Response Spectra

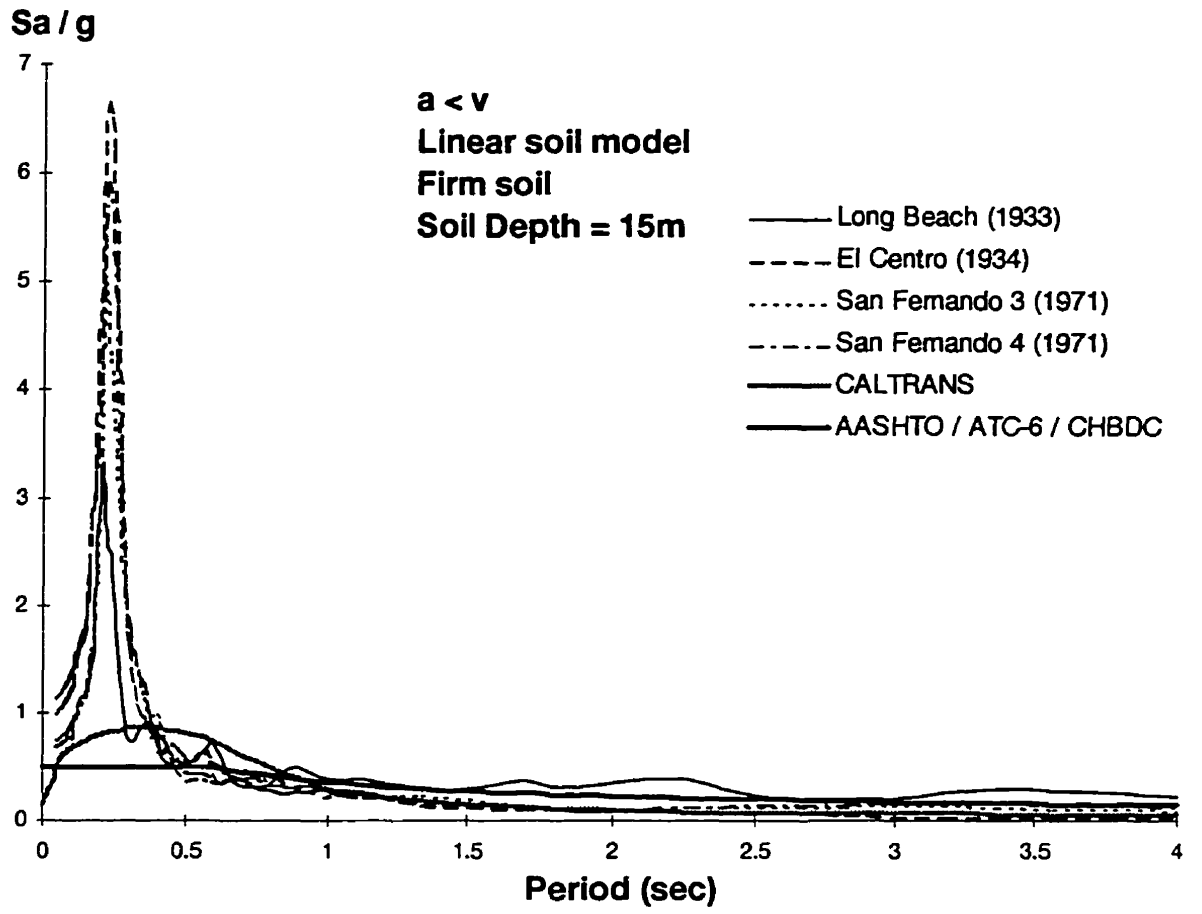

Figure 4.25 Comparison Of Response Spectra For Linear Model of Firm Soil with 15m Depths Subjected Low a/v Earthquakes To Code Design Response Spectra

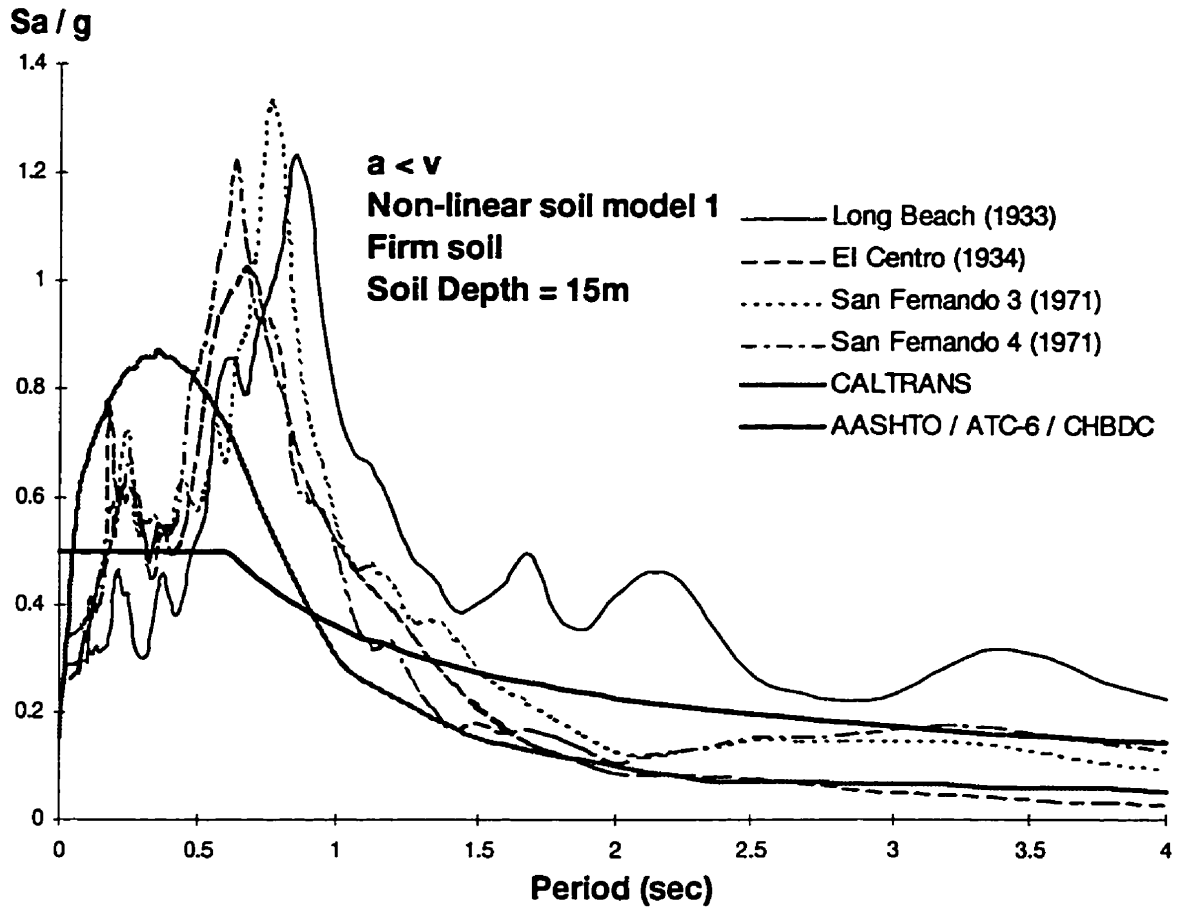

Figure 4.26 Comparison Of Response Spectra For Nonlinear Model 1 of Firm Soil with 15m Depths Subjected Low a/v Earthquakes To Code Design Response Spectra

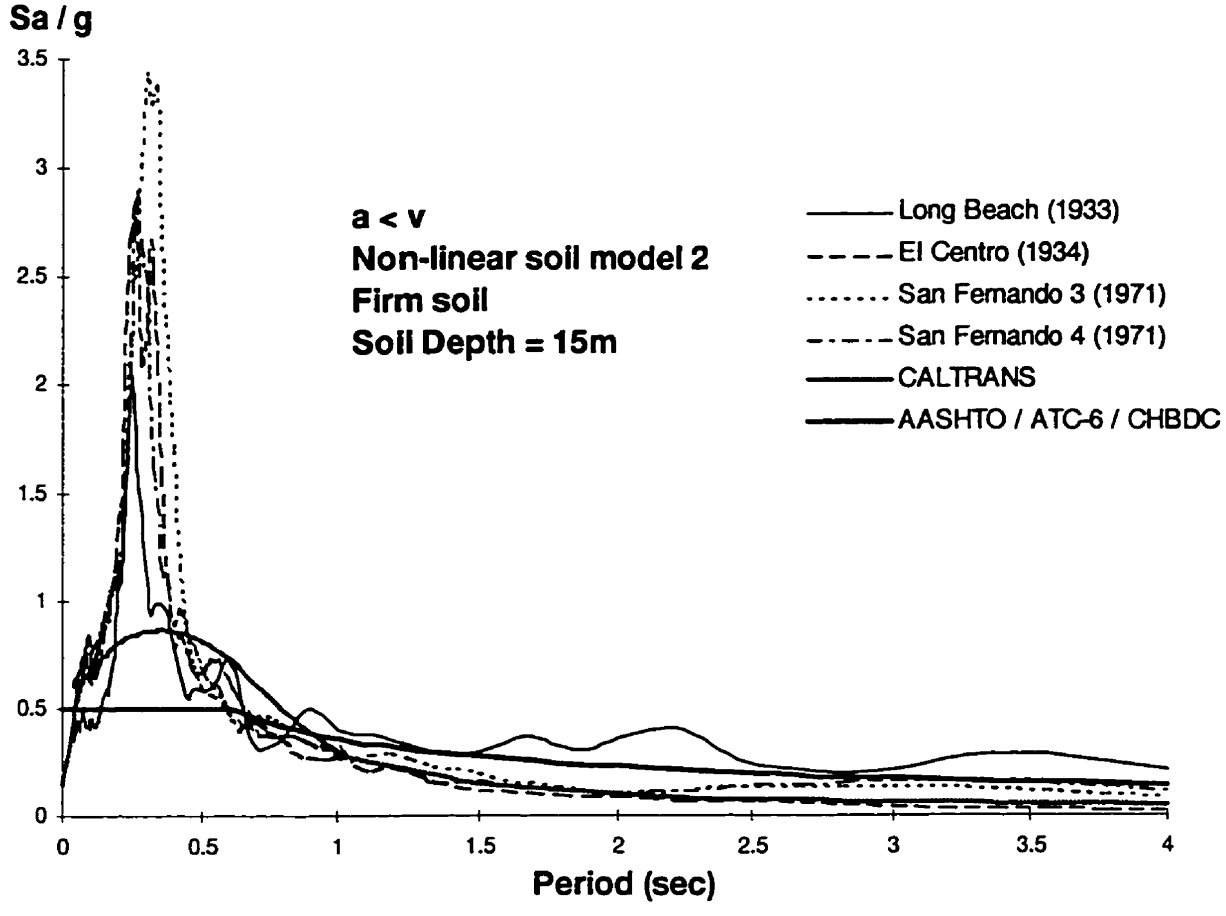

Figure 4.27 Comparison Of Response Spectra For Nonlinear Model 2 of Firm Soil with 15m Depths Subjected Low a/v Earthquakes To Code Design Response Spectra

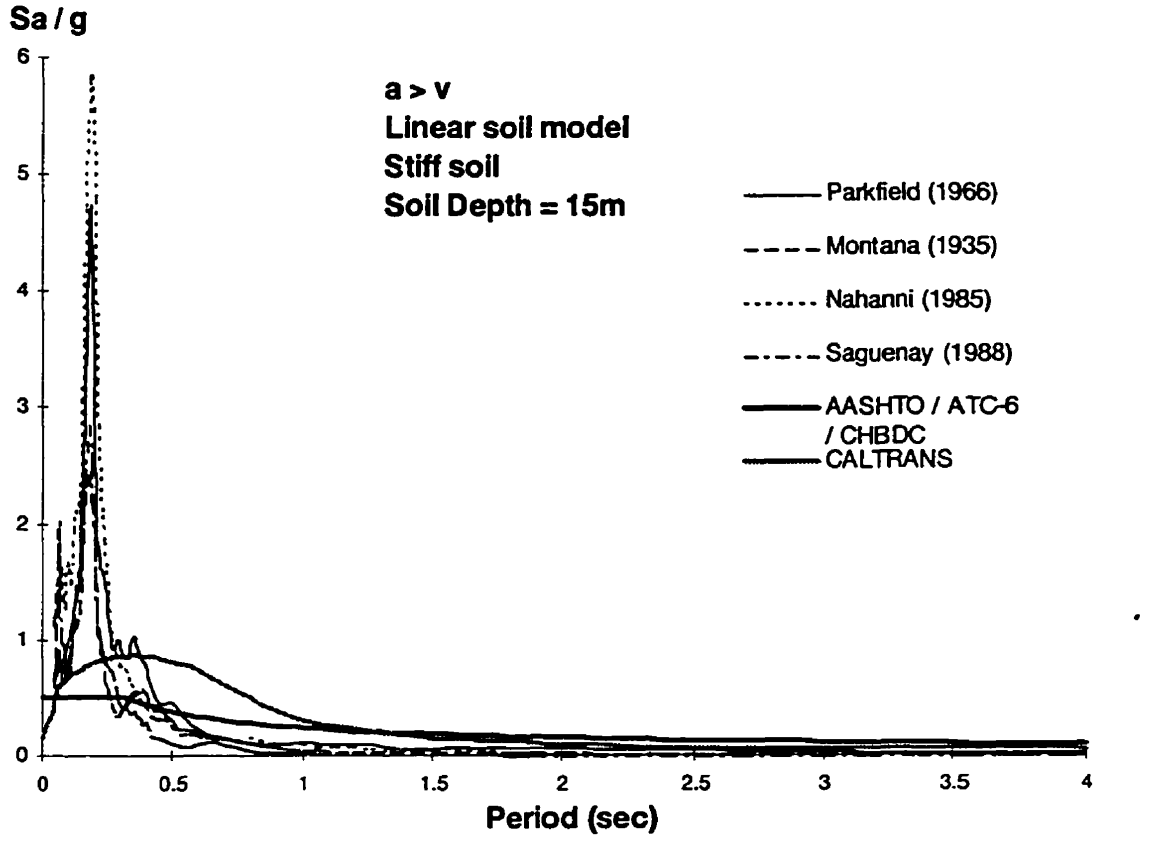

Figure 4.28 Comparison Of Response Spectra For Linear Model of Stiff Soil with 15m Depths Subjected High a/v Earthquakes To Code Design Response Spectra

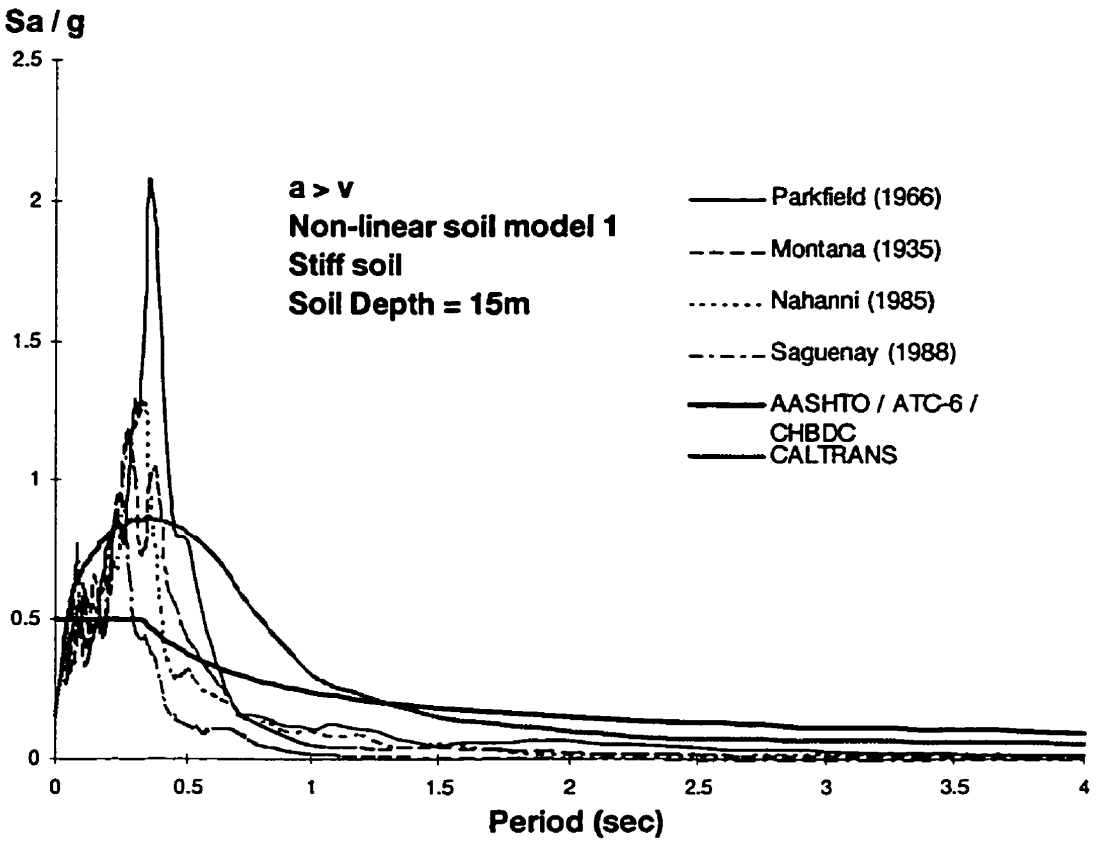

Figure 4.29 Comparison Of Response Spectra For Nonlinear Model 1 of Stiff Soil with 15m Depths Subjected High a/v Earthquakes To Code Design Response Spectra

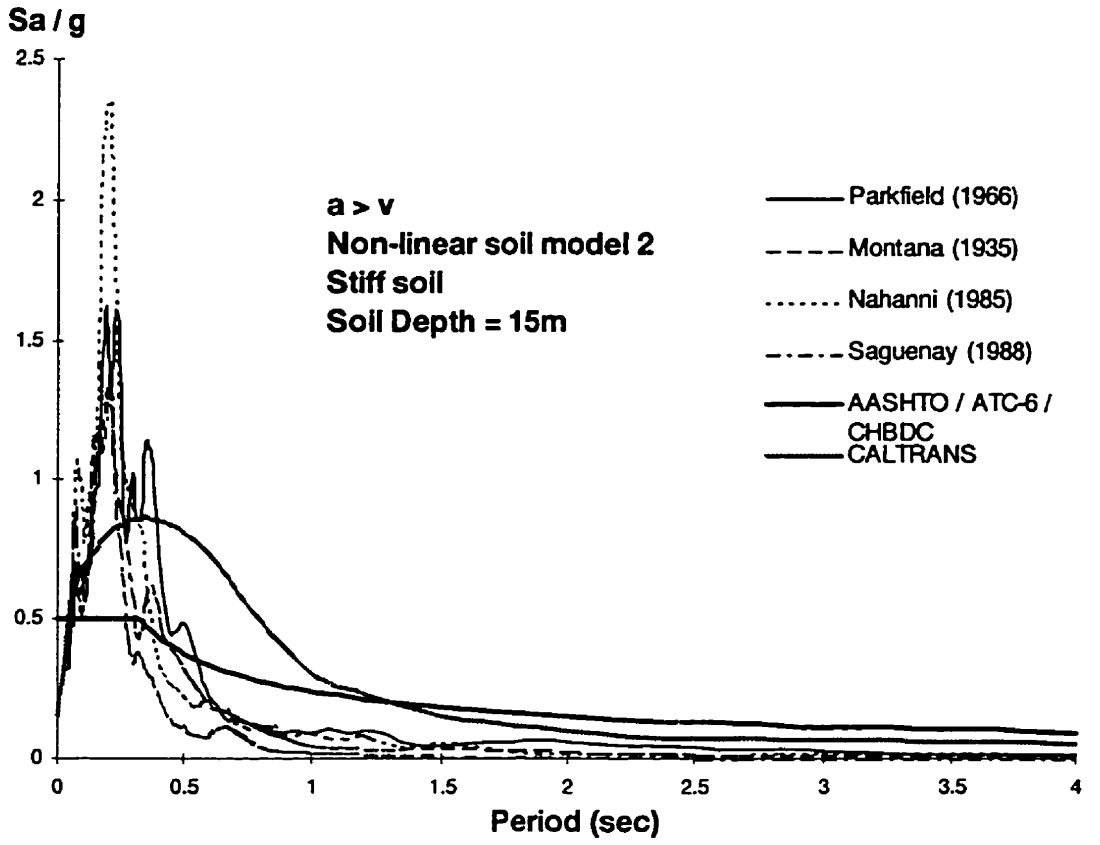

Figure 4.30 Comparison Of Response Spectra For Nonlinear Model 2 of Stiff Soil with 15m Depths Subjected High a/v Earthquakes To Code Design Response Spectra

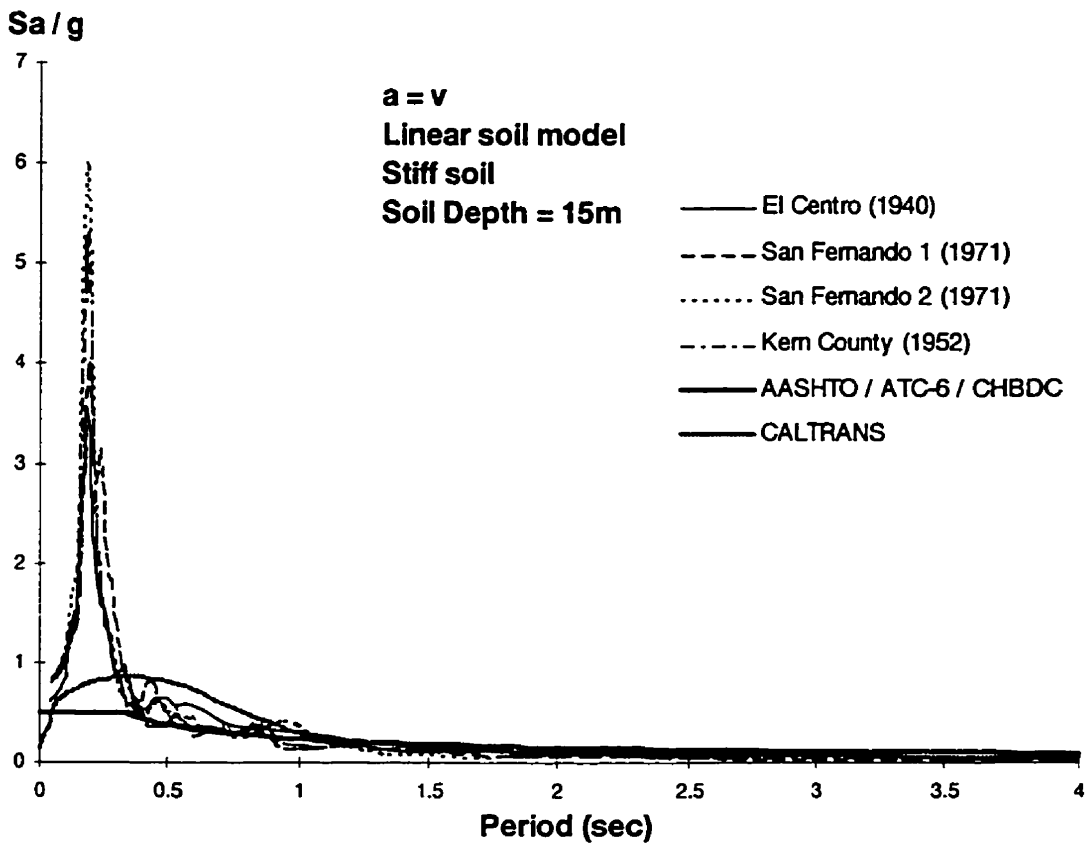

Figure 4.31 Comparison Of Response Spectra For Linear Model of Stiff Soil with 15m Depths Subjected Intermediate a/v Earthquakes To Code Design Response Spectra

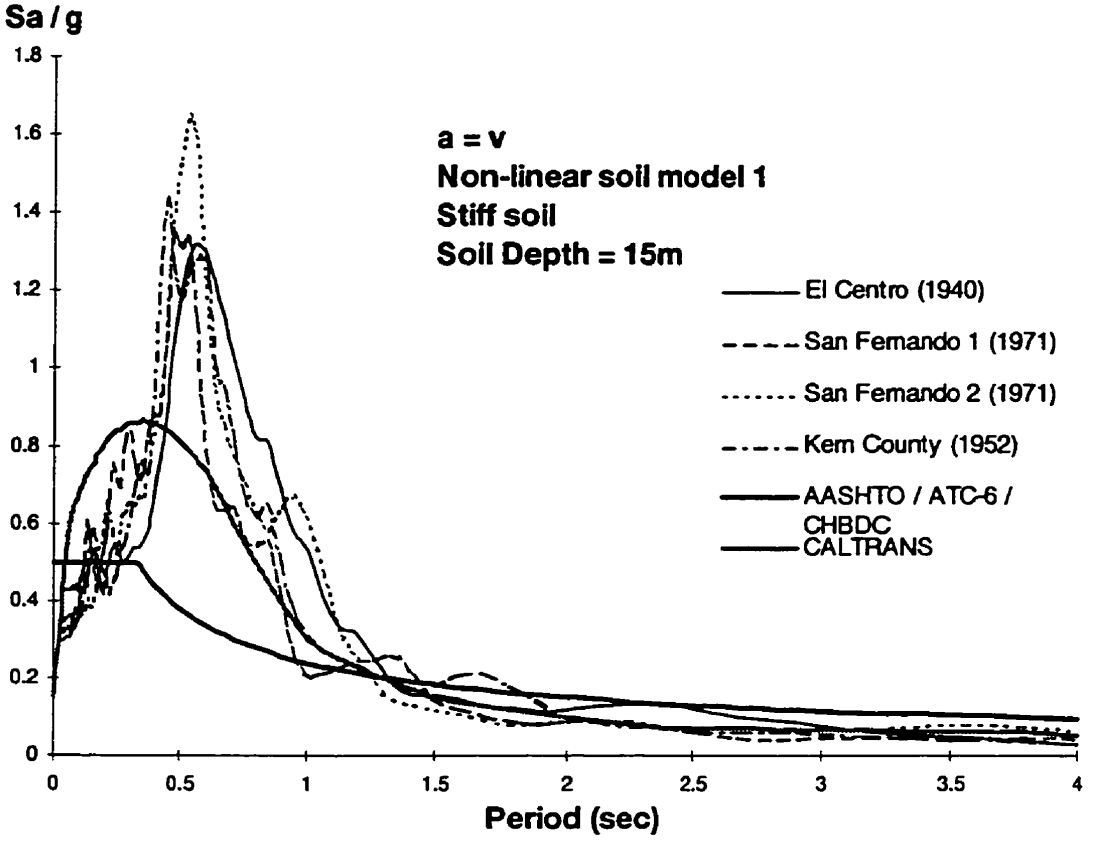

Figure 4.32 Comparison Of Response Spectra For Nonlinear Model 1 of Stiff Soil with 15m Depths Subjected Intermediate a/v Earthquakes To Code Design Response Spectra

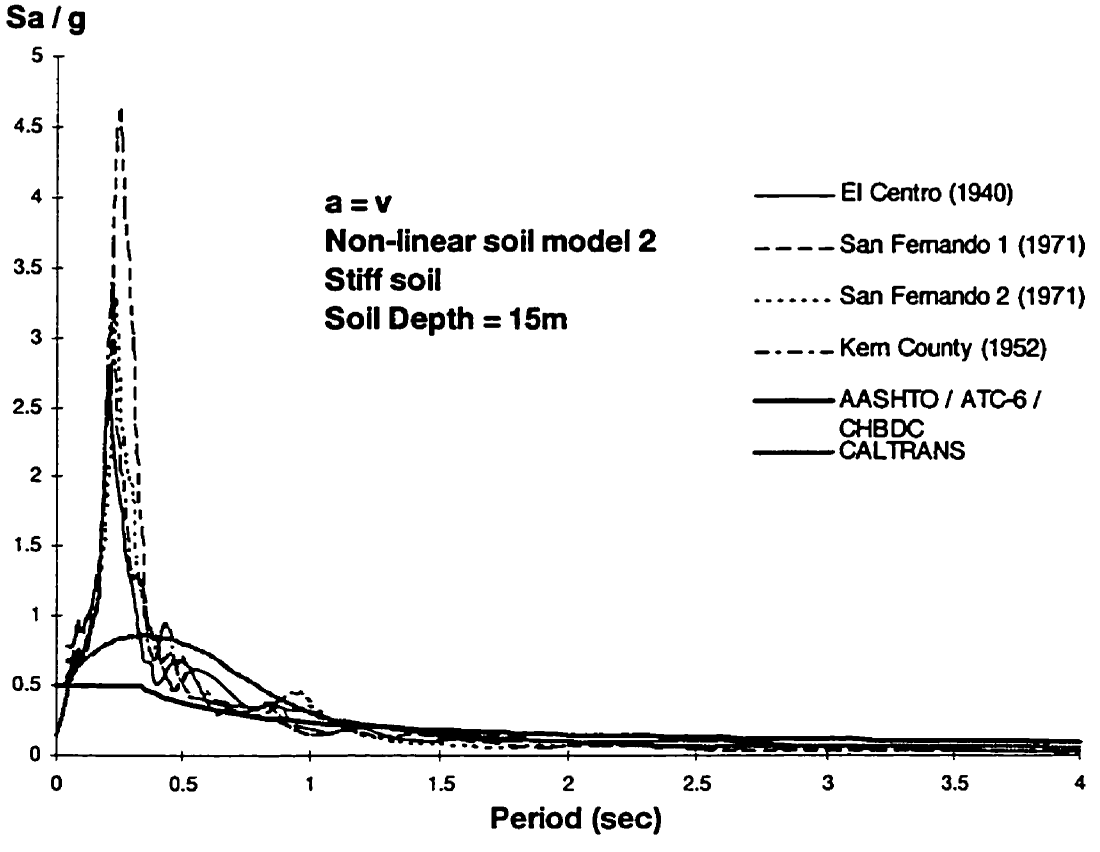

Figure 4.33 Comparison Of Response Spectra For Nonlinear Model 2 of Firm Soil with 15m Depths Subjected Intermediate a/v Earthquakes To Code Design Response Spectra

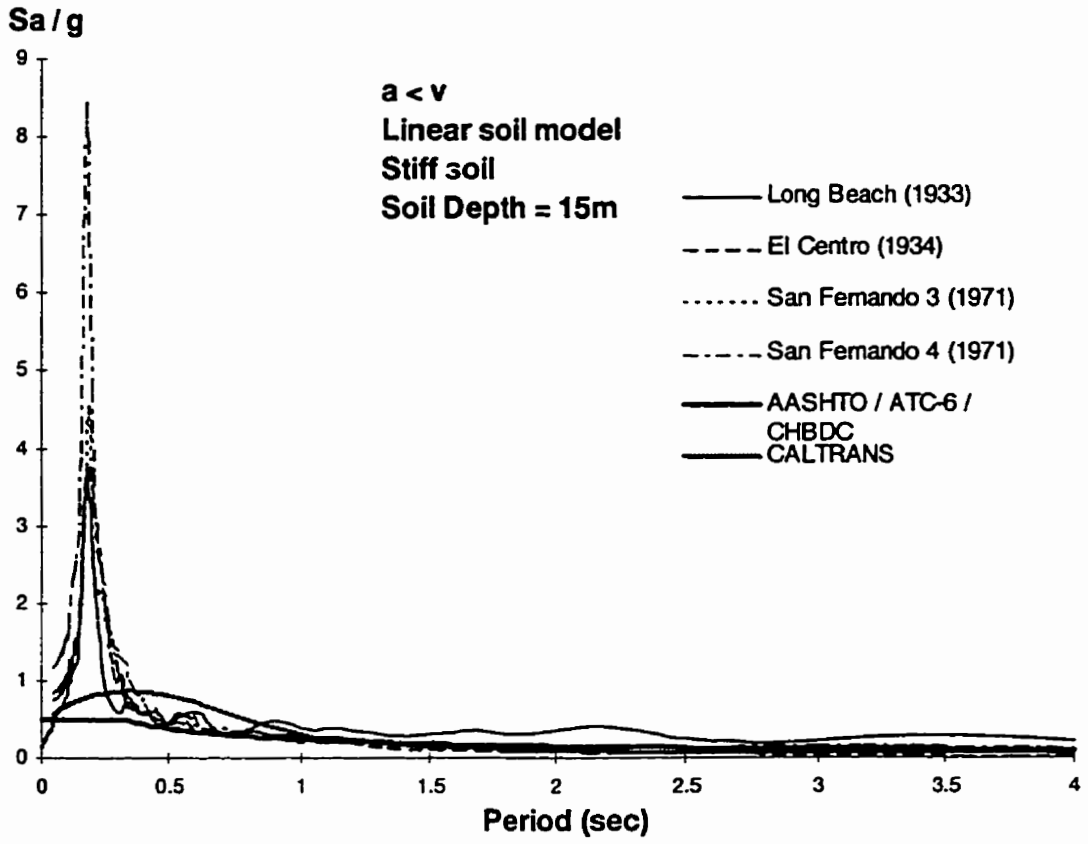

Figure 4.34 Comparison Of Response Spectra For Linear Model of Stiff Soil with 15m Depths Subjected Low a/v Earthquakes To Code Design Response Spectra

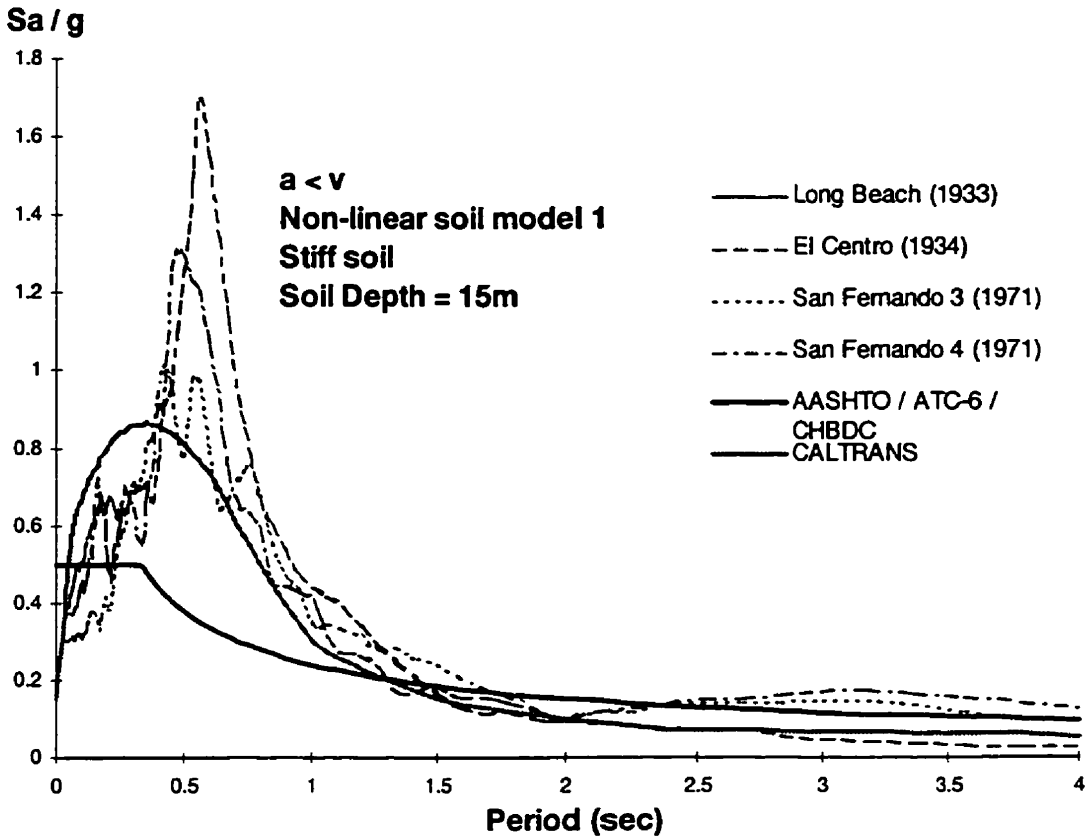

Figure 4.35 Comparison Of Response Spectra For Nonlinear Model 1 of Stiff Soil with 15m Depths Subjected Low a/v Earthquakes To Code Design Response Spectra

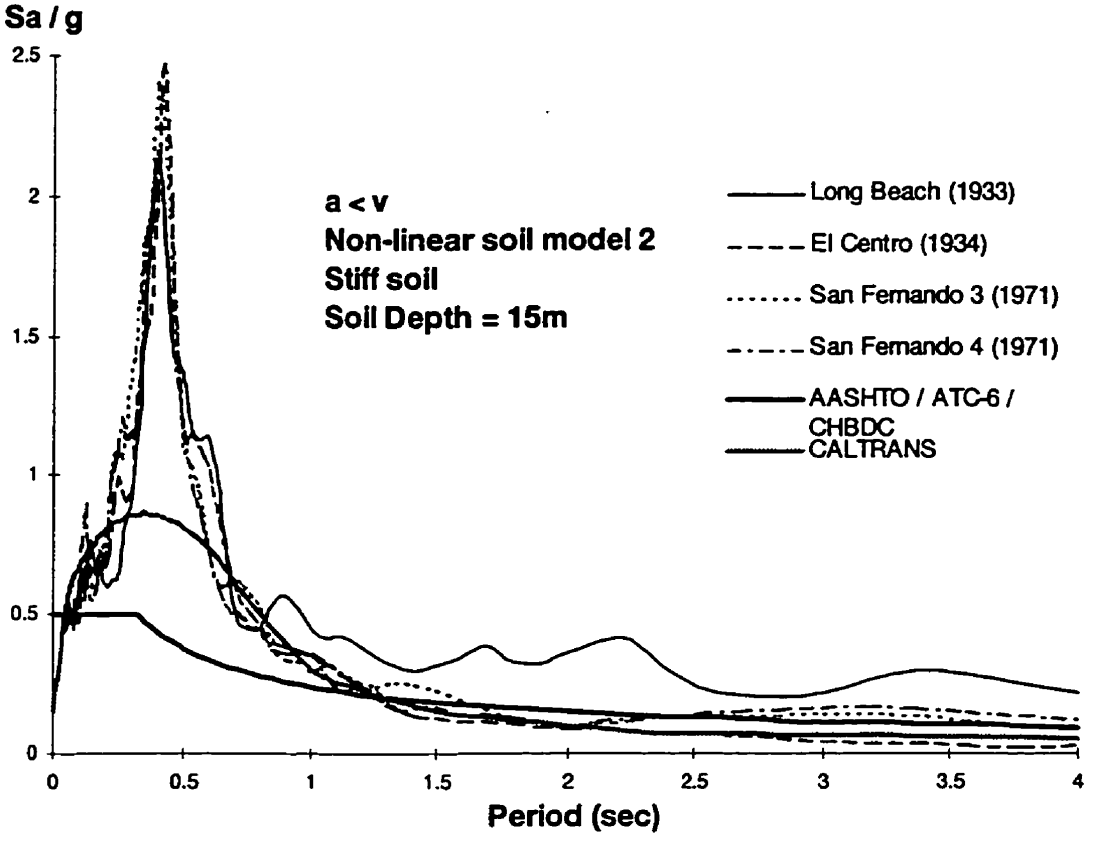

Figure 4.36 Comparison Of Response Spectra For Nonlinear Model 2 of Stiff Soil with 15m Depths Subjected Low a/v Earthquakes To Code Design Response Spectra

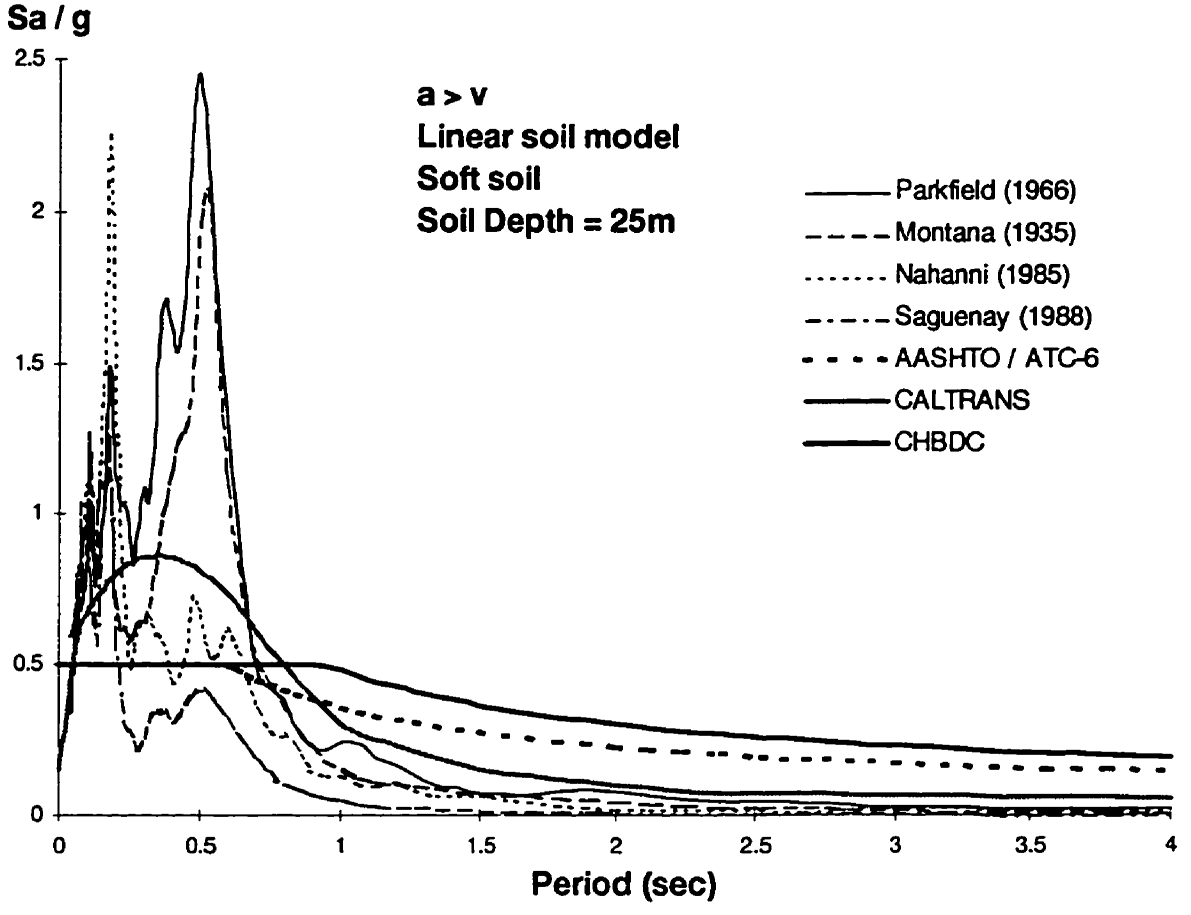

Figure 4.37 Comparison Of Response Spectra For Linear Model of Soft Soil with 25m Depths Subjected High a/v Earthquakes To Code Design Response Spectra

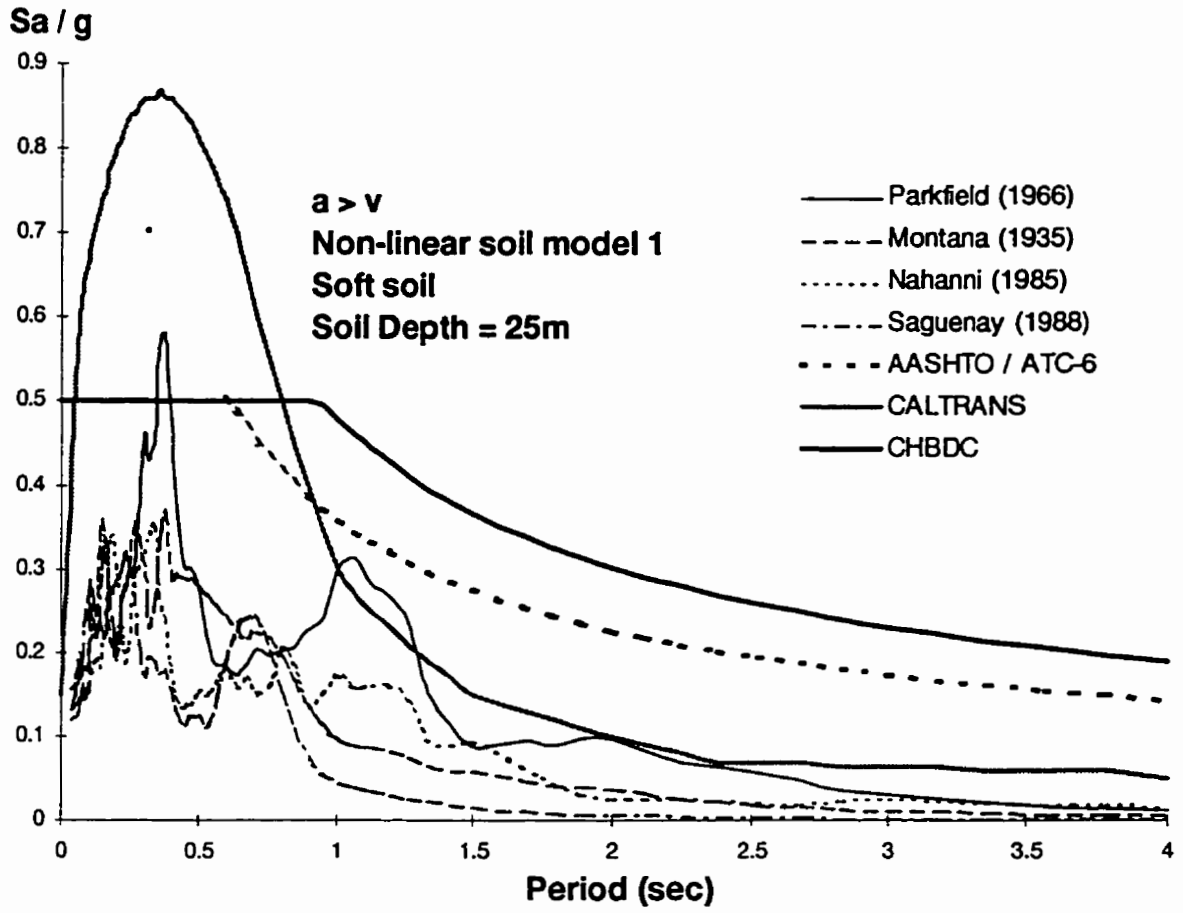

Figure 4.38 Comparison Of Response Spectra For Nonlinear Model 1 of Soft Soil with 25m Depths Subjected High a/v Earthquakes To Code Design Response Spectra

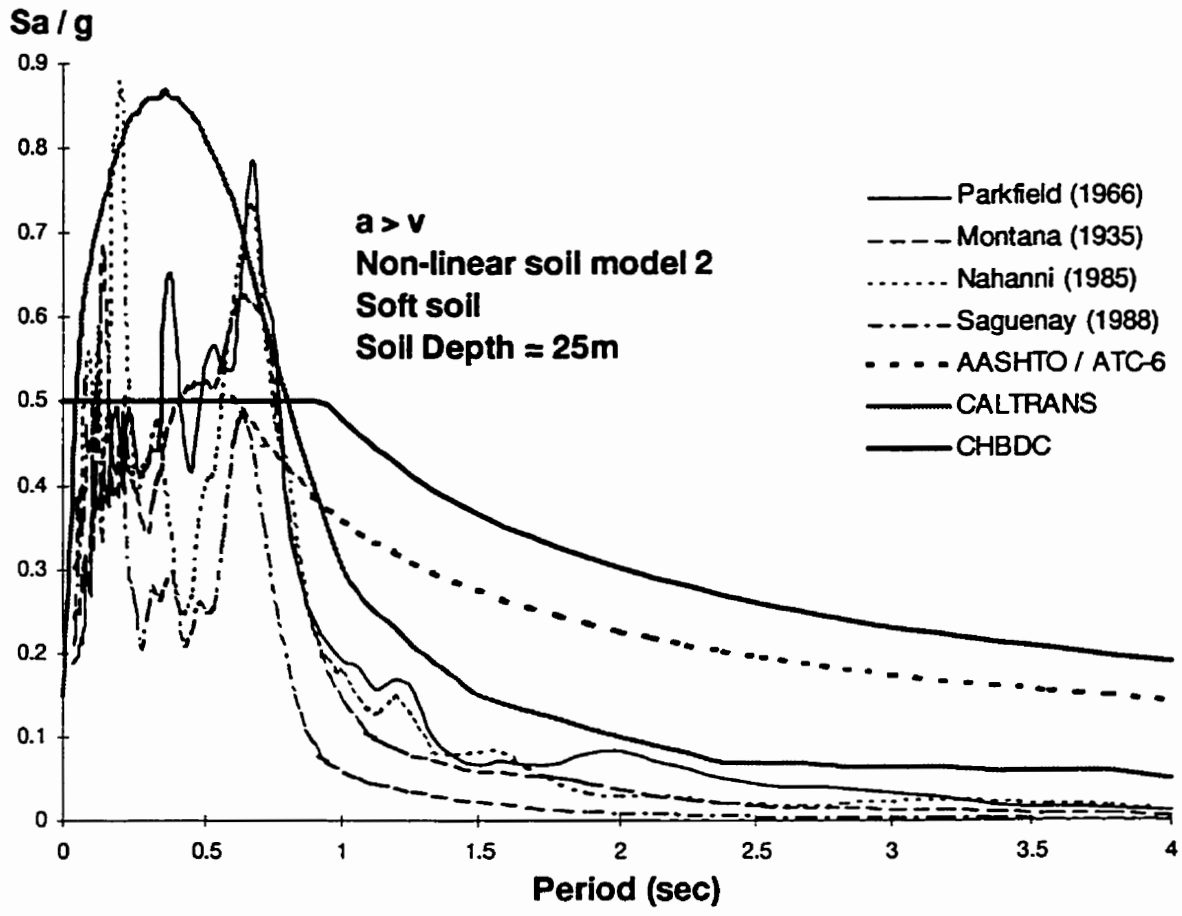

Figure 4.39 Comparison Of Response Spectra For Nonlinear Model 2 of Soft Soil with 25m Depths Subjected High a/v Earthquakes To Code Design Response Spectra

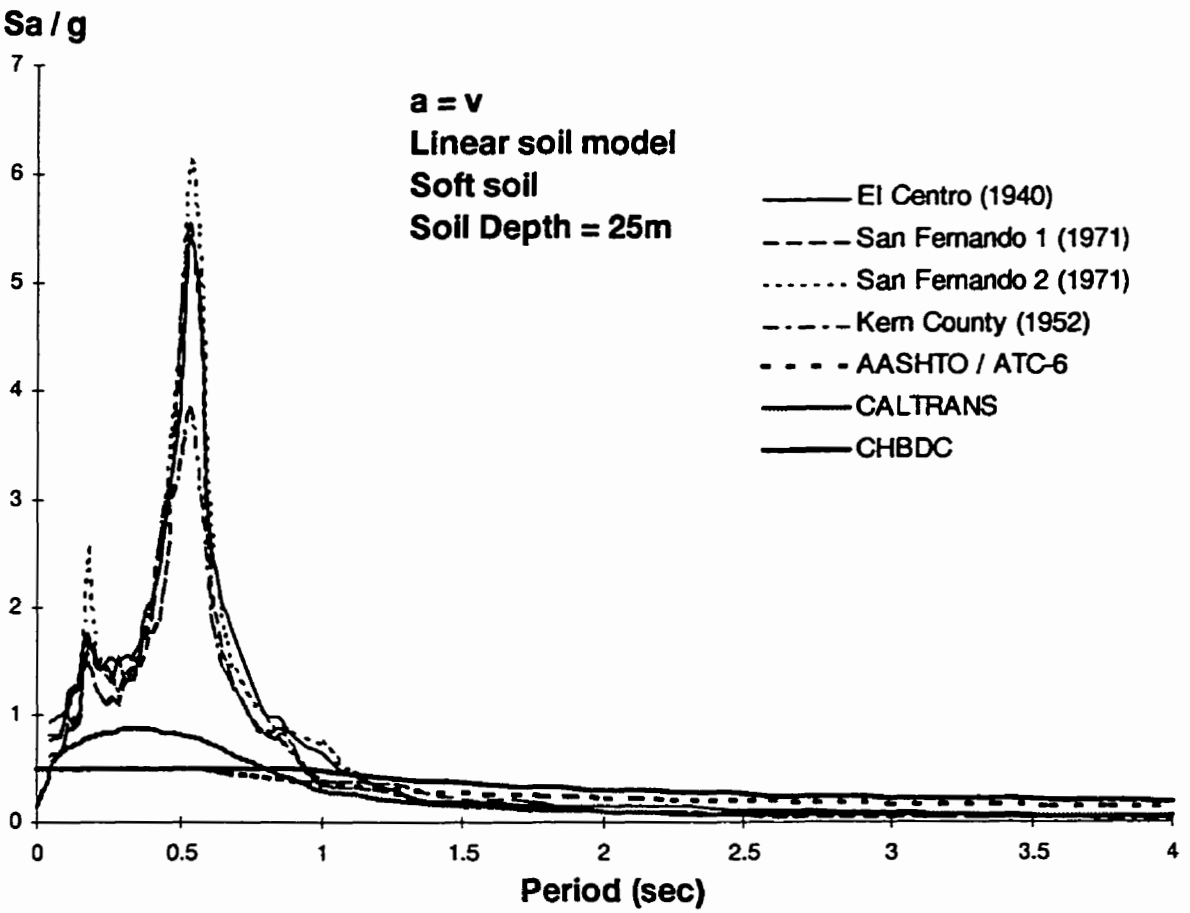

Figure 4.40 Comparison Of Response Spectra For Linear Model of Soft Soil with 25m Depths Subjected Intermediate a/v Earthquakes To Code Design Response Spectra

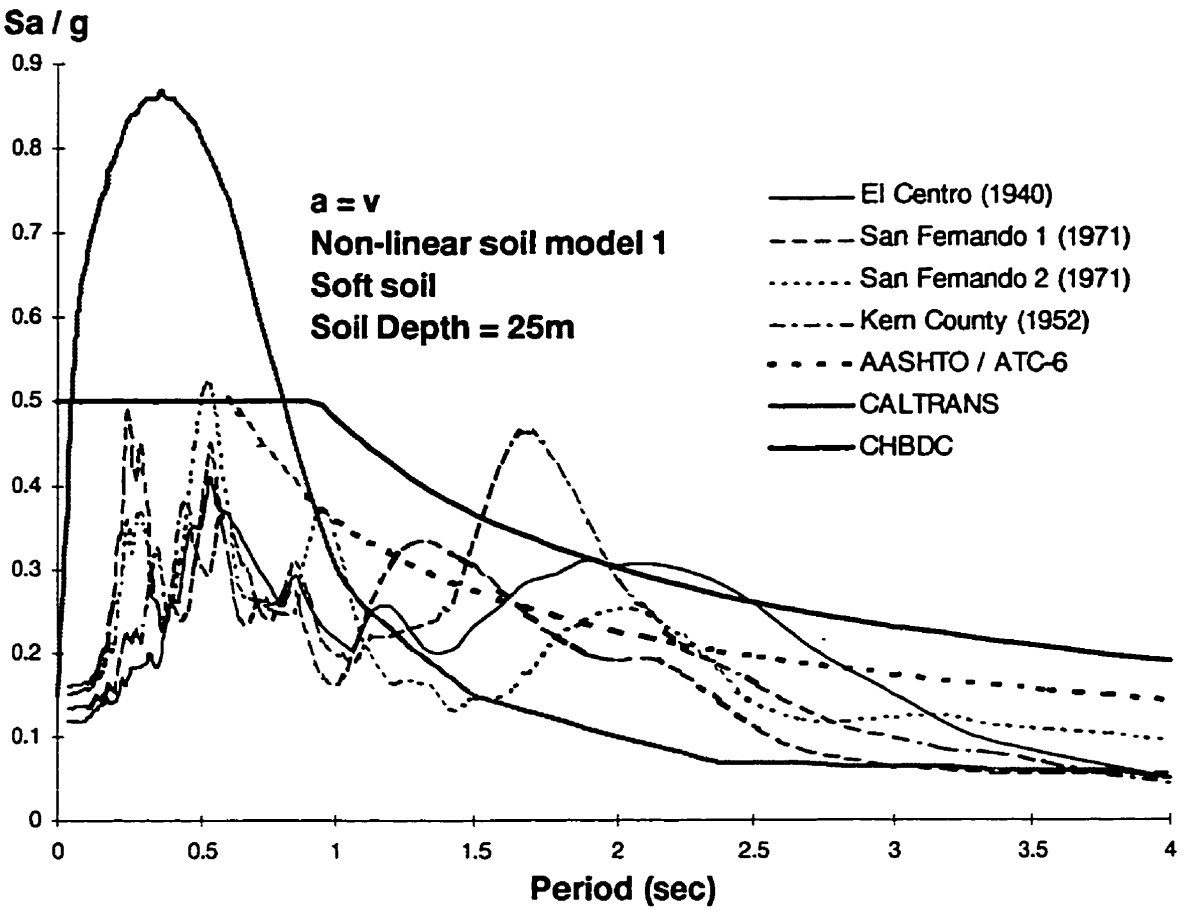

Figure 4.41 Comparison Of Response Spectra For Nonlinear Model 1 of Soft Soil with 25m Depths Subjected Intermediate a/v Earthquakes To Code Design Response Spectra

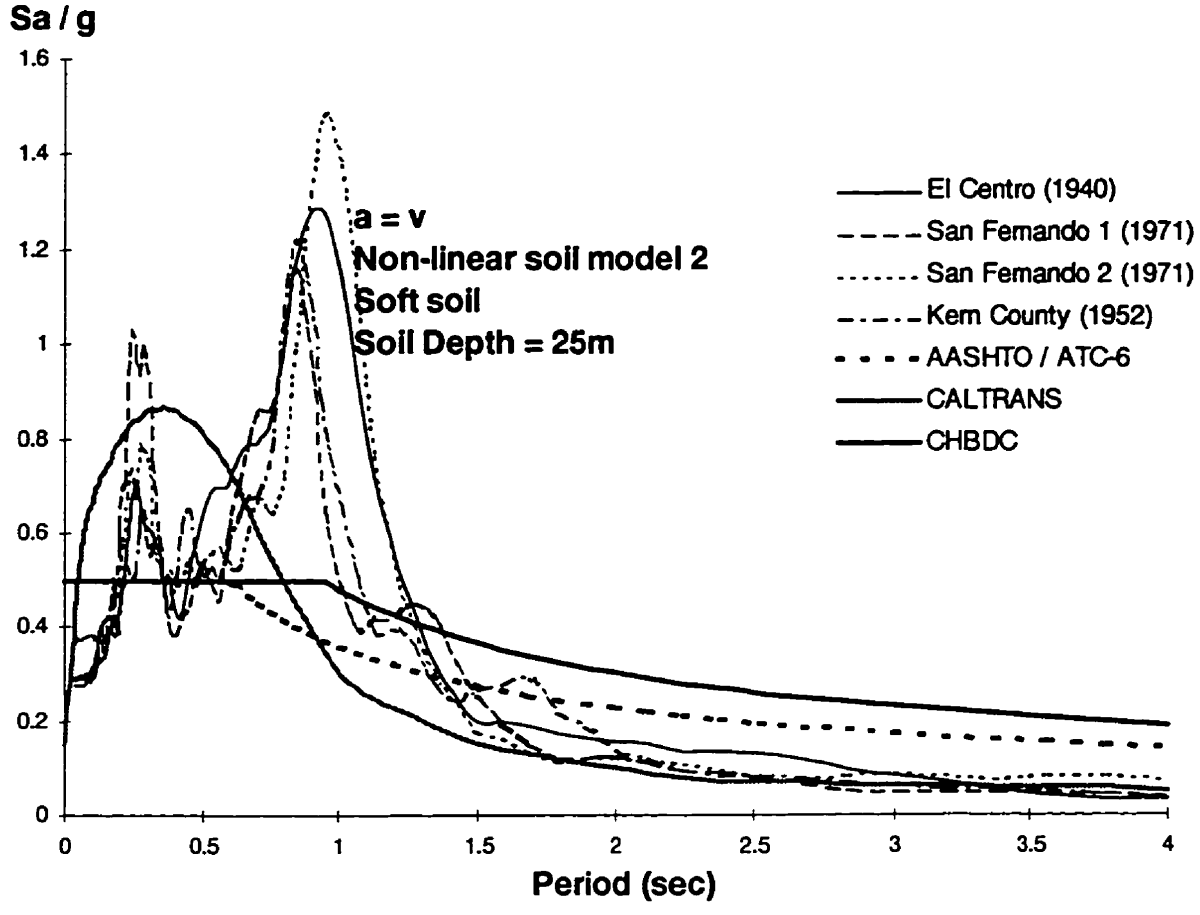

Figure 4.42 Comparison Of Response Spectra For Nonlinear Model 2 of Soft Soil with 25m Depths Subjected Intermediate a/v Earthquakes To Code Design Response Spectra

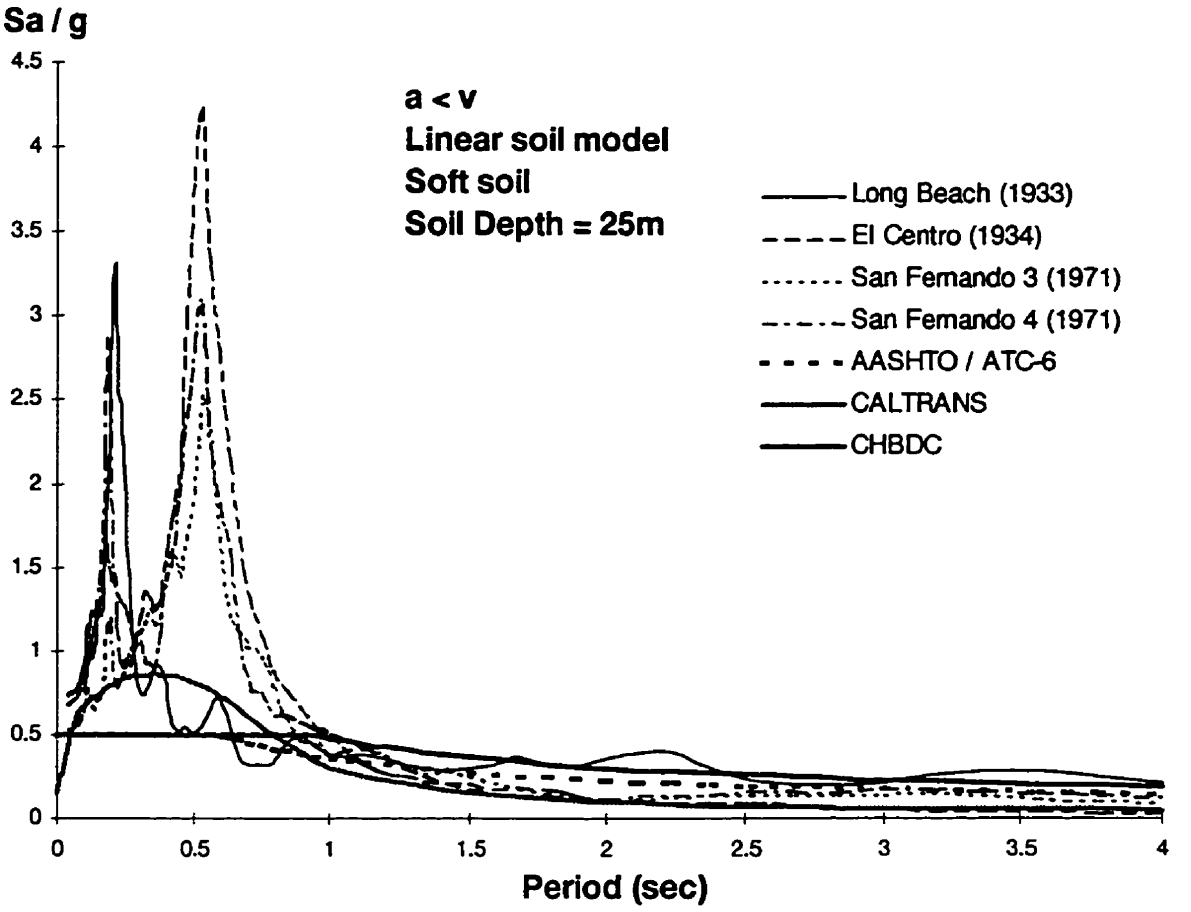

Figure 4.43 Comparison Of Response Spectra For Linear Model of Soft Soil with 25m Depths Subjected Low a/v Earthquakes To Code Design Response Spectra

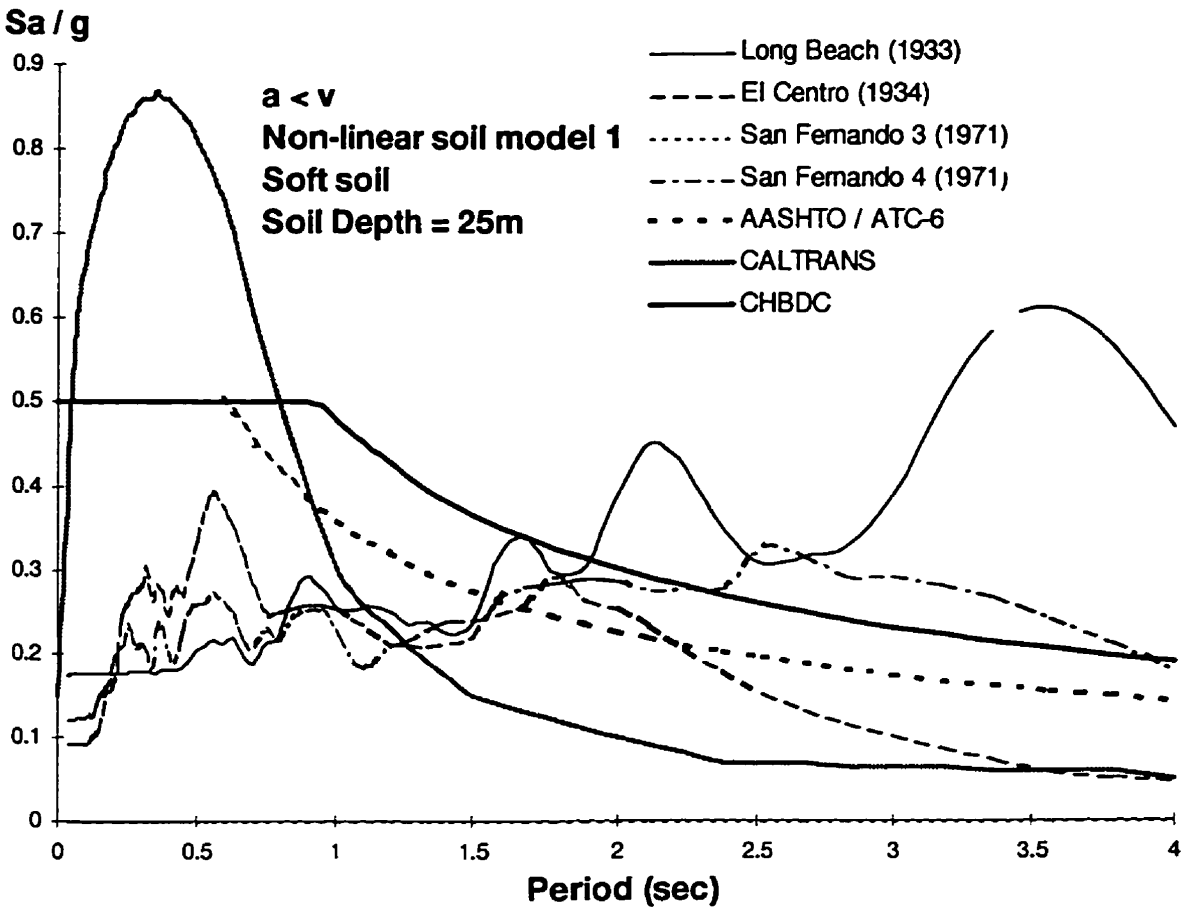

Figure 4.44 Comparison Of Response Spectra For Nonlinear Model 1 of Soft Soil with 25m Depths Subjected Low a/v Earthquakes To Code Design Response Spectra

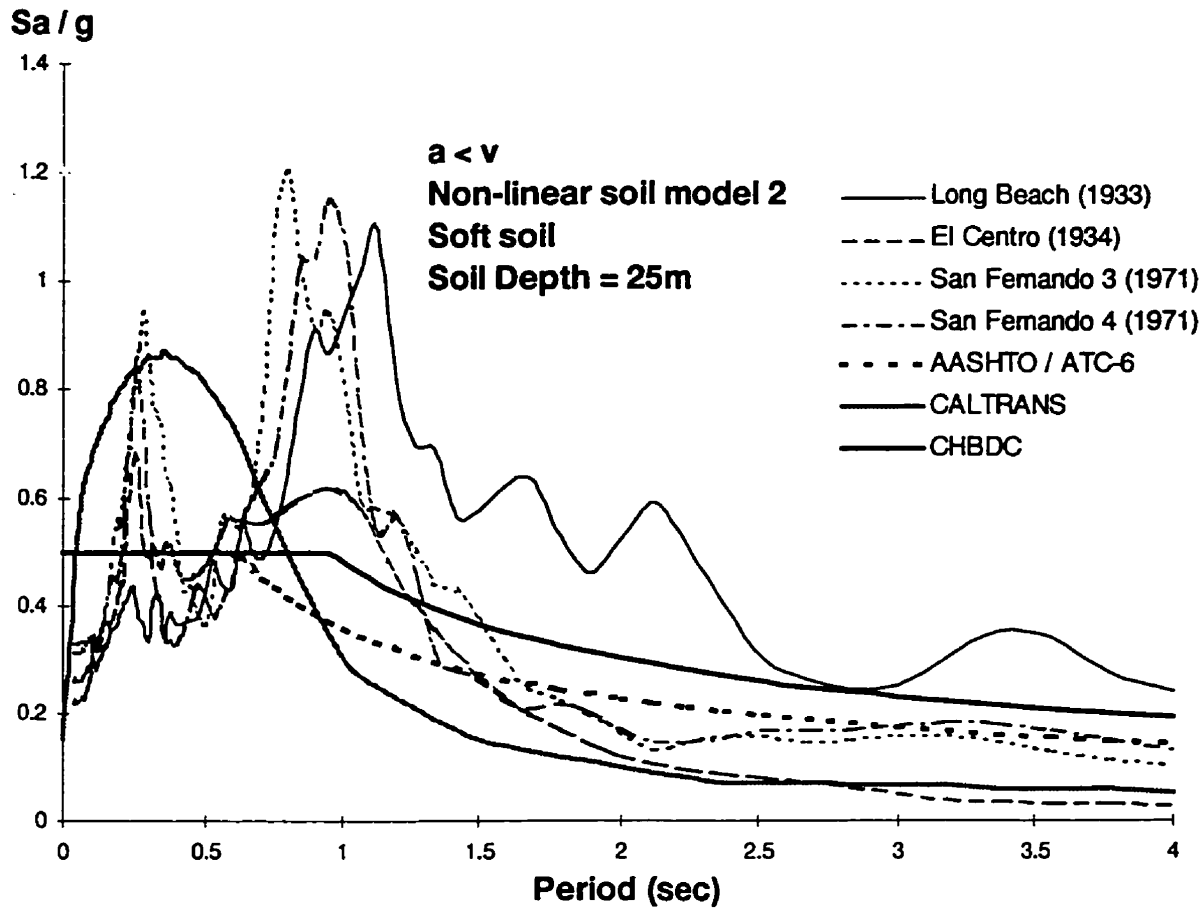

Figure 4.45 Comparison Of Response Spectra For Nonlinear Model 2 of Soft Soil with 25m Depths Subjected Low a/v Earthquakes To Code Design Response Spectra

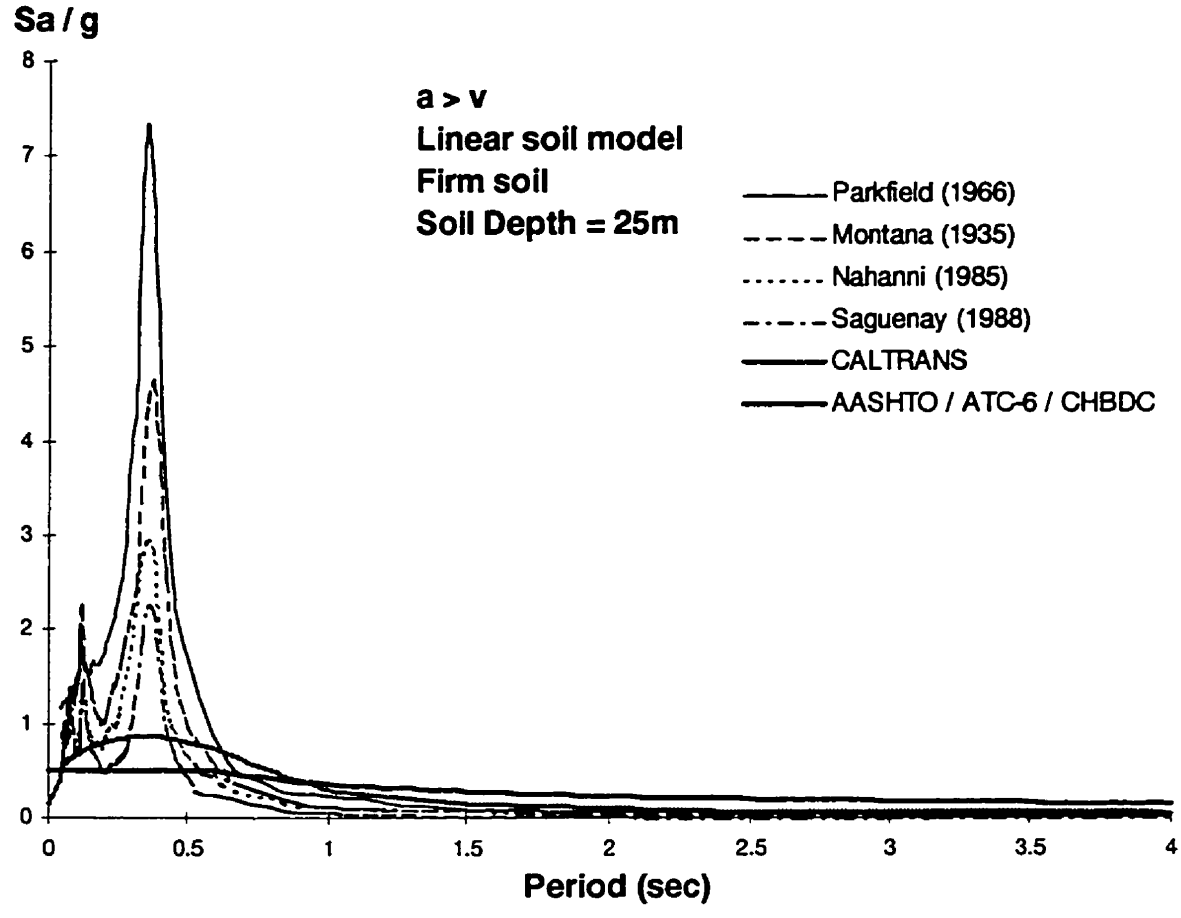

Figure 4.46 Comparison Of Response Spectra For Linear Model of Firm Soil with 25m Depths Subjected High a/v Earthquakes To Code Design Response Spectra

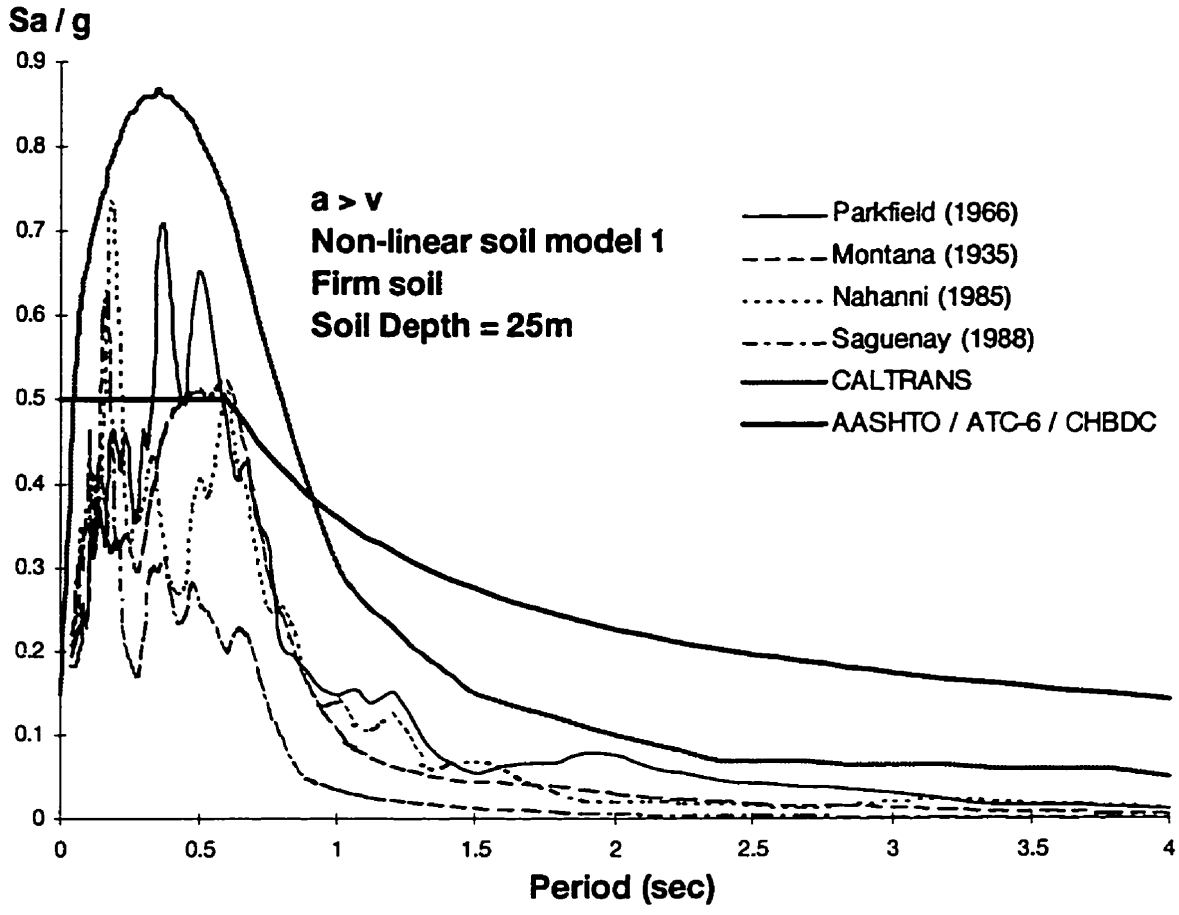

Figure 4.47 Comparison Of Response Spectra For Nonlinear Model 1 of Firm Soil with 25m Depths Subjected High a/v Earthquakes To Code Design Response Spectra

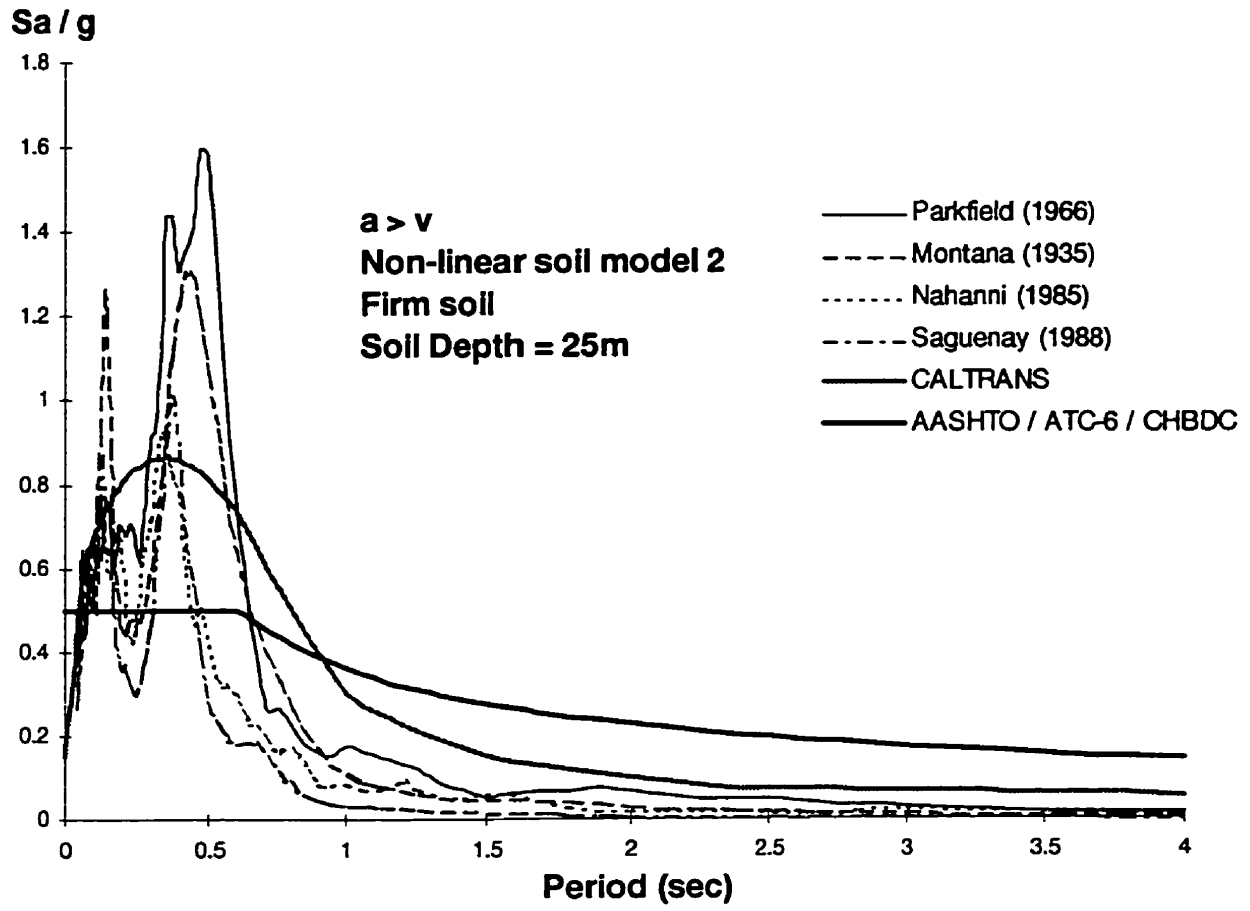

Figure 4.48 Comparison Of Response Spectra For Nonlinear Model 2 of Firm Soil with 25m Depths Subjected High a/v Earthquakes To Code Design Response Spectra

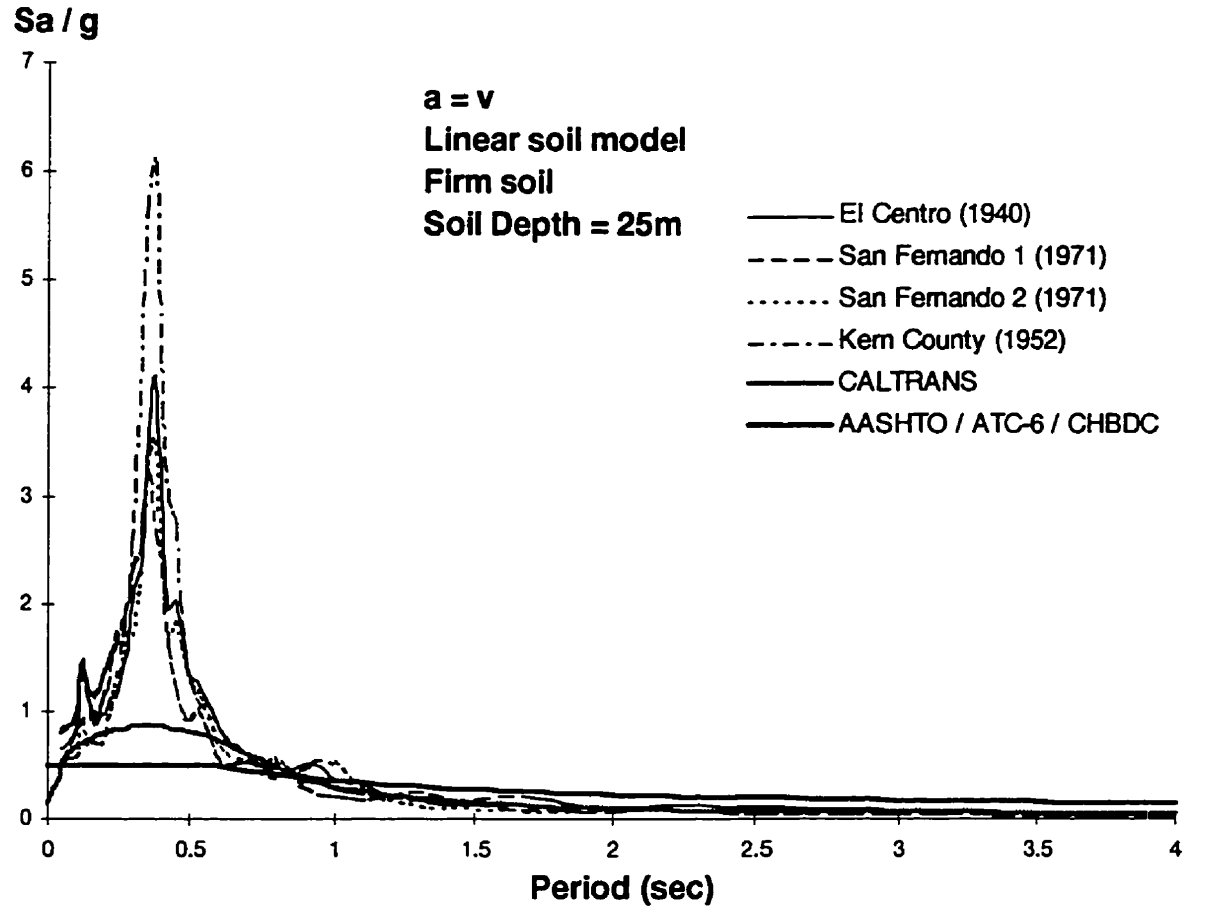

Figure 4.49 Comparison Of Response Spectra For Linear Model of Firm Soil with 25m Depths Subjected Intermediate a/v Earthquakes To Code Design Response Spectra

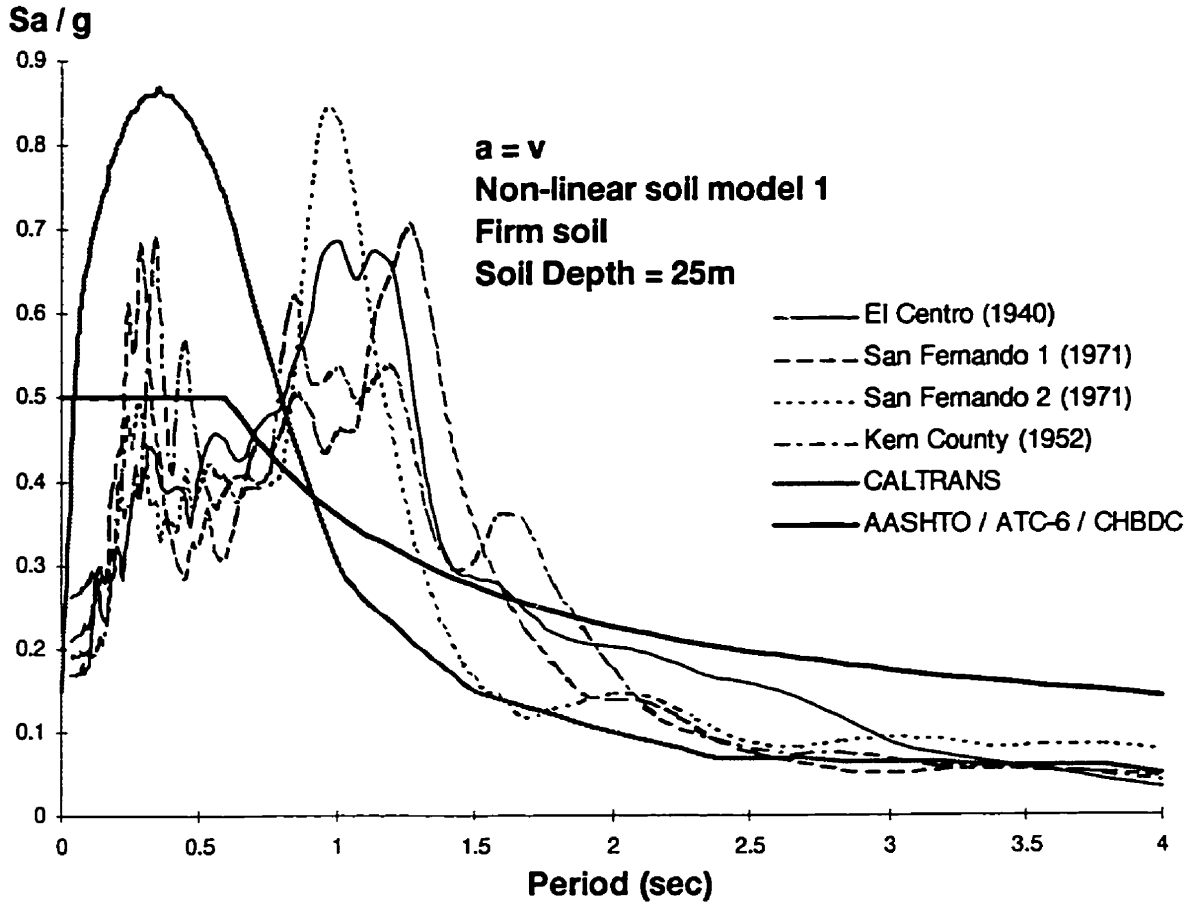

Figure 4.50 Comparison Of Response Spectra For Nonlinear Model 1 of Firm Soil with 25m Depths Subjected Intermediate a/v Earthquakes To Code Design Response Spectra

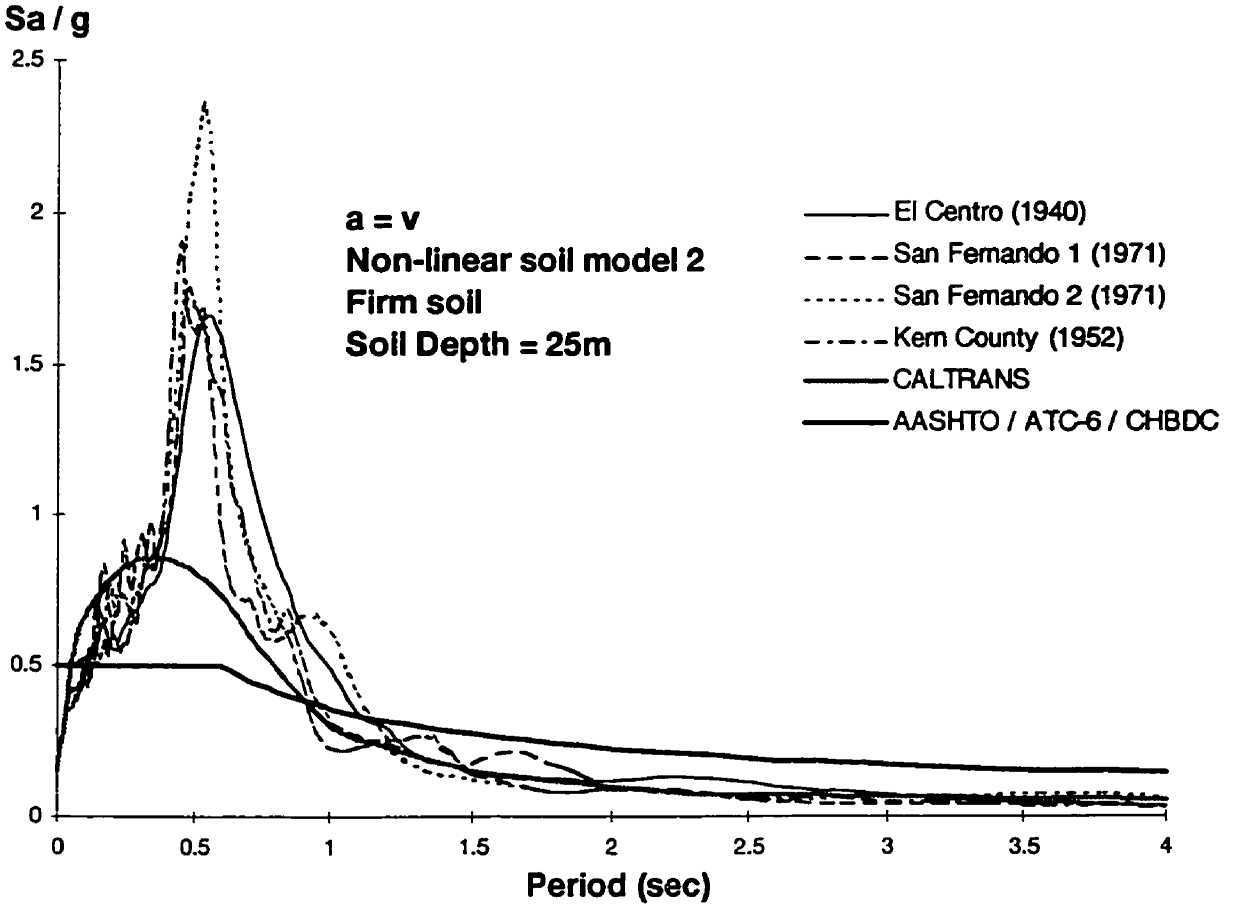

Figure 4.51 Comparison Of Response Spectra For Nonlinear Model 2 of Firm Soil with 25m Depths Subjected Intermediate a/v Earthquakes To Code Design Response Spectra

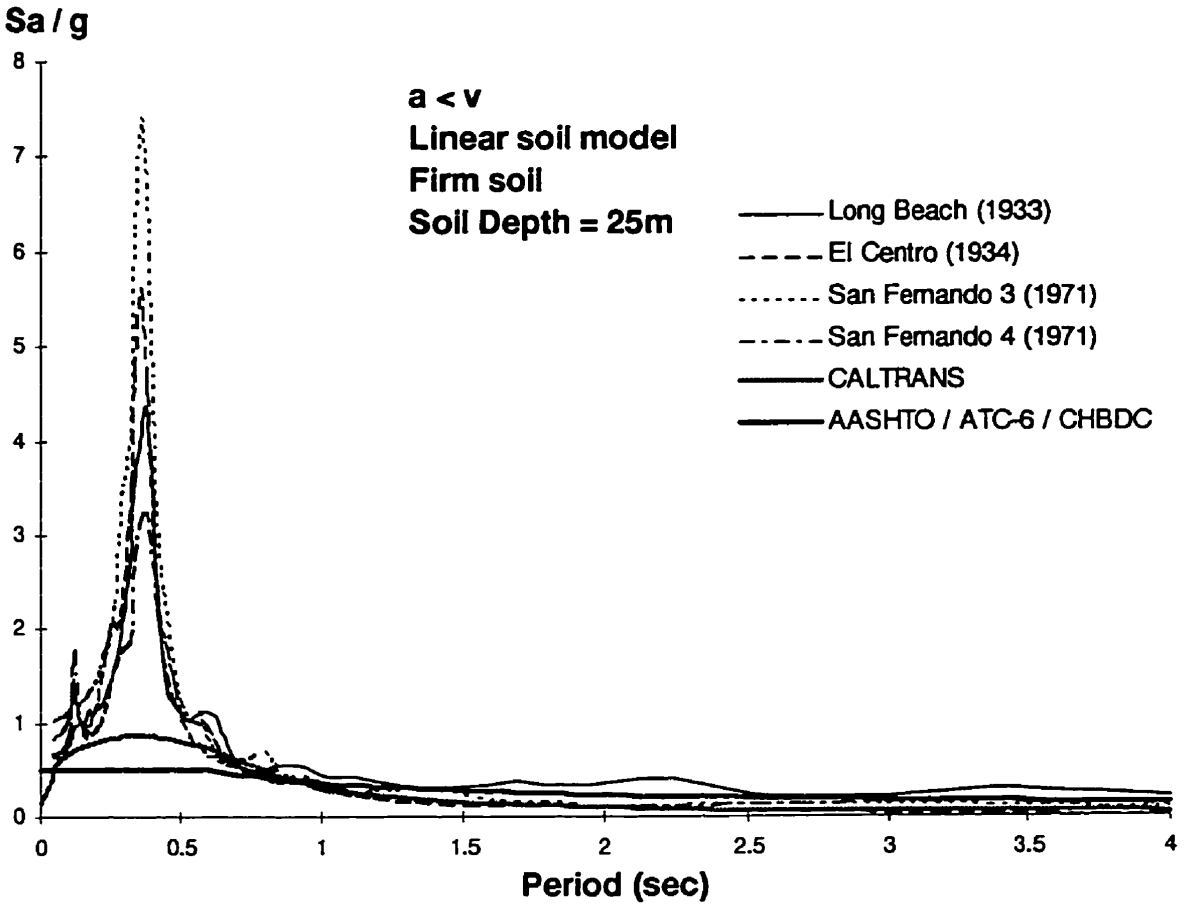

Figure 4.52 Comparison Of Response Spectra For Linear Model of Firm Soil with 25m Depths Subjected Low a/v Earthquakes To Code Design Response Spectra

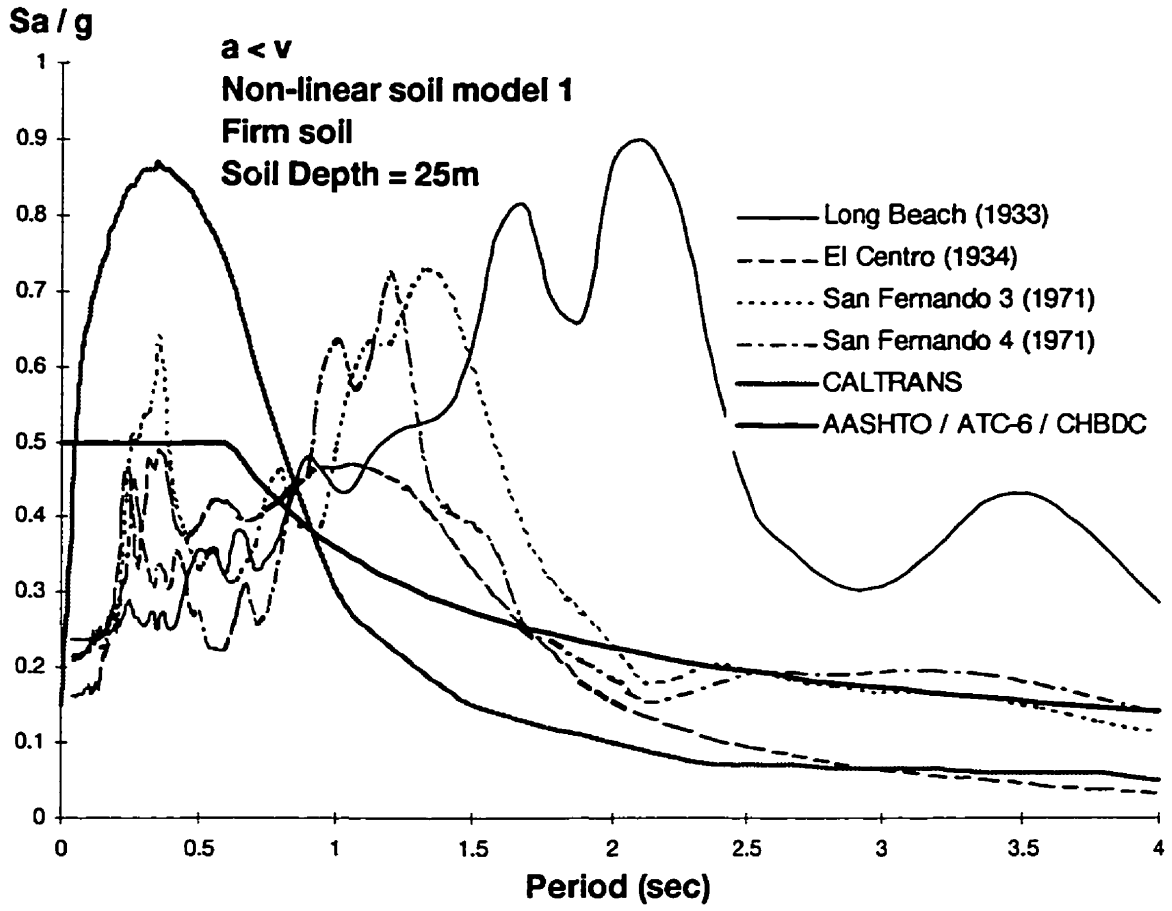

Figure 4.53 Comparison Of Response Spectra For Nonlinear Model 1 of Firm Soil with 25m Depths Subjected Low a/v Earthquakes To Code Design Response Spectra

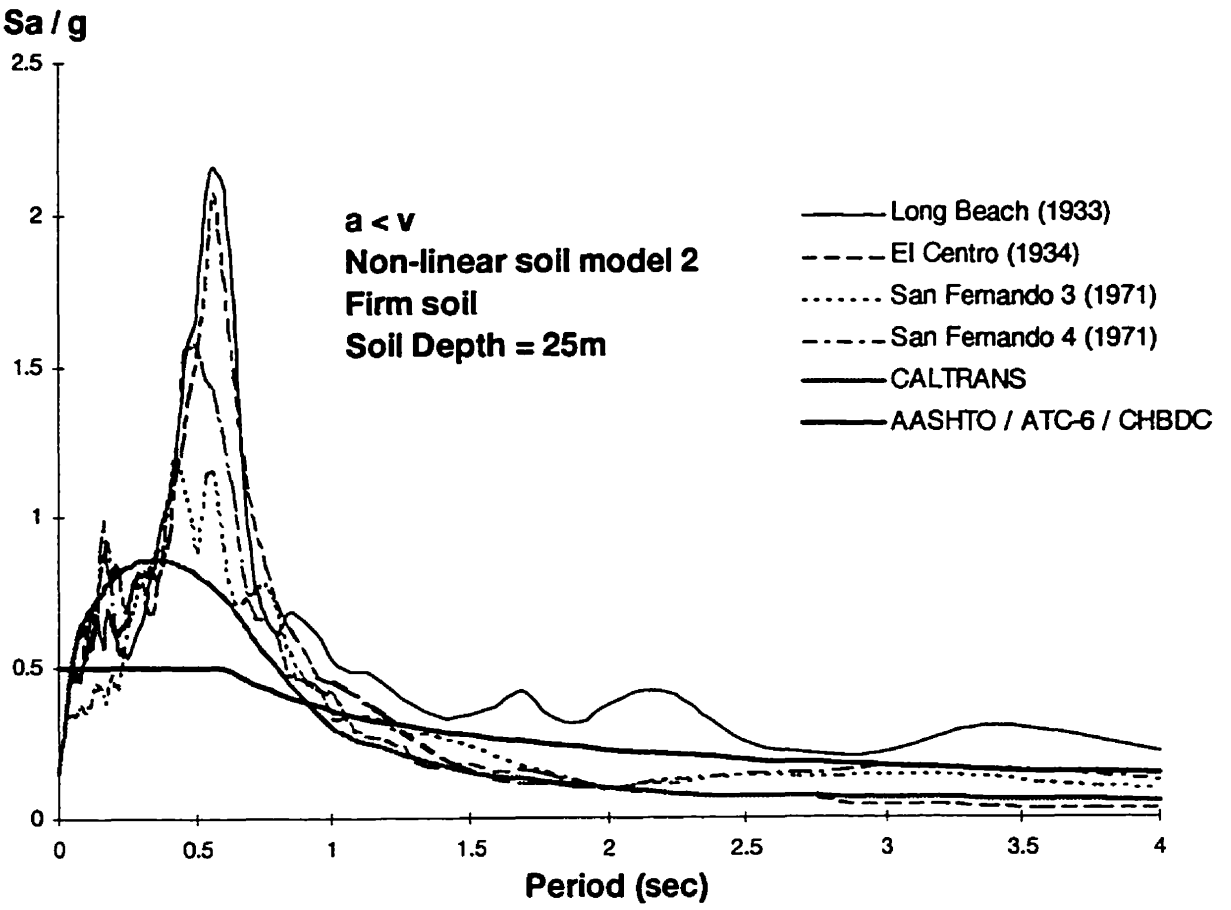

Figure 4.54 Comparison Of Response Spectra For Nonlinear Model 2 of Firm Soil with 25m Depths Subjected Low a/v Earthquakes To Code Design Response Spectra

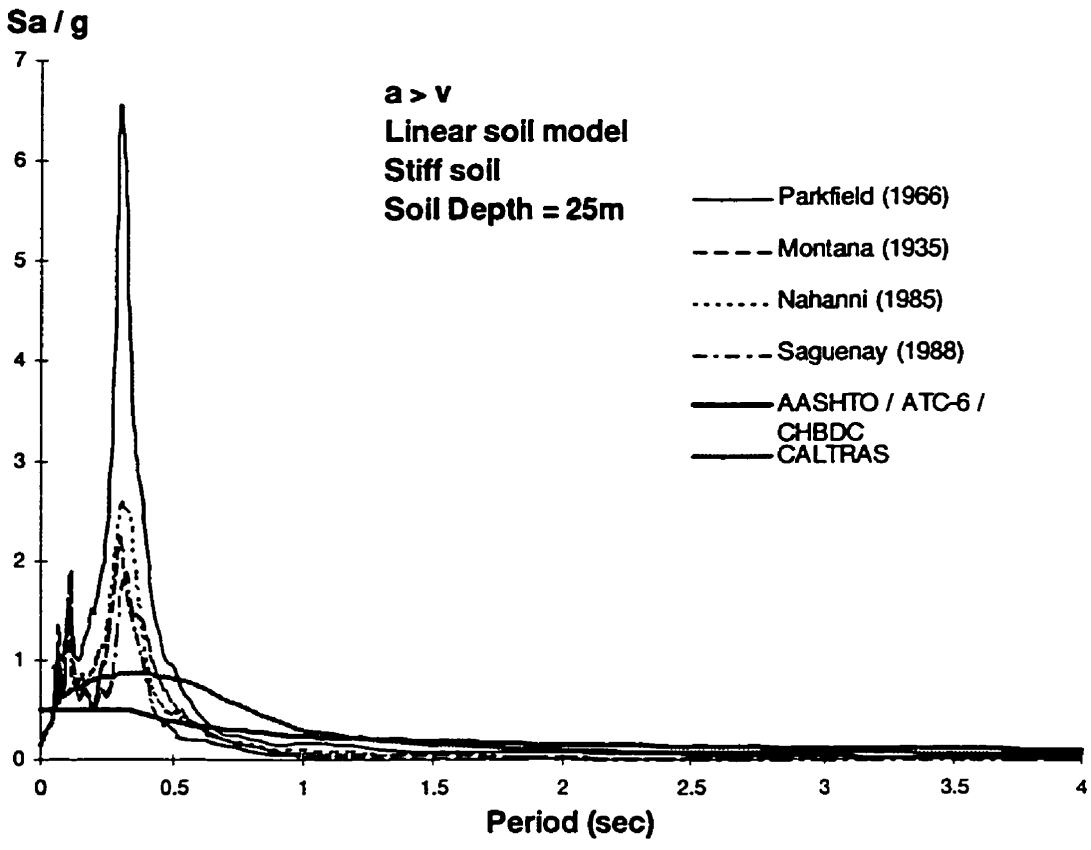

Figure 4.55 Comparison Of Response Spectra For Linear Model of Stiff Soil with 25m Depths Subjected High a/v Earthquakes To Code Design Response Spectra

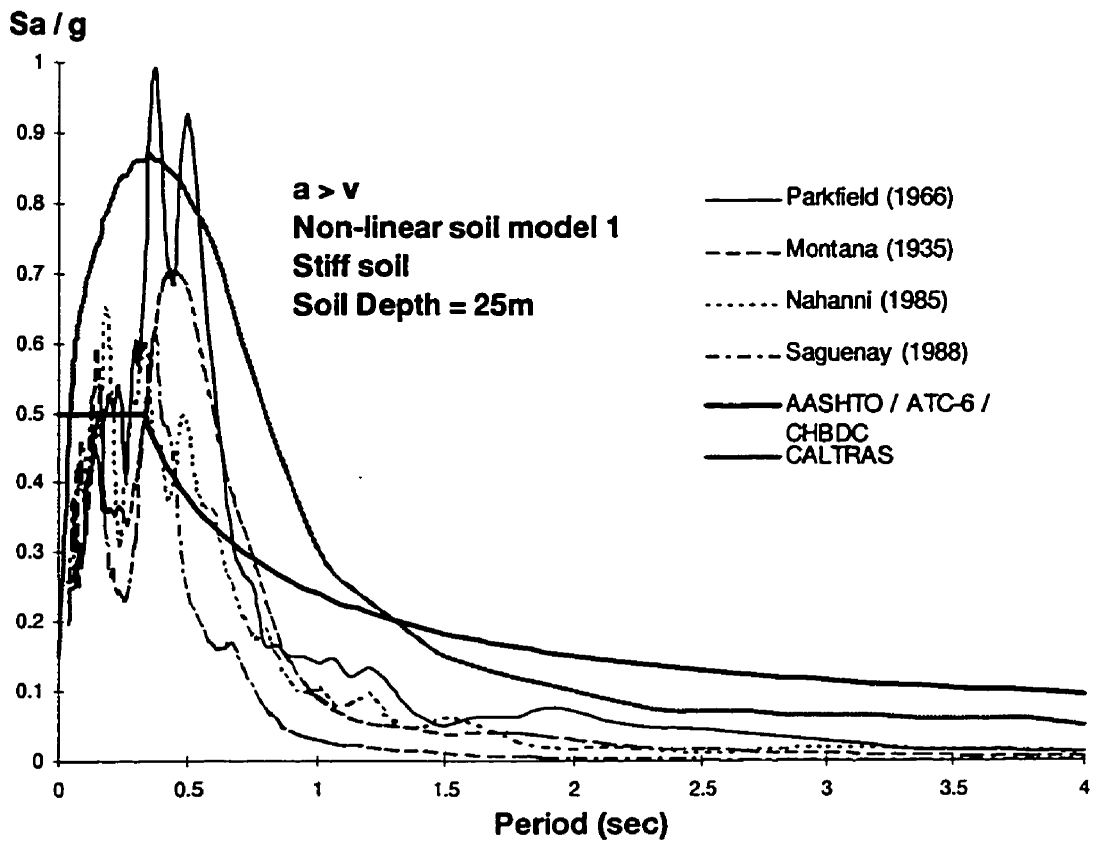

Figure 4.56 Comparison Of Response Spectra For Nonlinear Model 1 of Stiff Soil with 25m Depths Subjected High a/v Earthquakes To Code Design Response Spectra

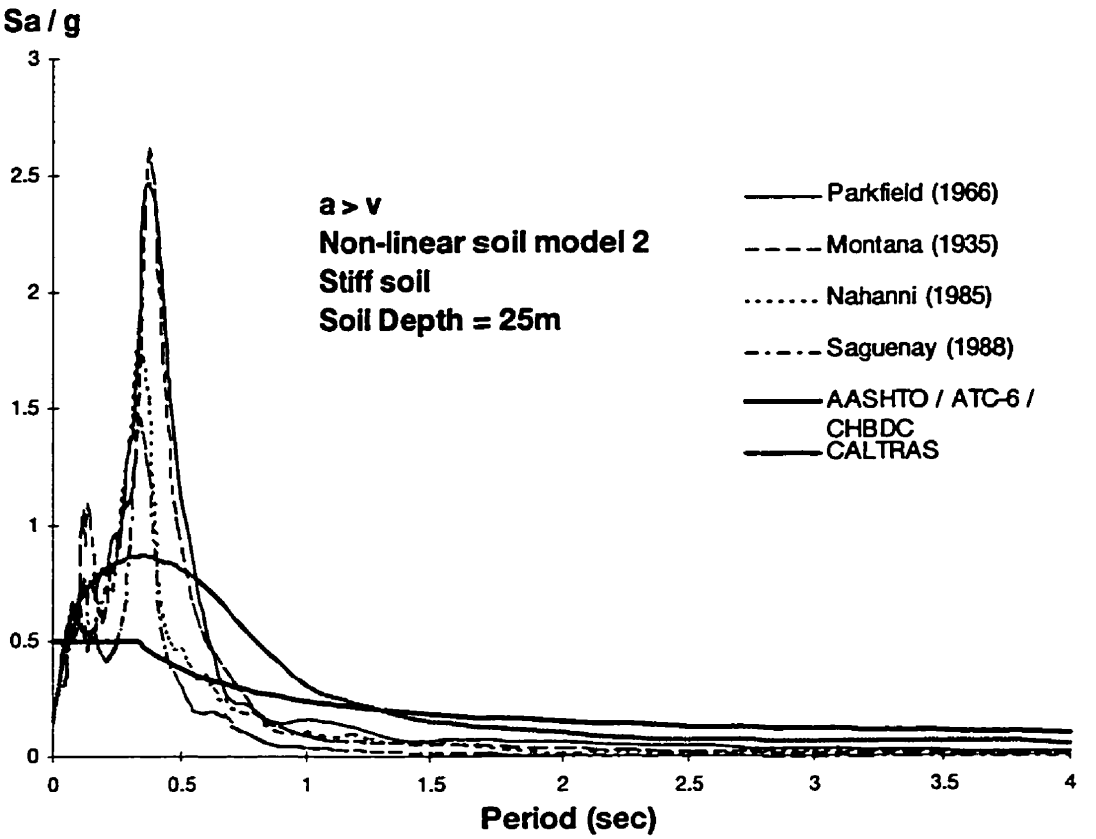

Figure 4.57 Comparison Of Response Spectra For Nonlinear Model 2 of Stiff Soil with 25m Depths Subjected High a/v Earthquakes To Code Design Response Spectra

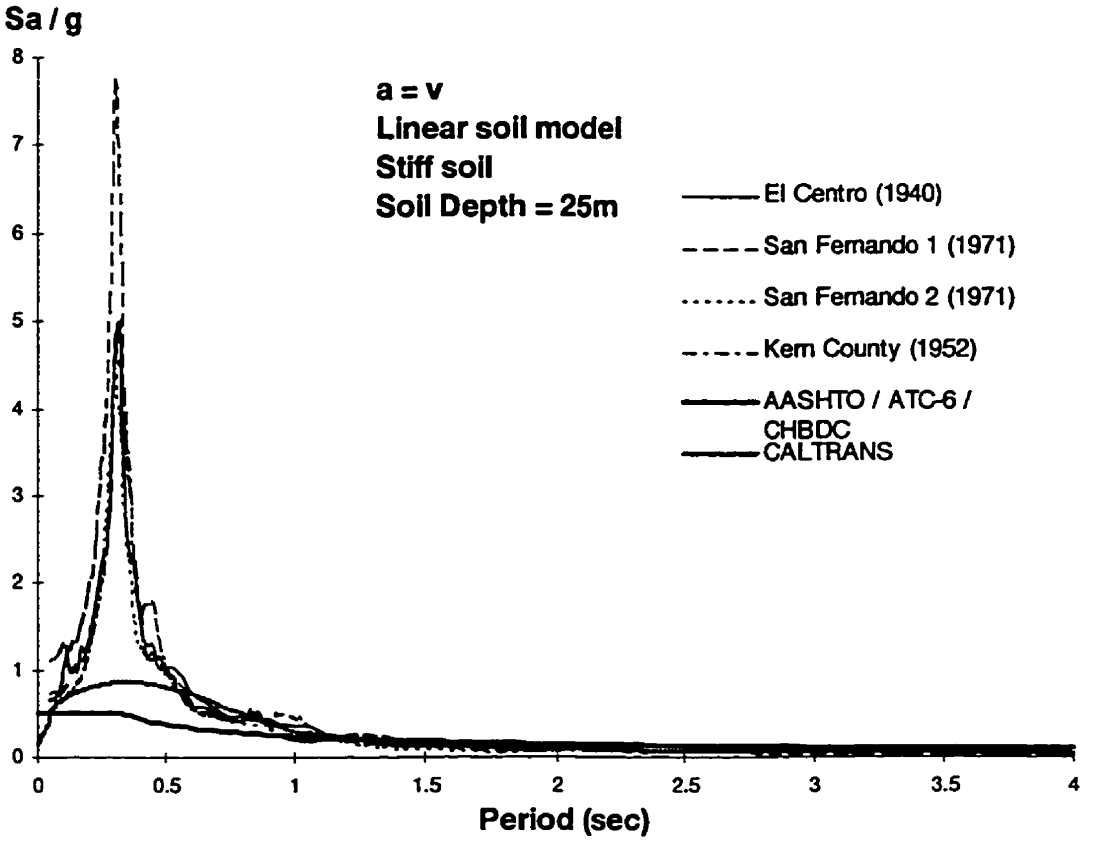

Figure 4.58 Comparison Of Response Spectra For Linear Model of Stiff Soil with 25m Depths Subjected Intermediate a/v Earthquakes To Code Design Response Spectra

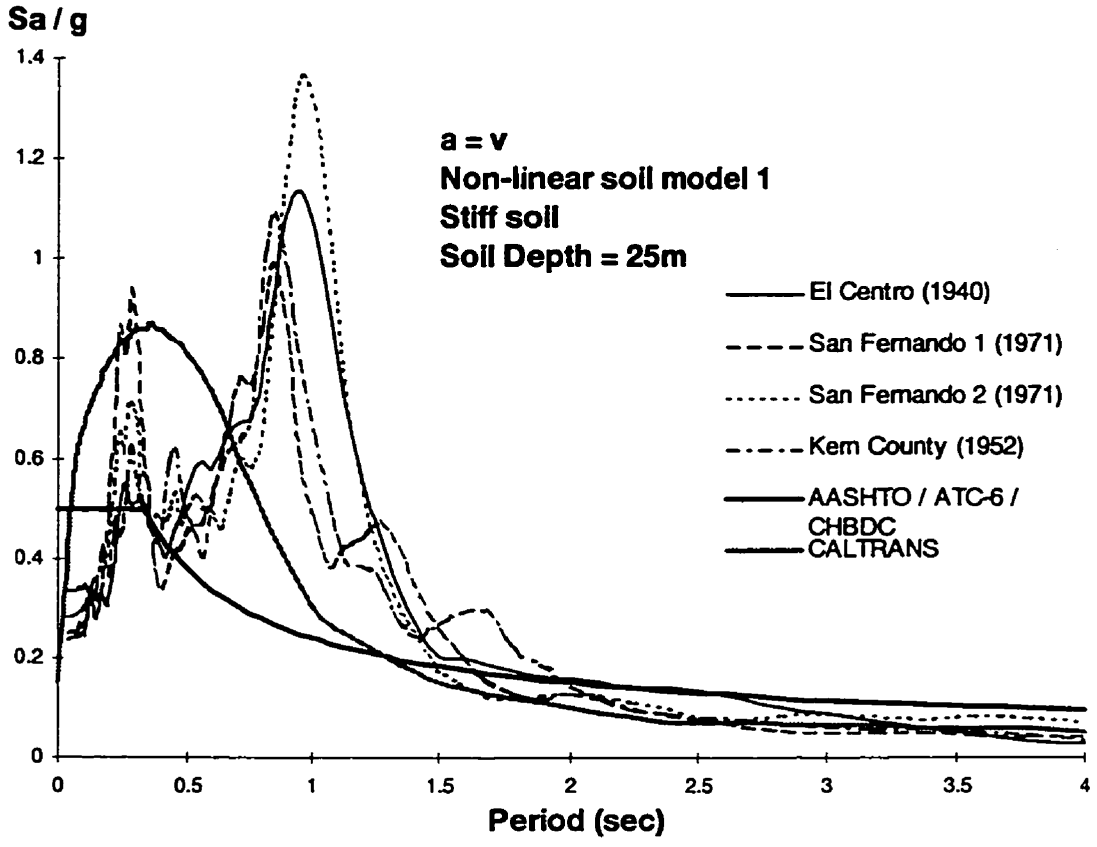

Figure 4.59 Comparison Of Response Spectra For Nonlinear Model 1 of Stiff Soil with 25m Depths Subjected Intermediate a/v Earthquakes To Code Design Response Spectra

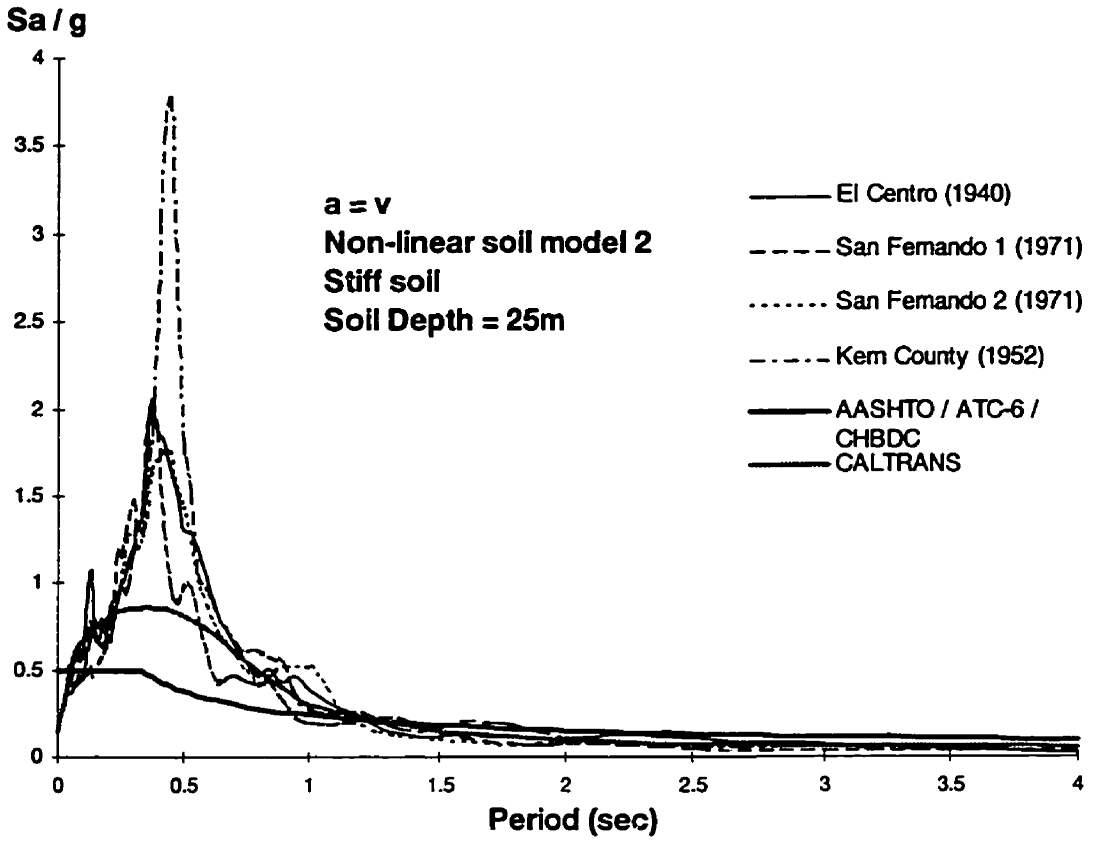

Figure 4.60 Comparison Of Response Spectra For Nonlinear Model 2 of Firm Soil with 25m Depths Subjected Intermediate a/v Earthquakes To Code Design Response Spectra

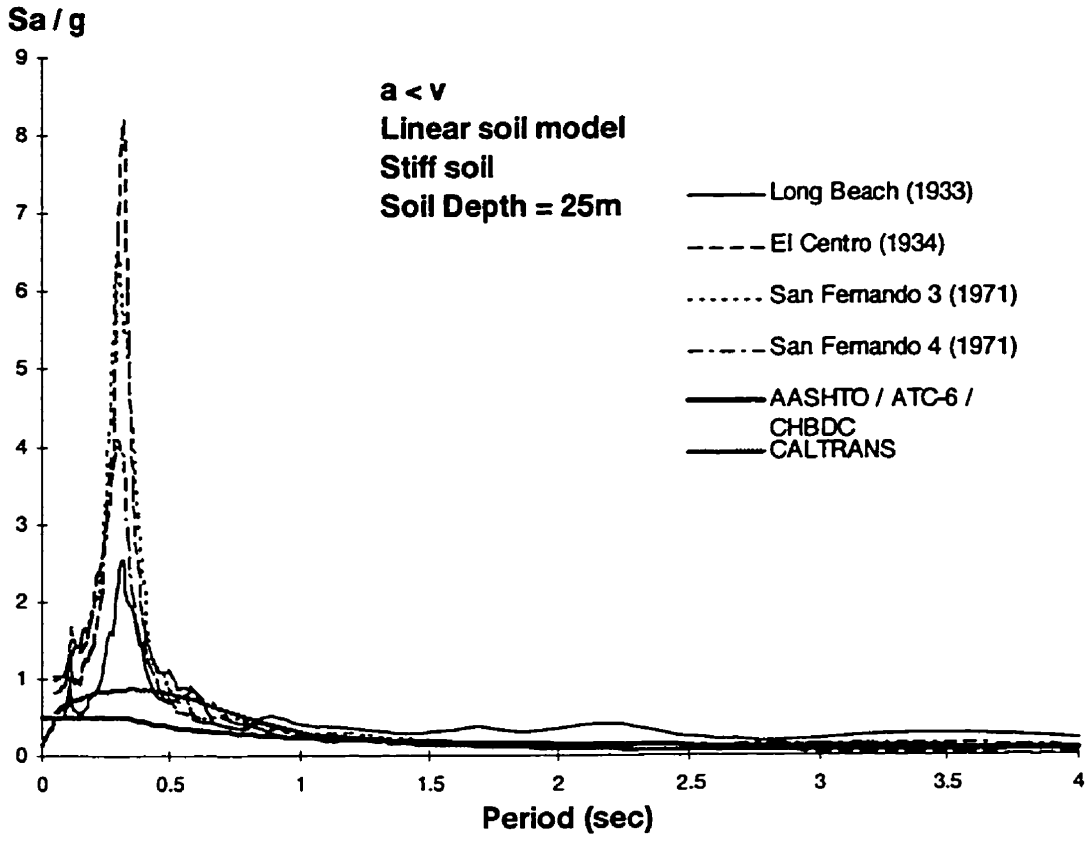

Figure 4.61 Comparison Of Response Spectra For Linear Model of Stiff Soil with 25m Depths Subjected Low a/v Earthquakes To Code Design Response Spectra

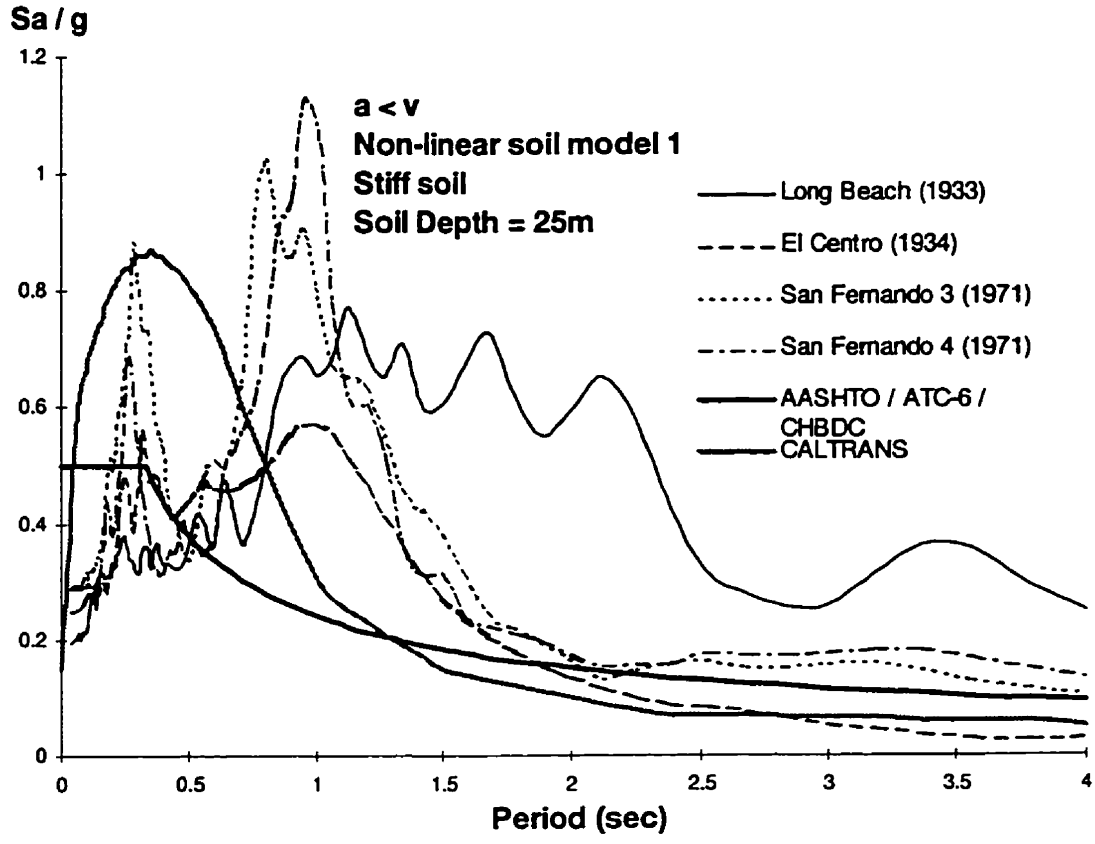

Figure 4.62 Comparison Of Response Spectra For Nonlinear Model 1 of Stiff Soil with 25m Depths Subjected Low a/v Earthquakes To Code Design Response Spectra

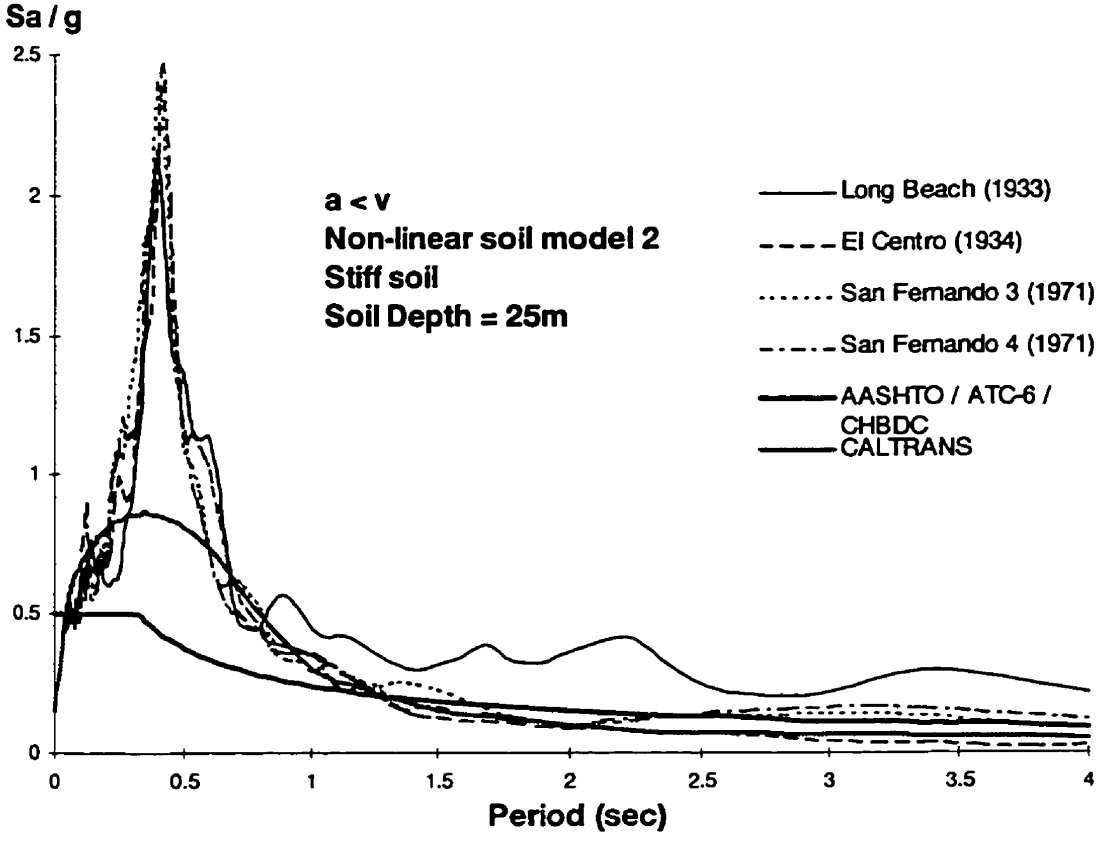

Figure 4.63 Comparison Of Response Spectra For Nonlinear Model 2 of Stiff Soil with 25m Depths Subjected Low a/v Earthquakes To Code Design Response Spectra

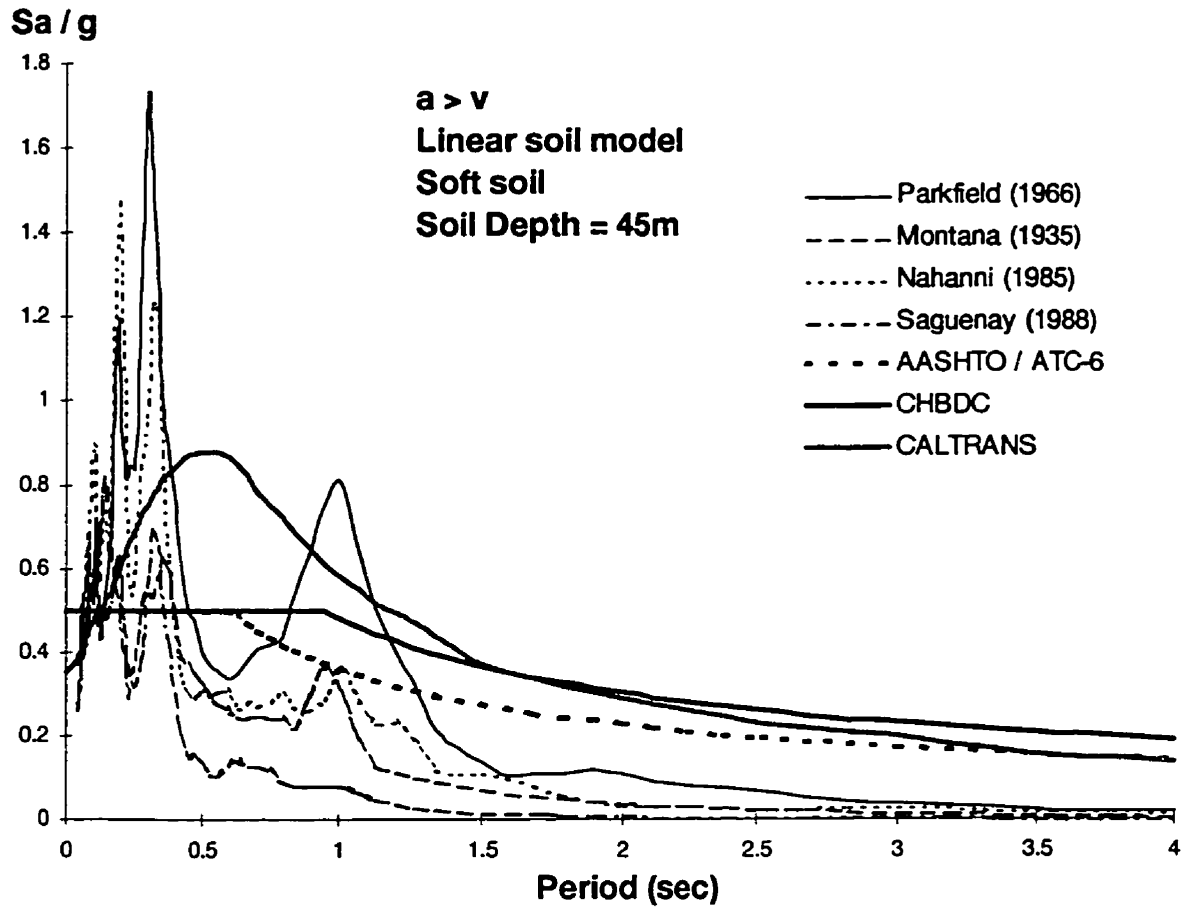

Figure 4.64 Comparison Of Response Spectra For Linear Model of Soft Soil with 45m Depths Subjected High a/v Earthquakes To Code Design Response Spectra

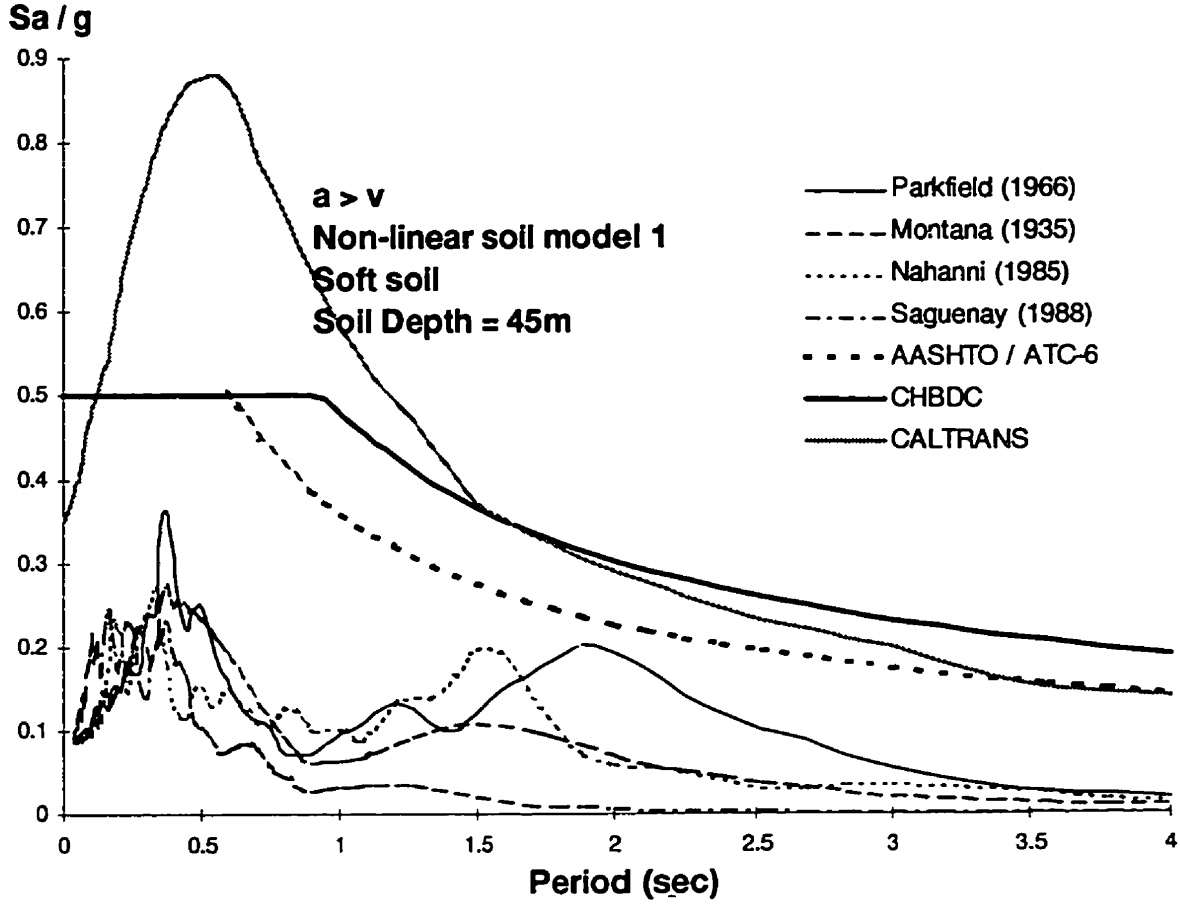

Figure 4.65 Comparison Of Response Spectra For Nonlinear Model 1 of Soft Soil with 45m Depths Subjected High a/v Earthquakes To Code Design Response Spectra

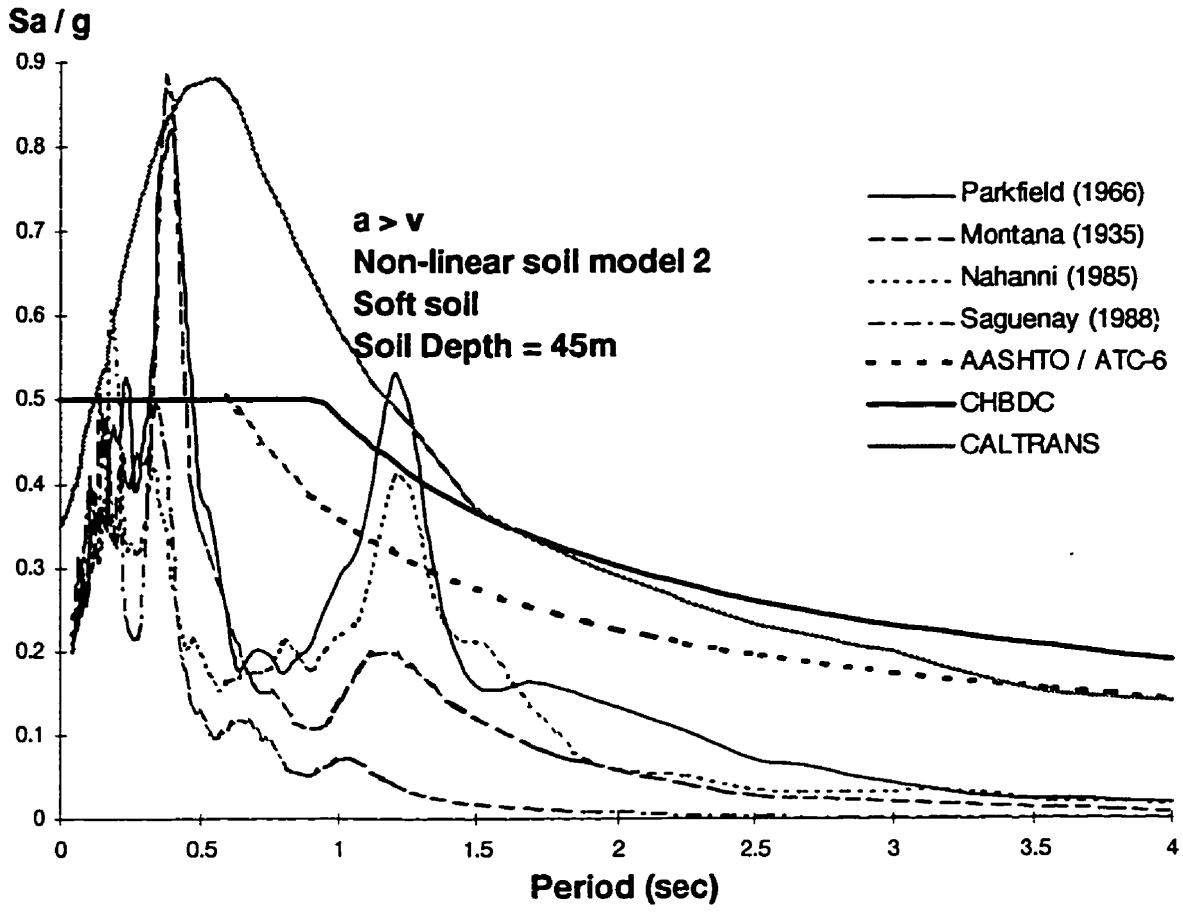

Figure 4.66 Comparison Of Response Spectra For Nonlinear Model 2 of Soft Soil with 45m Depths Subjected High a/v Earthquakes To Code Design Response Spectra

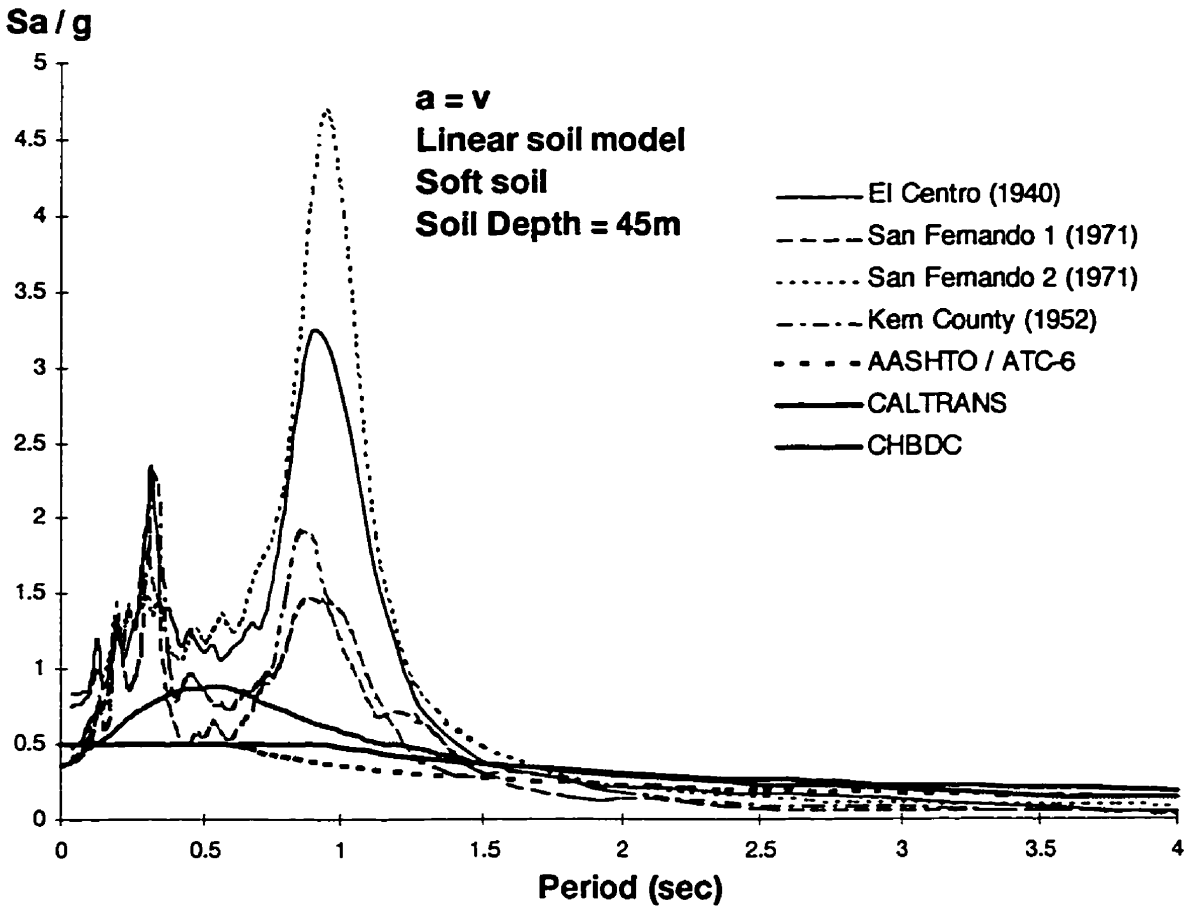

Figure 4.67 Comparison Of Response Spectra For Linear Model of Soft Soil with 45m Depths Subjected Intermediate a/v Earthquakes To Code Design Response Spectra

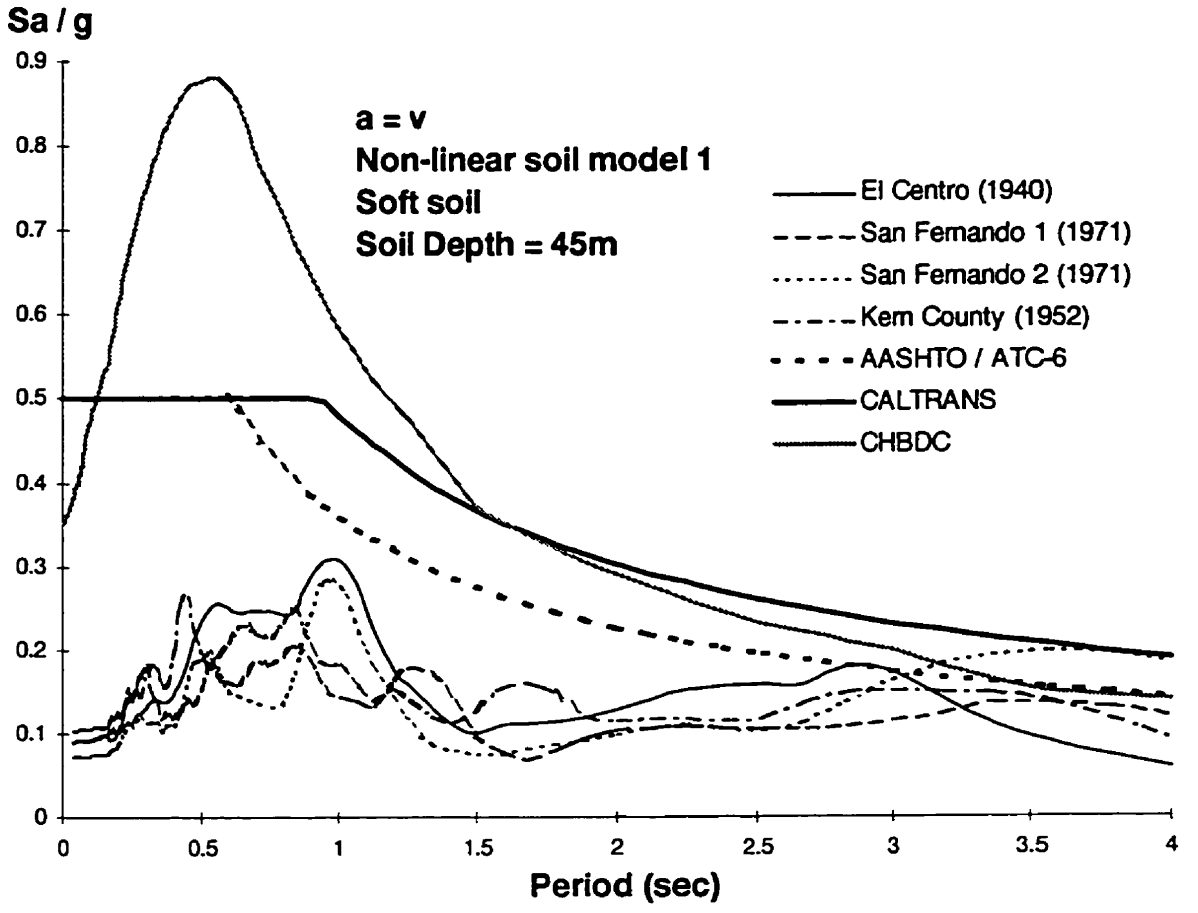

Figure 4.68 Comparison Of Response Spectra For Nonlinear Model 1 of Soft Soil with 45m Depths Subjected Intermediate a/v Earthquakes To Code Design Response Spectra

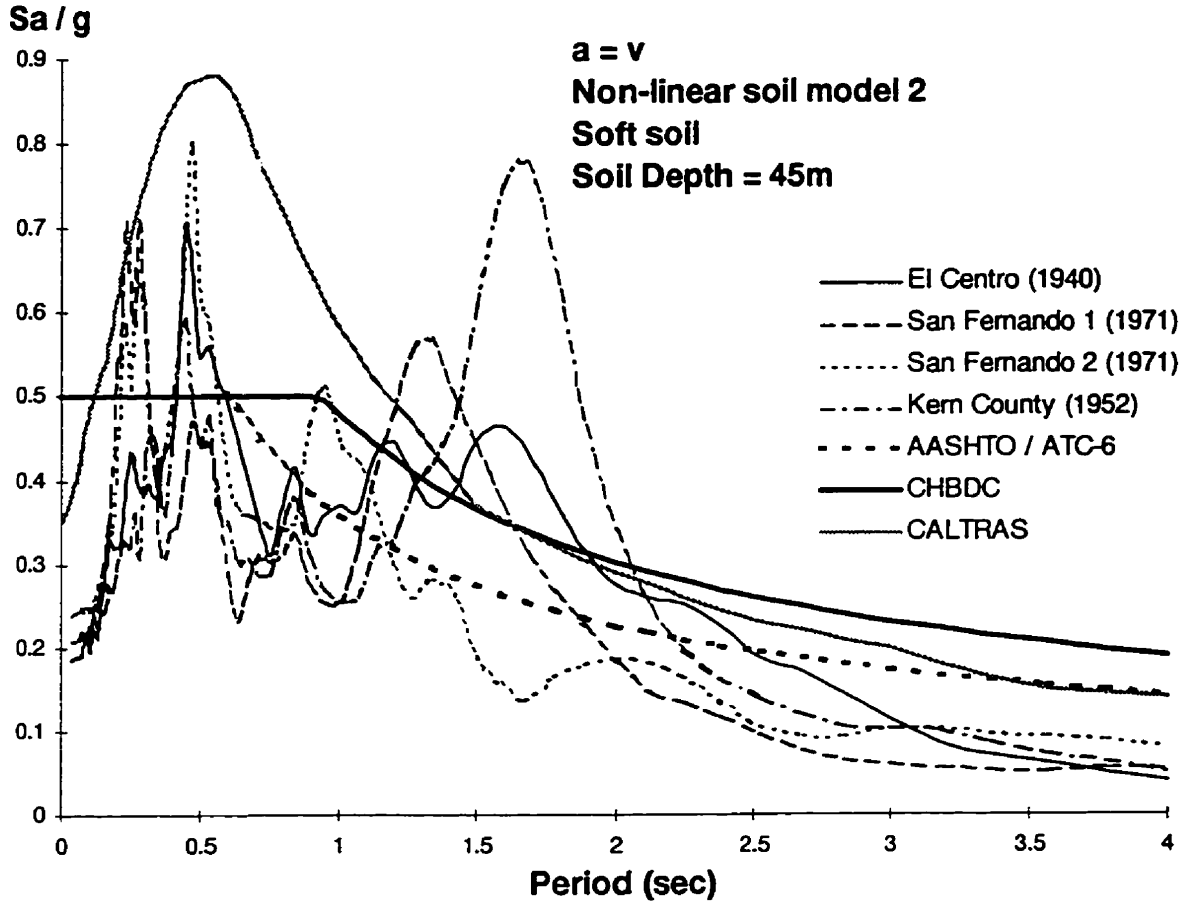

Figure 4.69 Comparison Of Response Spectra For Nonlinear Model 2 of Soft Soil with 45m Depths Subjected Intermediate a/v Earthquakes To Code Design Response Spectra

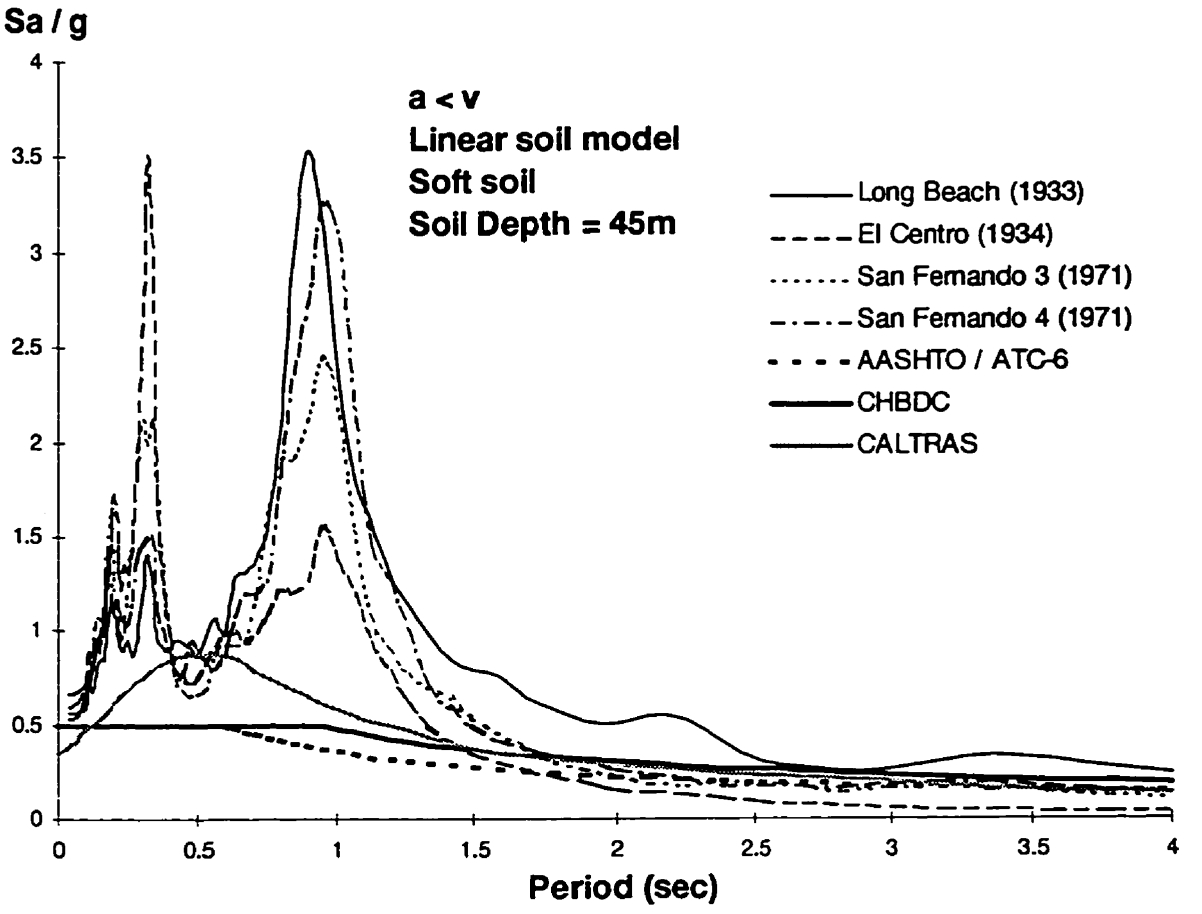

Figure 4.70 Comparison Of Response Spectra For Linear Model of Soft Soil with 45m Depths Subjected Low a/v Earthquakes To Code Design Response Spectra

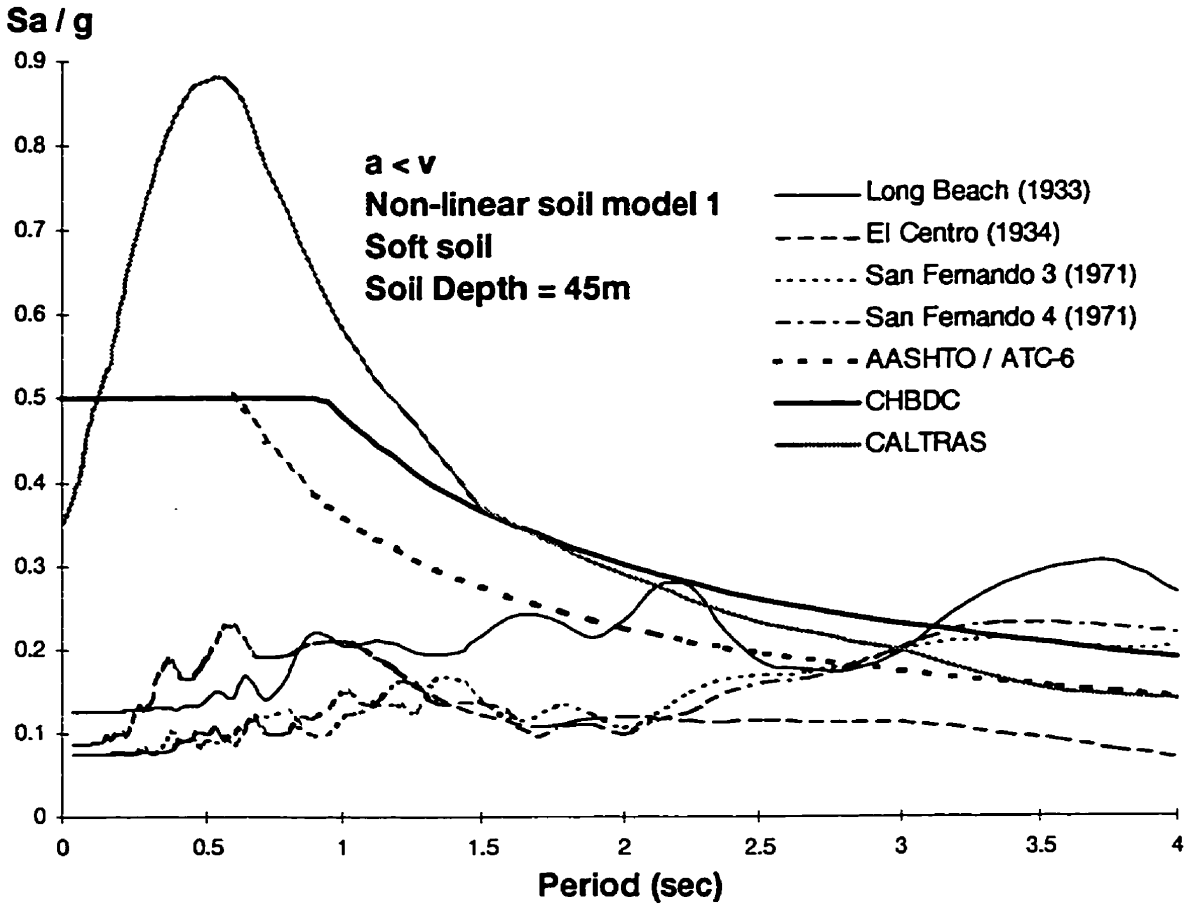

Figure 4.71 Comparison Of Response Spectra For Nonlinear Model 1 of Soft Soil with 45m Depths Subjected Low a/v Earthquakes To Code Design Response Spectra

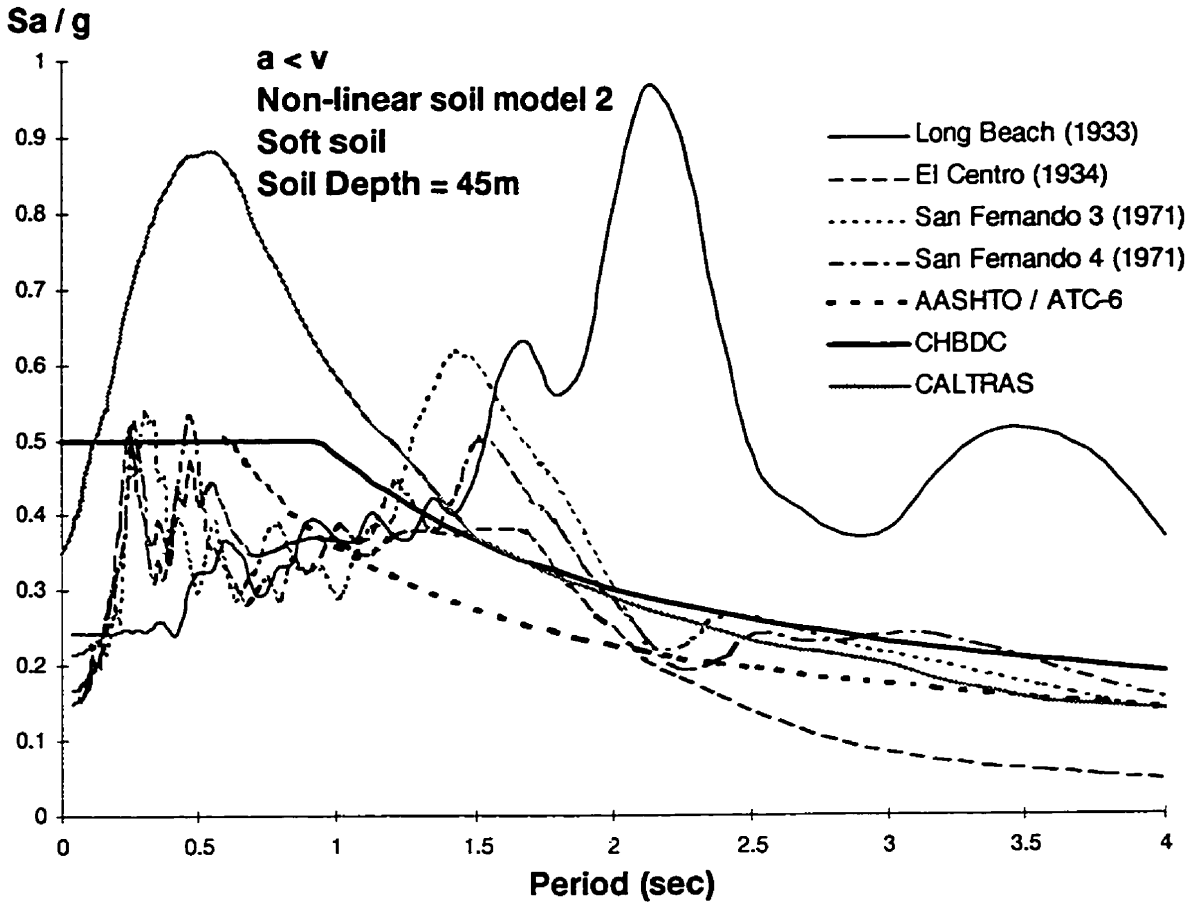

Figure 4.72 Comparison Of Response Spectra For Nonlinear Model 2 of Soft Soil with 45m Depths Subjected Low a/v Earthquakes To Code Design Response Spectra

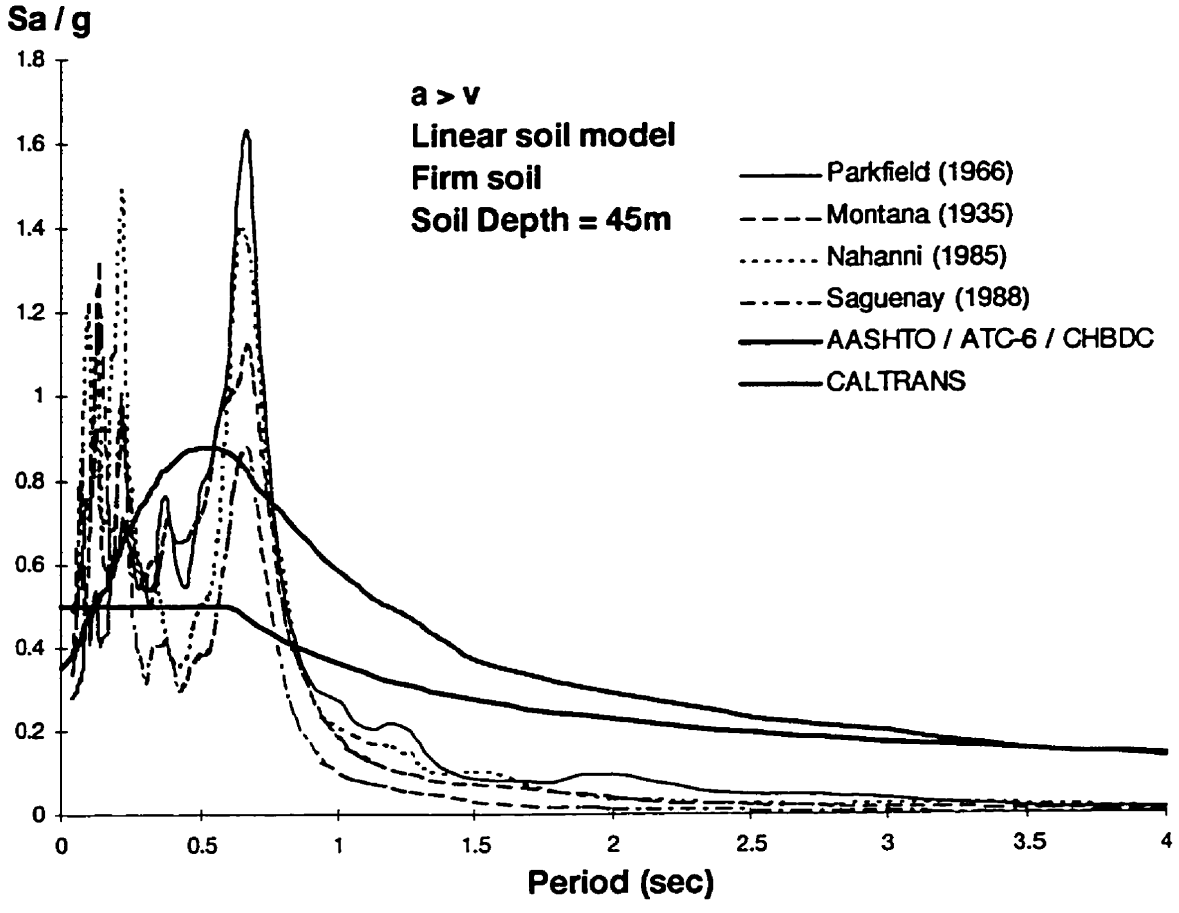

Figure 4.73 Comparison Of Response Spectra For Linear Model of Firm Soil with 45m Depths Subjected High a/v Earthquakes To Code Design Response Spectra

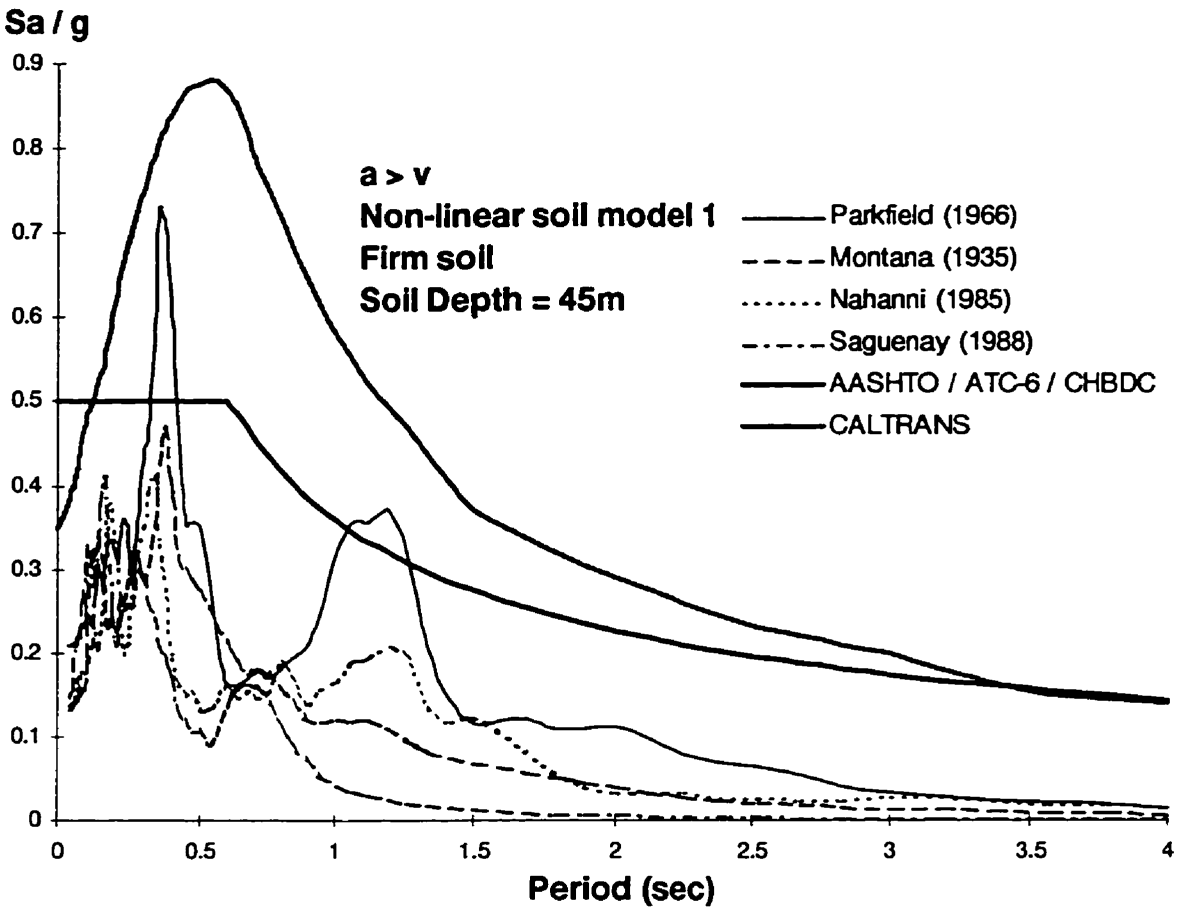

Figure 4.74 Comparison Of Response Spectra For Nonlinear Model 1 of Firm Soil with 45m Depths Subjected High a/v Earthquakes To Code Design Response Spectra

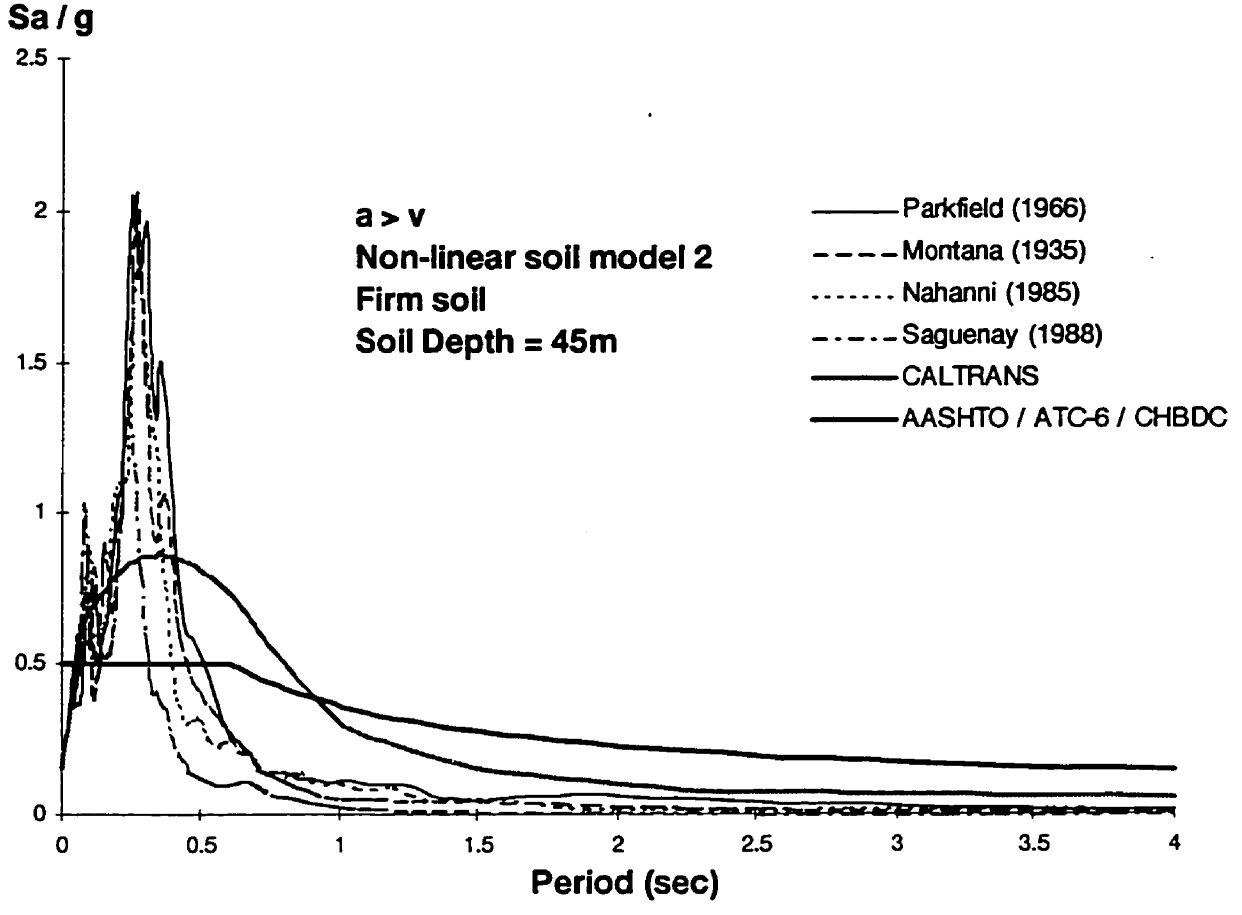

Figure 4.75 Comparison Of Response Spectra For Nonlinear Model 2 of Firm Soil with 45m Depths Subjected High a/v Earthquakes To Code Design Response Spectra

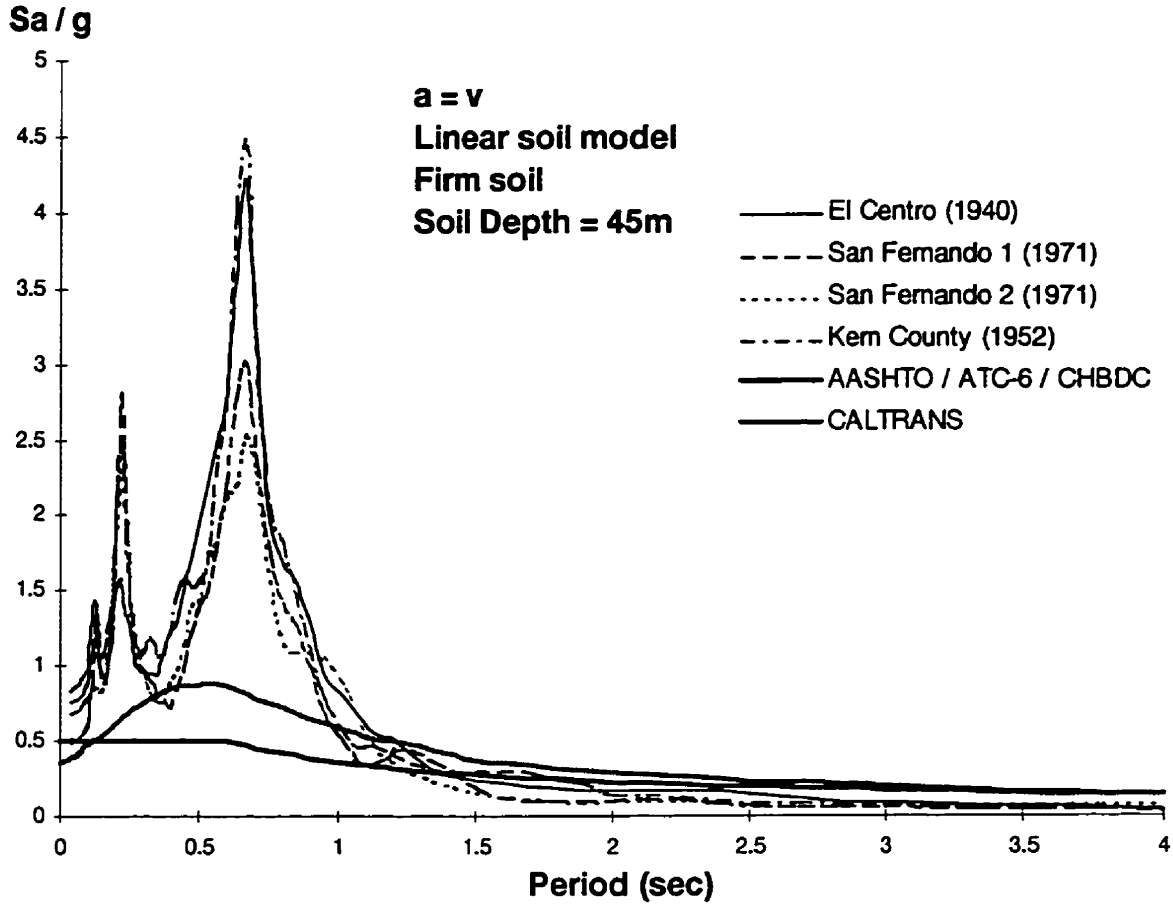

Figure 4.76 Comparison Of Response Spectra For Linear Model of Firm Soil with 45m Depths Subjected Intermediate a/v Earthquakes To Code Design Response Spectra

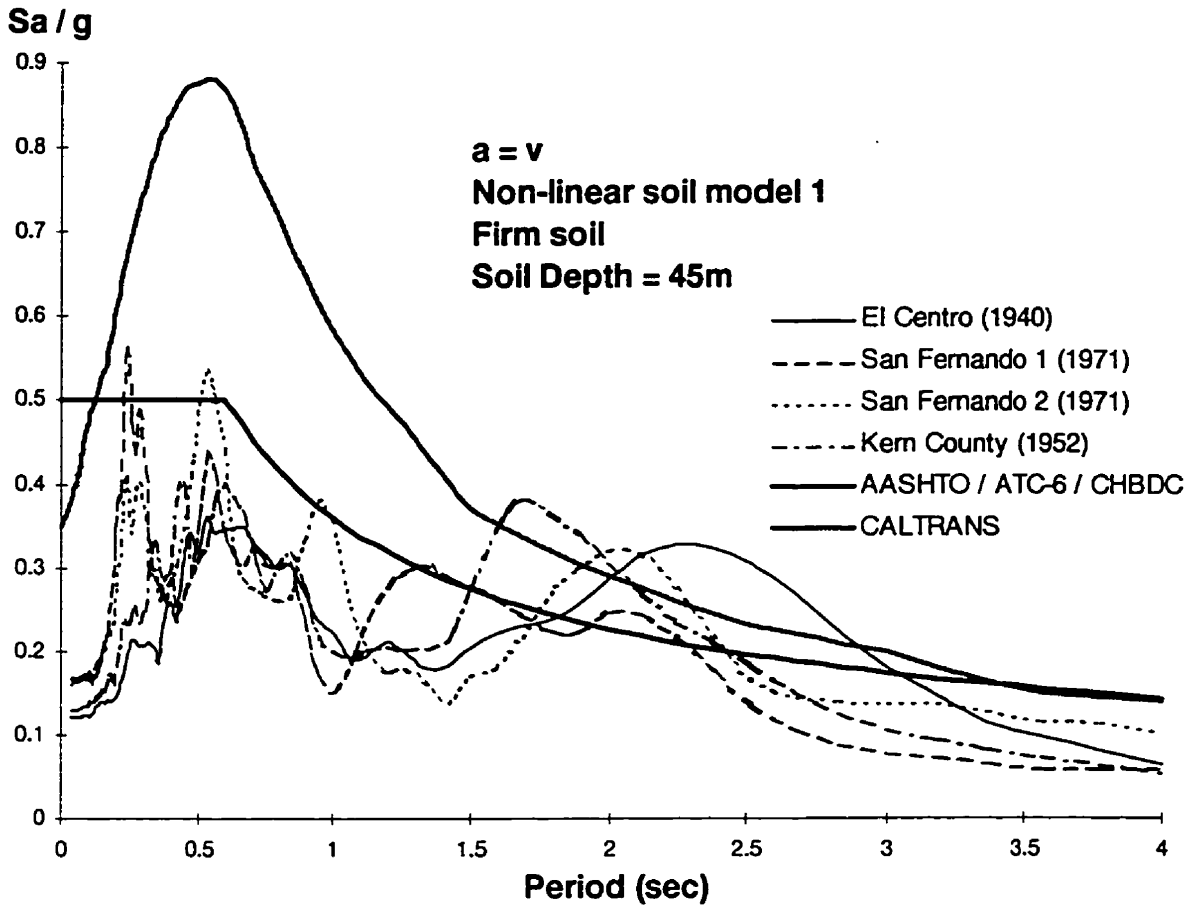

Figure 4.77 Comparison Of Response Spectra For Nonlinear Model 1 of Firm Soil with 45m Depths Subjected Intermediate a/v Earthquakes To Code Design Response Spectra

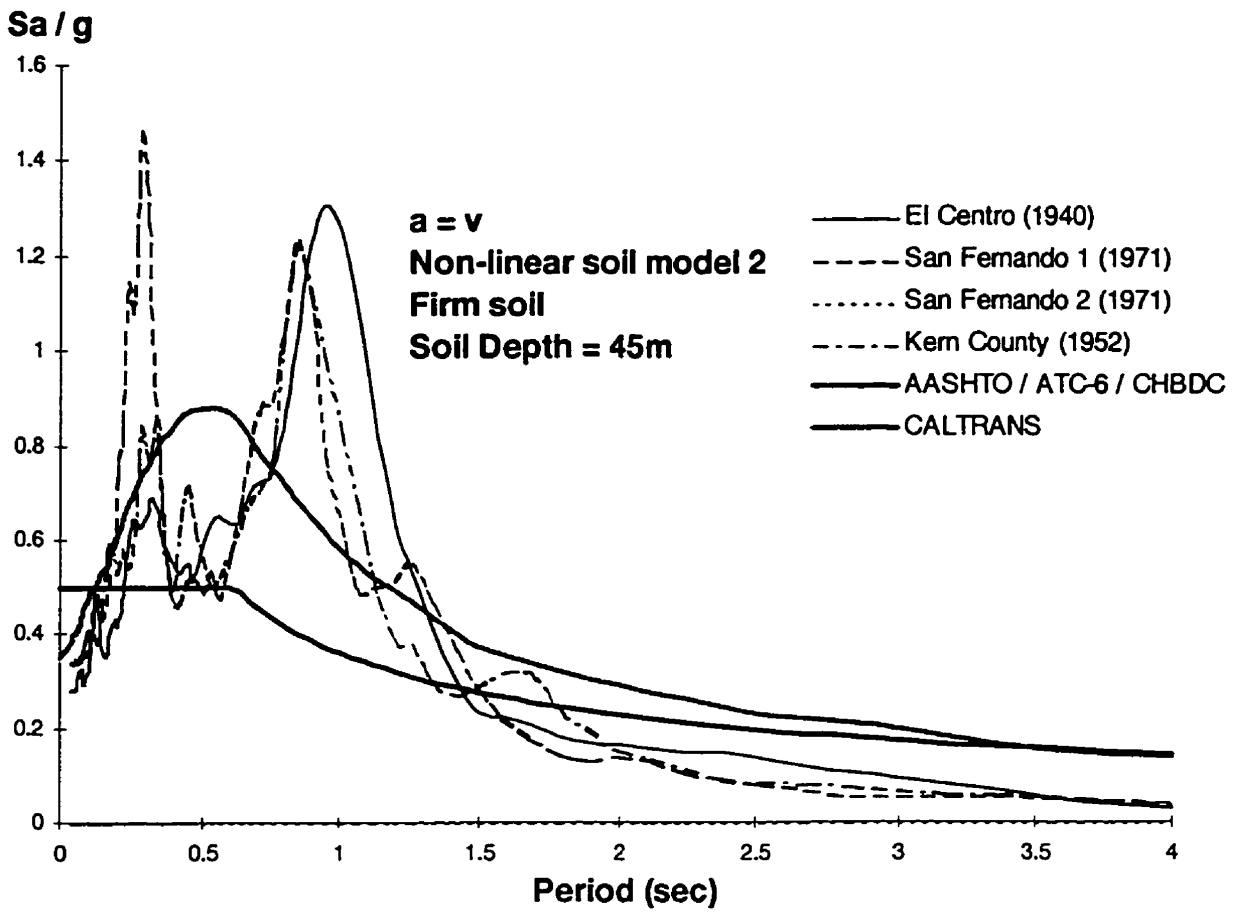

Figure 4.78 Comparison Of Response Spectra For Nonlinear Model 2 of Firm Soil with 45m Depths Subjected Intermediate a/v Earthquakes To Code Design Response Spectra

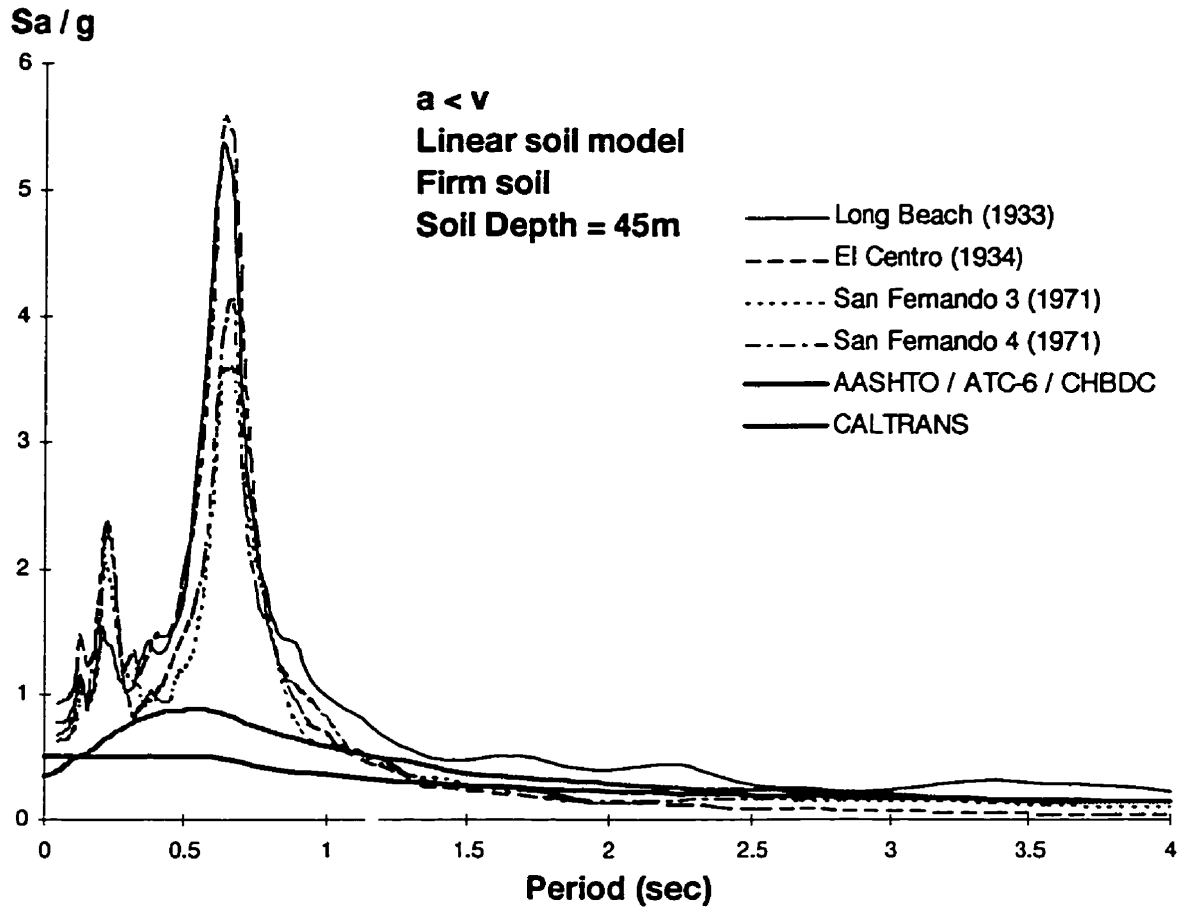

Figure 4.79 Comparison Of Response Spectra For Linear Model of Firm Soil with 45m Depths Subjected Low a/v Earthquakes To Code Design Response Spectra

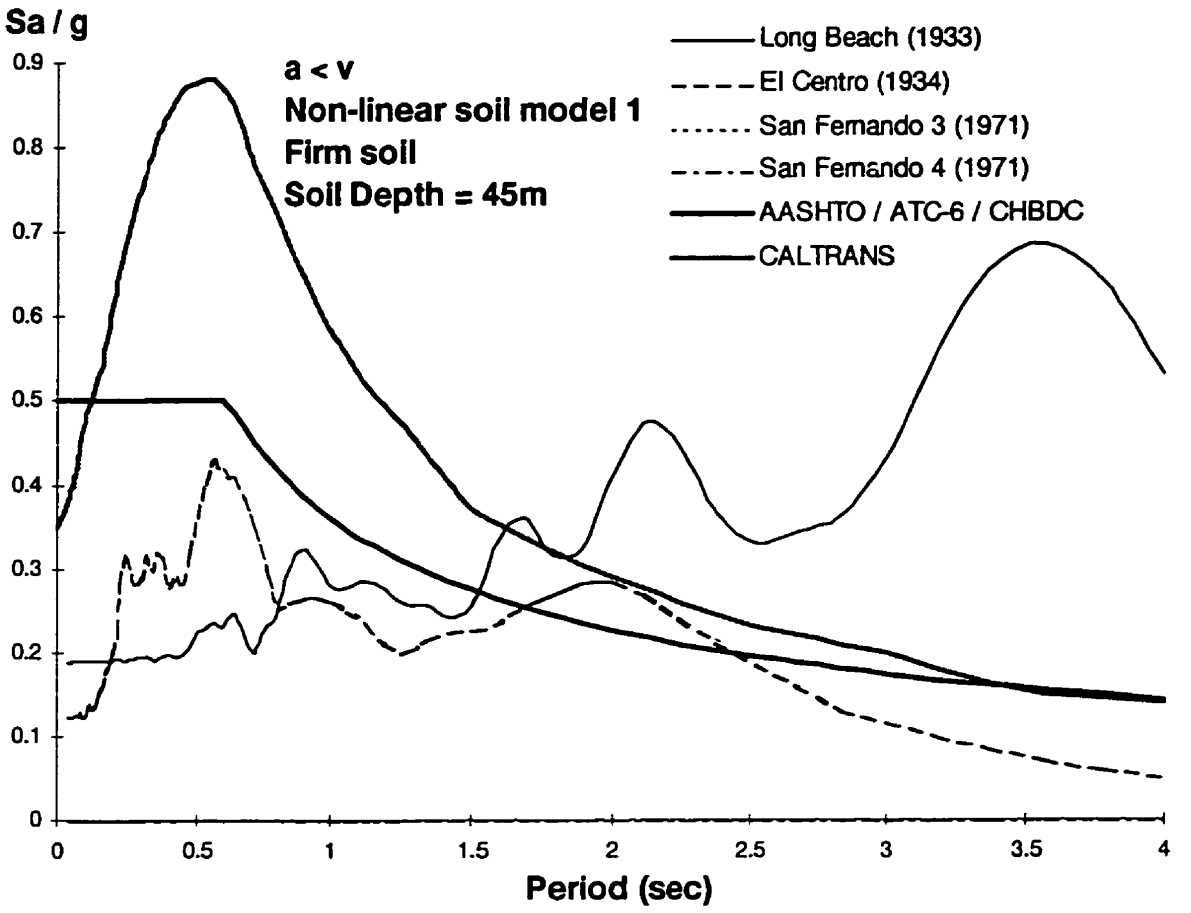

Figure 4.80 Comparison Of Response Spectra For Nonlinear Model 1 of Firm Soil with 45m Depths Subjected Low a/v Earthquakes To Code Design Response Spectra

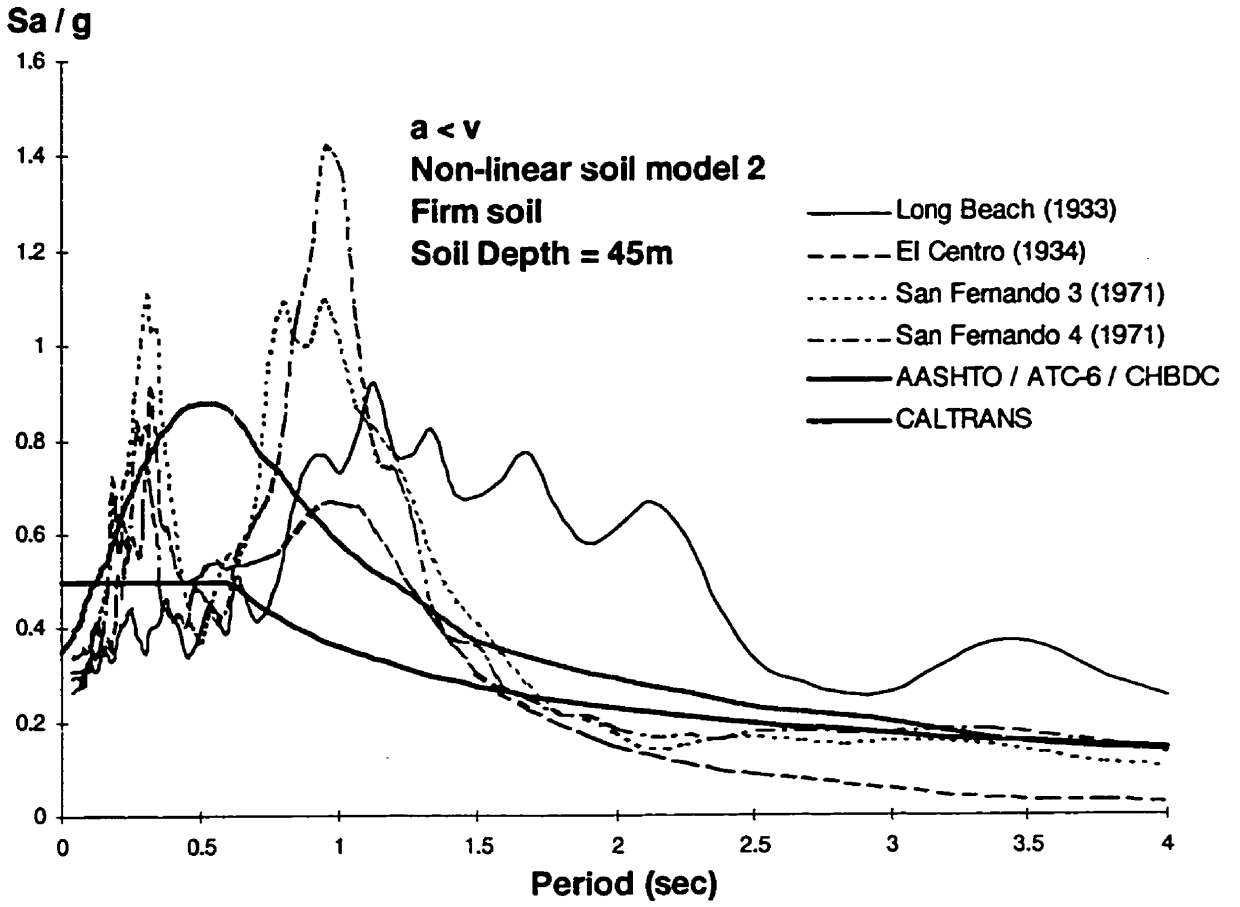

Figure 4.81 Comparison Of Response Spectra For Nonlinear Model 2 of Firm Soil with 45m Depths Subjected Low a/v Earthquakes To Code Design Response Spectra

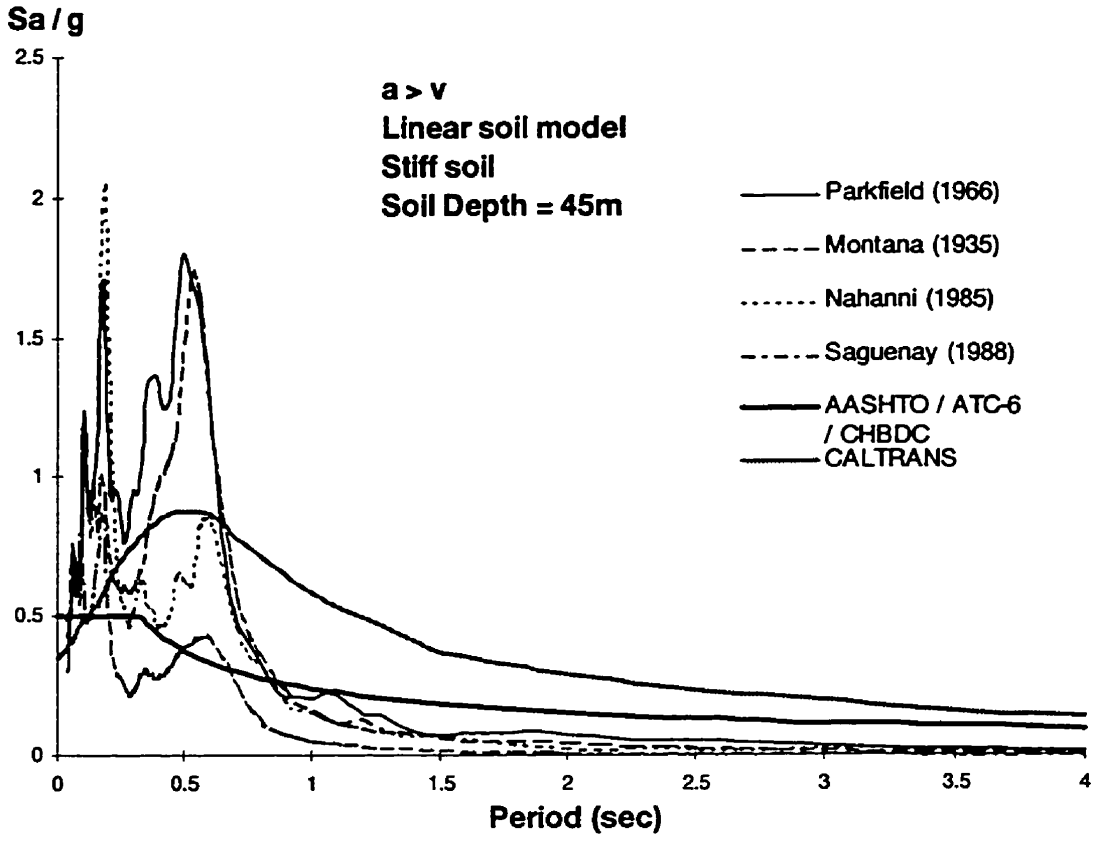

Figure 4.82 Comparison Of Response Spectra For Linear Model of Stiff Soil with 45m Depths Subjected High a/v Earthquakes To Code Design Response Spectra

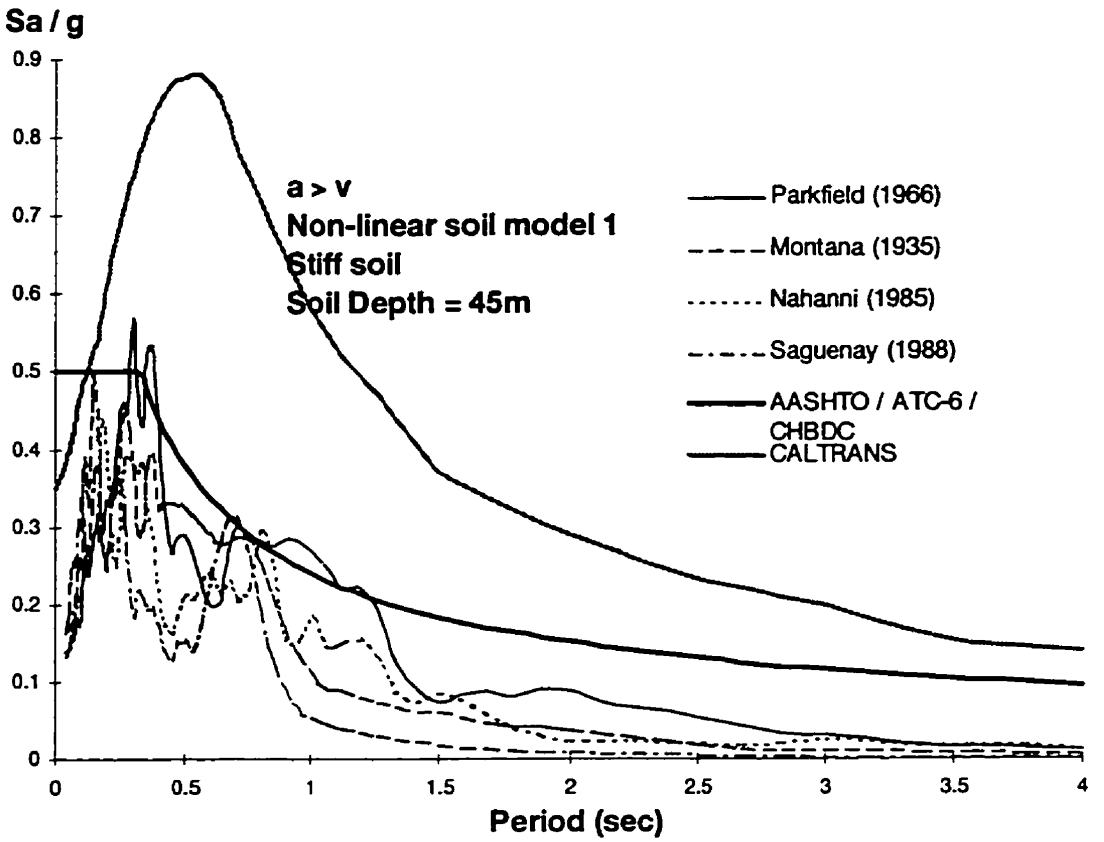

Figure 4.83 Comparison Of Response Spectra For Nonlinear Model 1 of Stiff Soil with 45m Depths Subjected High a/v Earthquakes To Code Design Response Spectra

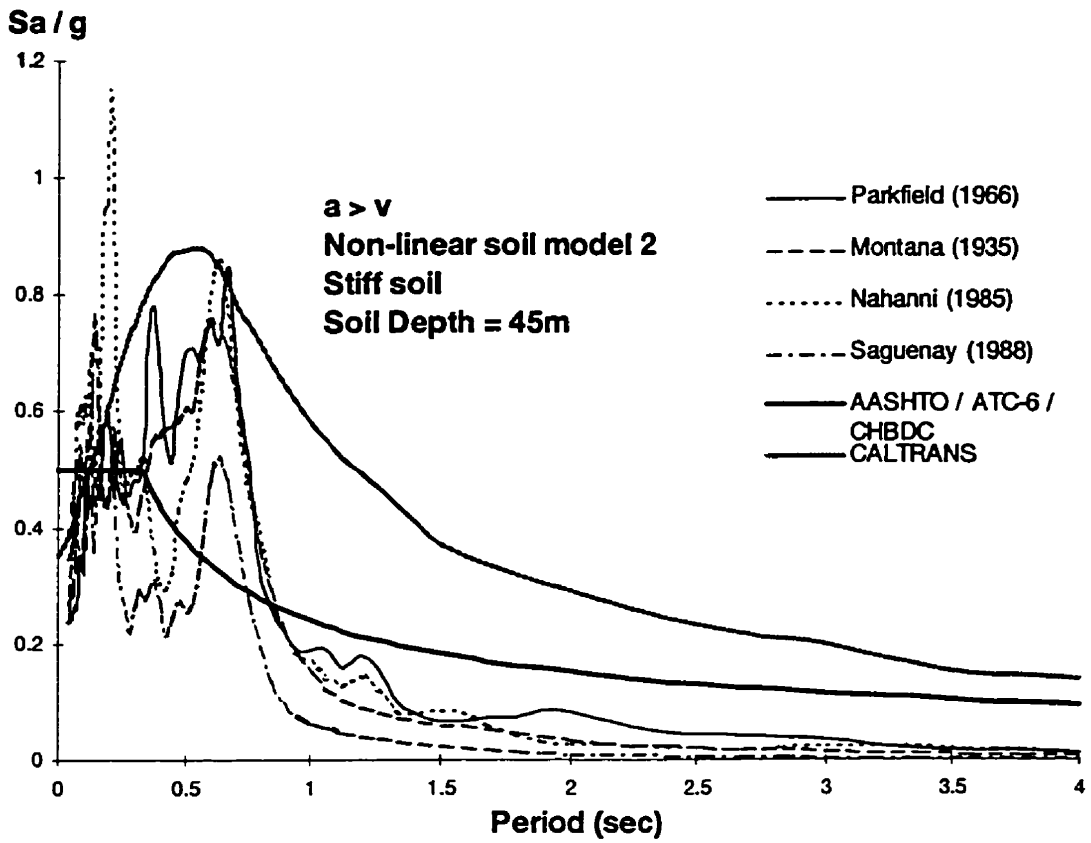

Figure 4.84 Comparison Of Response Spectra For Nonlinear Model 2 of Stiff Soil with 45m Depths Subjected High a/v Earthquakes To Code Design Response Spectra

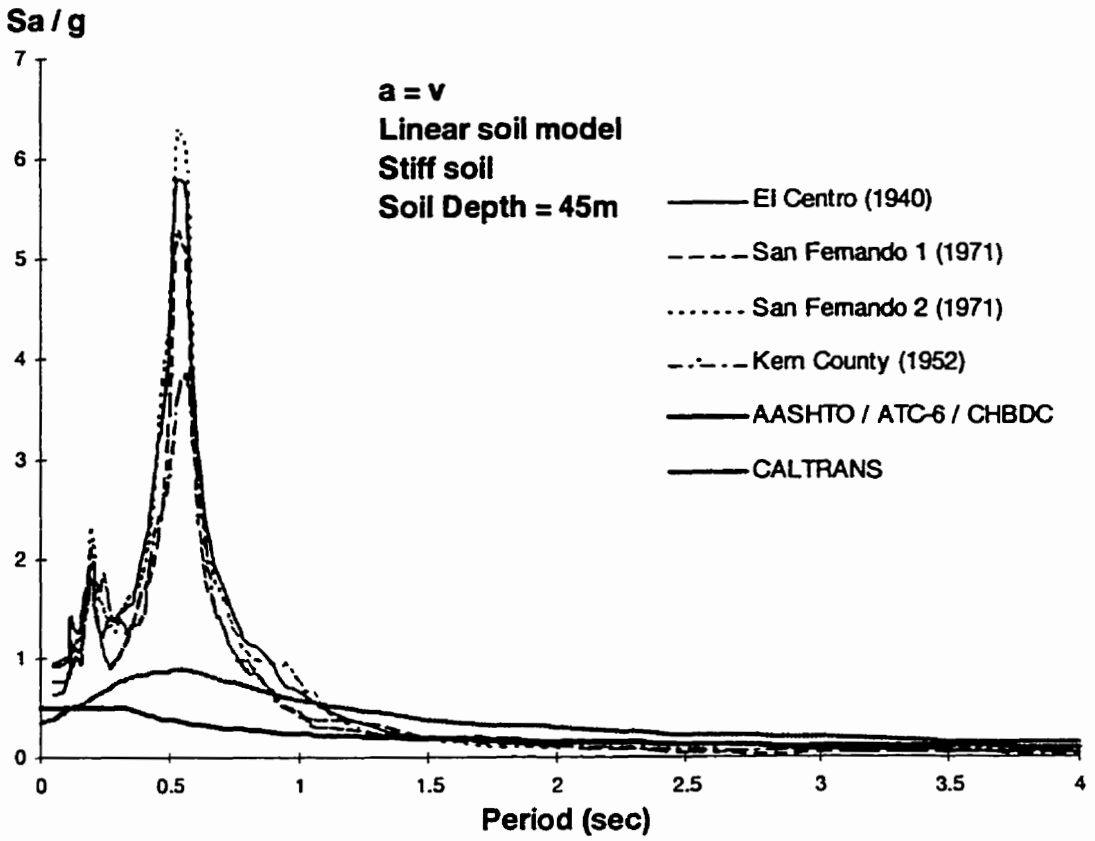

Figure 4.85 Comparison Of Response Spectra For Linear Model of Stiff Soil with 45m Depths Subjected Intermediate a/v Earthquakes To Code Design Response Spectra

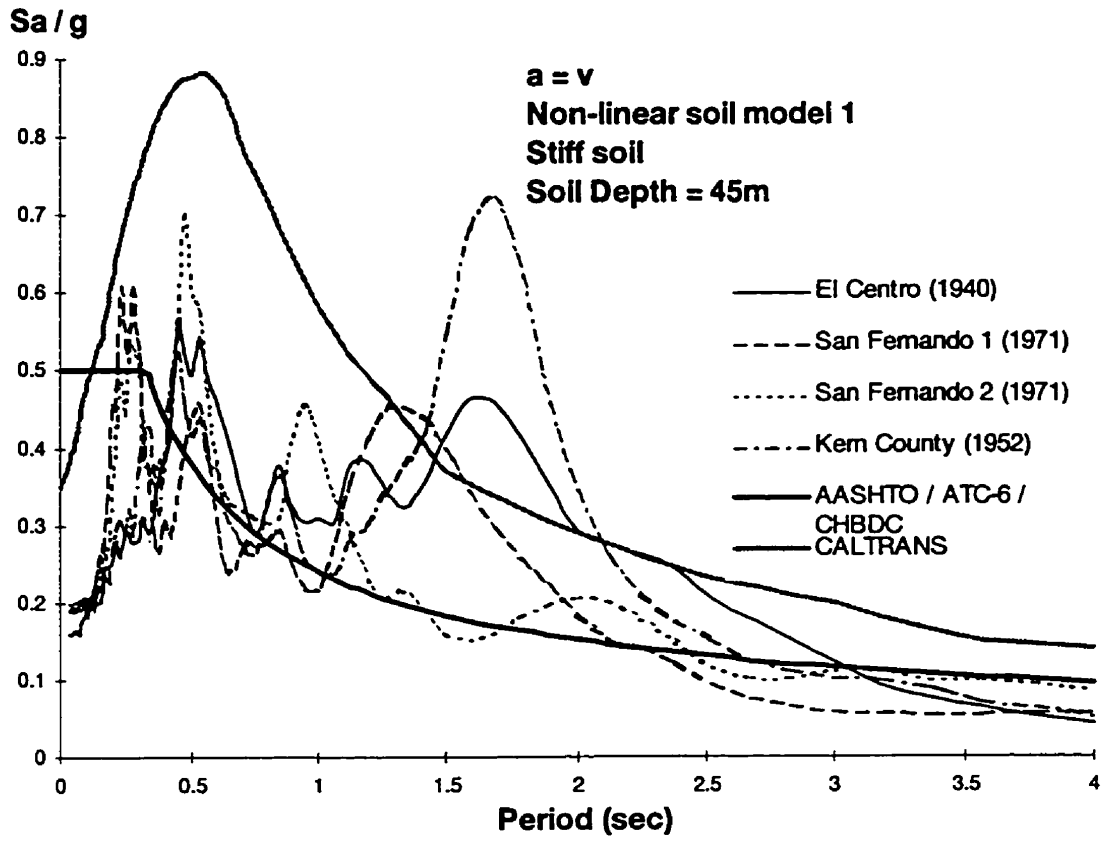

Figure 4.86 Comparison Of Response Spectra For Nonlinear Model 1 of Stiff Soil with 45m Depths Subjected Intermediate a/v Earthquakes To Code Design Response Spectra

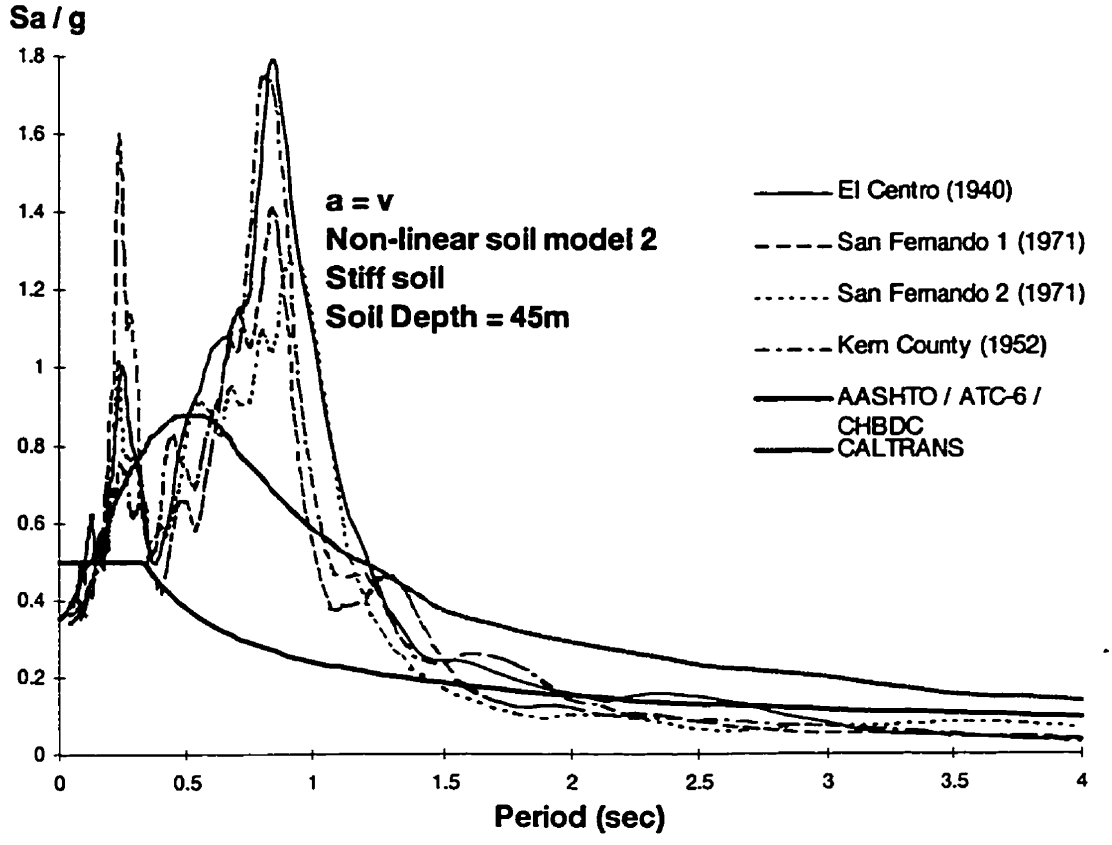

Figure 4.87 Comparison Of Response Spectra For Nonlinear Model 2 of Firm Soil with 45m Depths Subjected Intermediate a/v Earthquakes To Code Design Response Spectra

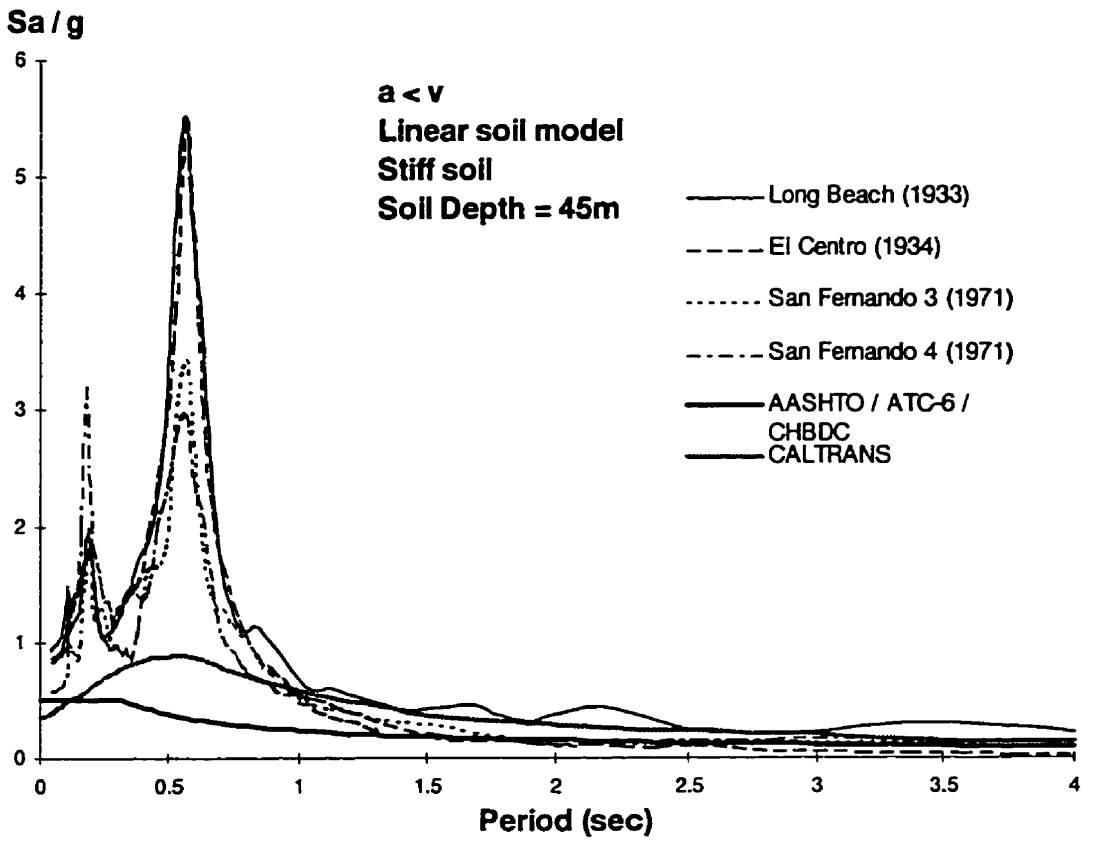

Figure 4.88 Comparison Of Response Spectra For Linear Model of Stiff Soil with 45m Depths Subjected Low a/v Earthquakes To Code Design Response Spectra

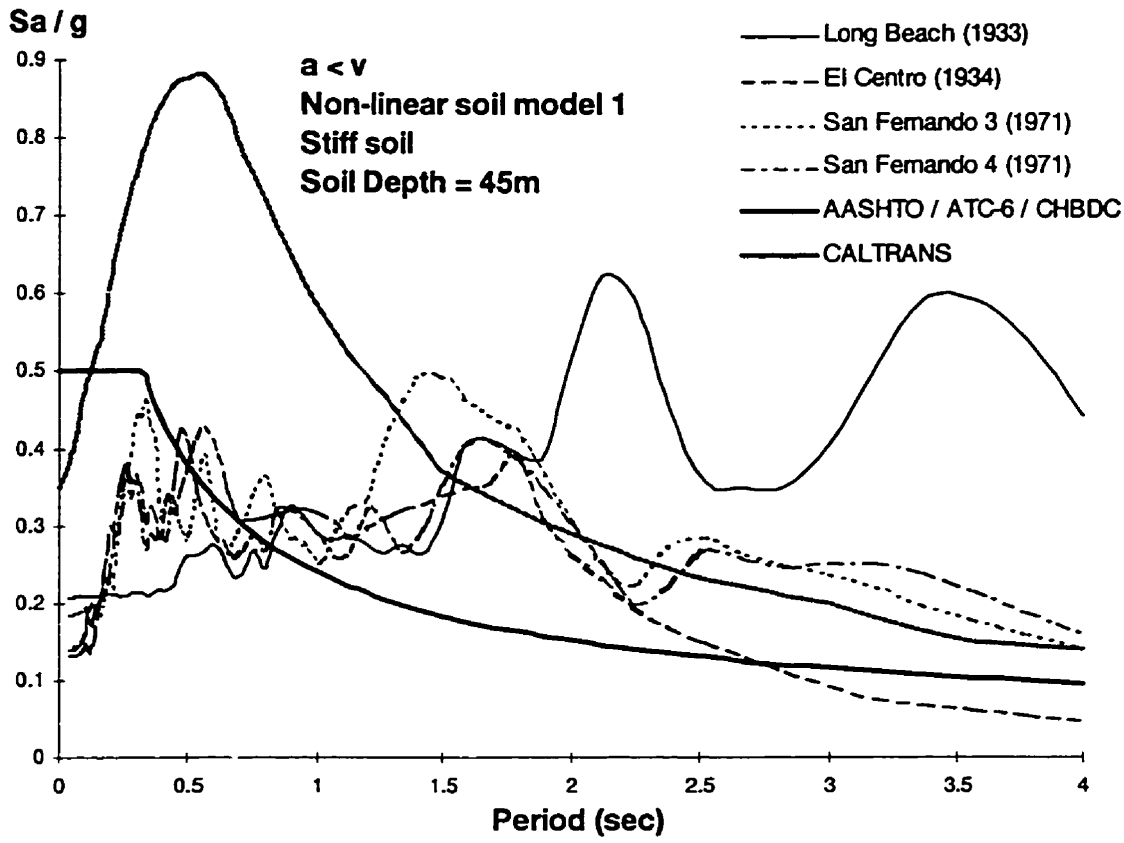

Figure 4.89 Comparison Of Response Spectra For Nonlinear Model 1 of Stiff Soil with 45m Depths Subjected Low a/v Earthquakes To Code Design Response Spectra

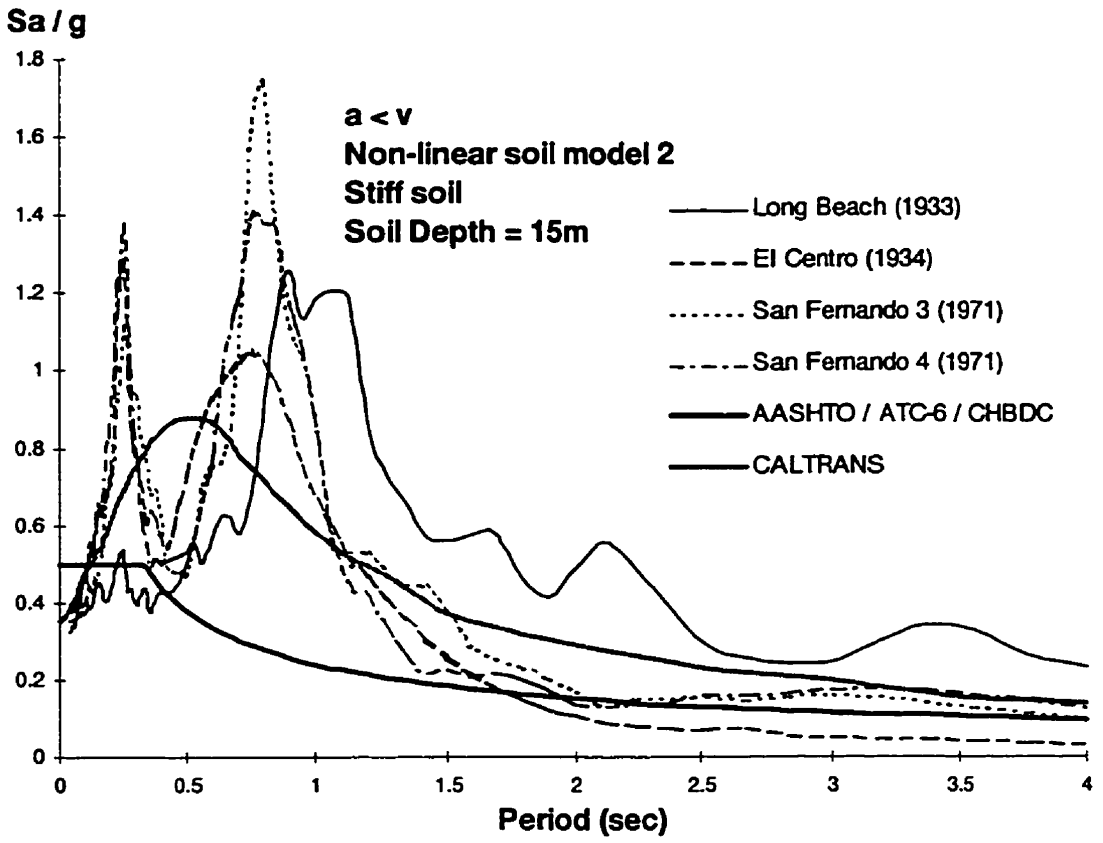

Figure 4.90 Comparison Of Response Spectra For Nonlinear Model 2 of Stiff Soil with 45m Depths Subjected Low a/v Earthquakes To Code Design Response Spectra

CHAPTER 5 SUMMARY AND CONCLUSIONS

5.1 Summary and Conclusions

In this study, some important aspects of the earthquake resistant design for highway bridges and the code design procedures commonly used in North America are reviewed. The seismic resistant design concept, design philosophy and the recent advances and technology in earthquake engineering as implied in the current seismic design codes are discussed. A conceptual comparison of the design objectives and design approaches of some of the commonly used codes and standards in the U.S. and Canada for the earthquake resistant design of bridges are presented. The effects of local soil deposits subjected to different input ground motions are investigated. The free field surface response spectra are generated by considering three different soil types, soft, firm, and stiff, with three depths, 15 m, 25 m and 45 m, as well as bedrock response spectra. For each specified soil type, three sets of input ground motions with high, intermediate and low a/v ratios and three different soil models (one linear and two nonlinear models) are used. Thus, a total of 84 sets of response spectra are obtained, which are compared with the design spectra in the AASHTO, ATC-6 and CALTRANS. The main conclusions are summarized as follows:

1. The surface ground motion is greatly affected by the properties of the soil deposit and the characteristics of the input ground motions. In view of this observation, which has been confirmed in the present study, the selection of appropriate design earthquakes is

particularly important for bridges constructed on sites identified with high amplification potential.

2. Local soil amplification effects are sensitive to the type and depth of soil deposits as well as to the dynamic properties of the soils. In general, the spectral responses obtained by using nonlinear soil models are considerably lower than those obtained for the linear soil model. For a specified soil type, the shape of the response spectra calculated by using different nonlinear soil models can be quite different. Consequently, it is important to obtain reliable soil property data for accurate calibration of the soil model used for design.

3. By comparing the calculated elastic response spectra of each soil case with the design load spectra specified in the current seismic design codes, it is found that the design loads specified by the codes are unconservative under a wide range of circumstance and period ranges. The CALTRANS design spectrum shows a better agreement in general than AASHTO, ATC and CHBDC.

5.2 Recommendations for Further Work

In order to continue studies on the subject of the earthquake resistant design for highway bridges, there are some important fields along this direction that deserve further studies, such as:

1. Further study on nonlinear behaviour of the bridge structure system and evaluation of the response reduction factor R are required. This study of site response effects is based on elastic structural response, which is considered to be adequate for design of bridge joints and connections.

2. The influence of underlying soil deposits on the ductile behaviour of bridge structure needs to be further investigated.

3. A uniform layer of soil deposits is assumed in this study, and this may not be adequate. Further studies on the effects of more complex geometric characteristics of local soils are needed, since the surface ground motion has been found to be very sensitive to the soil properties.

4. The adequacy of the seismic design codes for different types of highway bridges should be investigated.

REFERENCES

AASHO 1965 and AASHTO 1983, 1993, Standard Specifications for Highway Bridges, American Association of State Highway Officials, Washington, DC.

Anderson, D., Mitchell, D. and Tinawi R., 1995, Performance of Concrete Bridges During the 1995 Hyogoken-Nanbu (Kobe) Earthquake: The Hyogo-ken Nanbu (Kobe) Earthquake of 17 January 1995, Preliminary Reconnaissance Report, Canadian Association for Earthquake Engineering, April, pp. 115-152.

ATC. 1981, Seismic Design Guidelines for Highway Bridges. Report No. ATC-6, Applied Technology Council, Palo Alto, CA.

Barenberg, M.E. and Foutch, D.A., 1987. Evaluation of Seismic Design Procedures for Highway Bridges, Journal of the Structural Engineering Vol. 114, No. 7, 1588 - 1605.

Basham, P.M., Anglin, F.M., and Berry, M.J., 1985, New (1985) Probabilistic Strong Seismic Ground Motion Maps of Canada, Bulletin of the Seismological Society of America, Vol. 75, No. 2, pp 563-595

Basham, P.M., 1995, Recent Advances in Understanding of Earthquake Potential and Seismic Hazard in Canada, Proceedings of Seventh Canadian Conference on Earthquake Engineering, June 1995, Montreal, pp 45-64.

Bruneau, M., Wilson, J.C. and Tremblay, R., 1995, Seismic Performance of Steel Bridges During the 1995 Hanshin-Awaji (Kobe, Japan) Earthquake: The Hyogo-ken Nanbu (Kobe) Earthquake of 17 January 1995, Preliminary Reconnaissance Report, Canadian Association for Earthquake Engineering, April, pp. 115-152.

CALTRANS., 1976, 1990, Bridge Design Specification, California Department of Transportation, Sacramento, CA.

Chapman, H.E., 1979, An Overview Of The State of Practice in Earthquake Resistant Design of Bridges in New Zealand, Proceedings of a Workshop on Earthquake Resistance of Highway Bridges, Applied Technology Council, Berkelay, California.

CHBDC, 1996, Canadian Highway Bridge Design Code, Seismic Committee of CHBDC

CSA, 1988, Design of highway bridges, CAN/CSA-S6-88, Canadian Standards Association, Rexdale, Ont.

Dobry, R. and Vucetic, M. 1987, Dynamic Properties and Seismic Response of Soft Clay Deposits. Proceedings of the International Symposium on Geotechnical Engineering of Soft Soils, Mexico City, Vol. 2, pp. 51-87.

Elhmadi, K., Heideberecht, A.C. and Hosni, S. 1990. Parametric Study of Seismic Site Response Effects, EERG Report 90-01, Earthquake Engineering Research group, McMarster University, Hamilton, Ont.

Elms, D.G. and Martin, G.R., 1979, Factors Involved in the Seismic Design Bridge Abutments, Proceedings of a Workshop on Earthquake Resistance of Highway Bridges, Applied Technology Council, Berkelay, California.

Fenves, G.L. and Serino, G. 1990 Soil-Structure Interaction in Buildings from Earthquake Records, Earthquake Spectra, Vol. 6, No. 4, pp. 641-655.

Gats, J.H., 1976, California Seismic Design Criteria for Bridges, Journal of the Structural Division, Vol. 102, No. ST12, pp. 2301-2314.

Gats, J.H., 1979, Factors Considered in the Development of the California Seismic Design Criteria for Bridges, Proceedings of a Workshop on Earthquake Resistance of Highway Bridges, Applied Technology Council, Berkelay, California.

Hall, W.J. and Newmark, N.M., 1979, Seismic Design of Bridges -- An Overview of Research Needs, Proceedings of a Workshop on Earthquake Resistance of Highway Bridges, Applied Technology Council, Berkeley, California, pp. 164-181.

Heideberecht, A.C. and Lu, C.Y., 1987, Evaluation of the Seismic Response Factor Introduced in the 1985 Edition of the National Building Code of Canada, Canadian Journal of Civil Engineering, 15, 382-388.

Heideberecht, A.C., Henderson, P., Naumoski N. and Pappin, J.W., 1990, Seismic Response and Design of Structures Located on Soft Clay Site, Canadian Geotechnical Journal, 27(3), pp. 330-341.

Housner, G.W. 1979, Earthquakes and Earthquake Engineering, Proceedings of Third Canadian Earthquake Engineering Conference, Montreal, 1979, pp. 1-15.

Housner, G.W. and Jennings, P.C. 1982, Earthquake Design Criteria, Earthquake Engineering Research Institute, Berkeley, California.

Hosni, S. and Heideberecht, A.C., 1994 Influence of Site Effects and Period-Dependent Force Modification Factors on the Seismic Response of Ductile Structures, Canadian Journal of Civil Engineering, 21, 596-604.

Imbsen, R. A., Nutt, R.V. and Penzien, J., 1979, Evaluation of Analytical Procedures Used in Bridge Seismic Design Practice, Proceedings of a Workshop on Earthquake Resistance of Highway Bridges, Applied Technology Council, Berkeley, California, pp. 468-474.

Japan Road Association, 1980, Specifications for Highway Bridges,.

JSCE., 1982, Bridge and Structural Committee, Japan Society of Civil Engineers, Earthquake-Resistant Design of Bridges, pp. 121-191.

Krawinkler, H., and Rahnama, M. 1992, Effects of Soft Soil on Design Spectra. Proceedings of the Tenth Would Conference on Earthquake Engineering, Madrid, Spain, Vol. 10, pp. 5841-5846.

Lysmer, J., Udaka, T., Tsai, C-F. and Seed, H.B., 1975, FLUSH - A Computer Program for Approximate 3-D Analysis of Soil-Structure Interaction Problem, Earthquake Engineering Research Center, University of California, Berkeley, Report No. EERC75-30, November, 1975

Mitchell, D., Adams, J., Ronad, H. D., Lo, R. C. and Weichert, D., 1986. Lessons from the 1985 Mexican Earthquake. Canadian Journal of Civil Engineering, 13, 535-557.

Mitchell, D., Tinawi, R., And Sexsmith, R. G., 1991. Performance of Bridges in 1989 Loma Prieta Earthquake - Lessons for Canadian Designers. Canadian Journal of Civil Engineering, 18, 711-734.

Moehle, J., Fenves, G., Mayes, R., Priestley, N., Seible, F., Uang, C.M., Werner, S., Aschheim, M., 1995, Highway Bridge and Traffic Management: Northridge Earthquake Reconnaissance Report, EERI, Earthquake Spectra, Special Supplement to Vol. 11, Feb. pp. 287-373.

Moehle, J., 1992, Displacement Design Criteria for RC Structures Subjected to Earthquakes, Earthquake Spectra, EERI, Vol. 8(3), August. pp. 403-428.

NBCC, 1985, 1995, National Building Code of Canada, Canadian Commission on the Building and Fire Codes and National Research Council of Canada

Naumoski, N., Tso, W.K. and Heideberecht, A.C., 1988, A Selection of Representative Strong Motion Earthquake Records Having Different A/V Ratios, EERG Report 88-01, Earthquake Engineering Research group, McMarster University, Hamilton, Ont.

Newmark, N.M., 1979, Earthquakes Resistant Design and ATC Provisions, Proceedings of Third Canadian Earthquake Engineering Conference, Montreal, 1979, pp. 609-645.

OHBDC 1979, 1983, 1991. Ontario Highway Bridge Design Code. Ontario Ministry of Transportation and Communications, Downsview, Ont.

Priestley, M.J.N., Seible, F. and Calvi, G.M., 1996, Seismic Design and Retrofit of Bridges, John Wiley & Sons, Inc.

Qi, X. and Moehle, J.P. 1991, Displacement Design Approach for Reinforced Concrete Structures Subjected to Earthquakes, Report No. UBC/EERC-91/2, Earthquake Engineering Research Center, University of California, Berkeley

Rainer, J.H. and Pernica, G., 1979, Dynamic Testing of a Modern Concrete Bridge, Canadian Journal of Civil Engineering, Vol. 6, No. 3, pp. 447-455.

Richards, R. and Elms, D.G., 1977, Seismic Behaviour of Retaining Walls and Bridge Abutments, Report No. 77-10, University of Canterbury, Christchurch, New Zealand, June.

Scott, R.F., Gibson, A.D., Somerville, P. Brogan, G.E., Hushmand, B. and Hall, J.F., 1995, Geotechnical Observations: Northridge Earthquake Reconnaissance Report, EERI, Earthquake Spectra, Special Supplement to Vol. 11, Feb. pp. 287-373.

Seed, H. B. and Idriss, I. M., 1970, Soil Moduli and Damping Factors for Dynamic Response Analysis, Earthquake Engineering Research Center, Report No. EERC 70-10, University of California, Berkeley, Dec. 1970.

Seed, H. B., Ugas, C., and Lysmer, J., 1976, Site Dependent Spectra for Earthquake Resistant Design, Bulletin of the Seismological Society of America, Vol. 66, No. 1.

Wallace W. and Moehle, J.P. 1990, Evaluation of ATC Requirements for Soil-Structure Interaction Using Data from The 3 March 1985 Chile Earthquake, Earthquake Spectra, Vol. 6, No. 3, pp. 593-611.

Wilson, E. L., Der Kiureghiam, A., and Bago, E.P., 1981, A Replacement for the SRSS Method in Seismic Analysis, Earthquake Engineering and Structural Dynamics, Vol. 9, pp. 187-194.

IMAGE EVALUATION
TEST TARGET (QA-3)

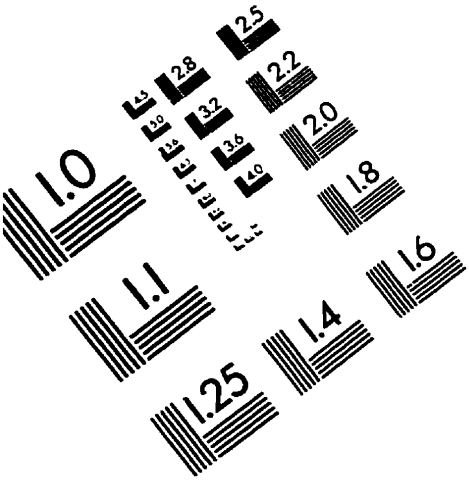

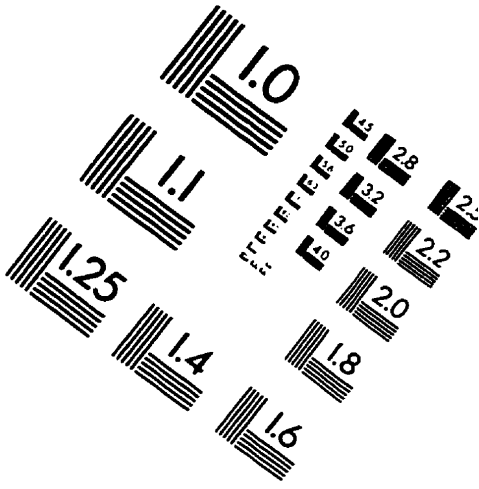

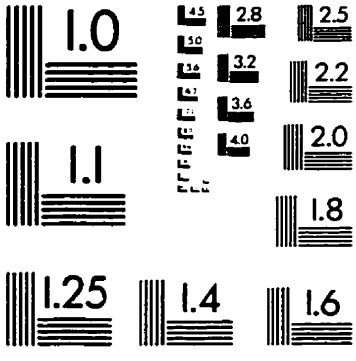

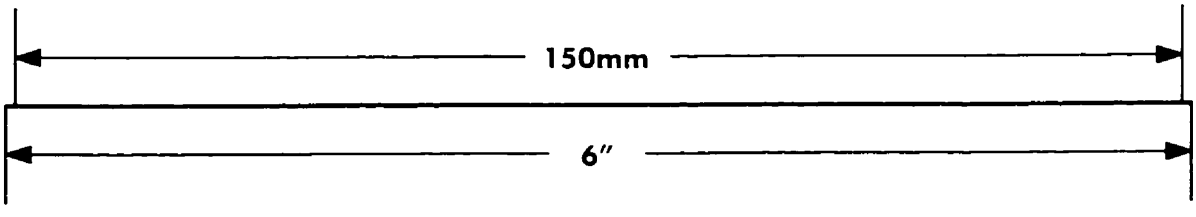

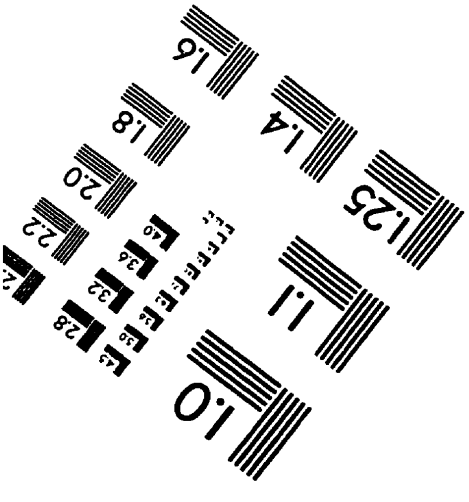

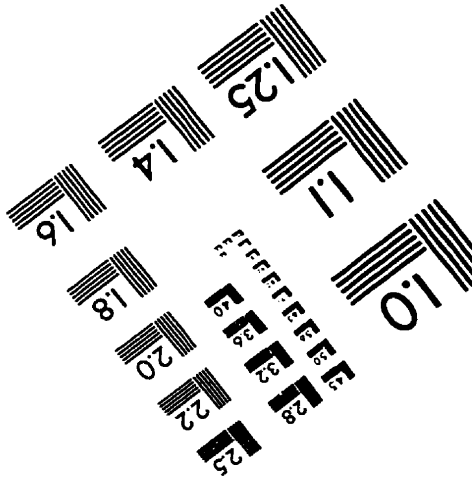

APPLIED IMAGE, Inc
1653 East Main Street
Rochester, NY 14609 USA
Phone: 716/482-0300
Fax: 716/288-5989